Hide and Seek: How Mycobacteria Evade and Manipulate Cellular Immune Responses

Christopher Jacob Cambier

A dissertation
submitted in partial fulfillment of the
requirements for the degree of

Doctor of Philosophy

University of Washington
2014

Reading Committee:
Lalita Ramakrishnan, Chair
Ram Savan
Kevin B. Urdahl

Program Authorized to Offer Degree:
Immunology

University of Washington

Abstract

Hide and Seek: How Mycobacteria Evade and Manipulate Cellular Immune Responses

Christopher Jacob Cambier

Chair of Supervisory Committee
Associate Professor Lalita Ramakrishnan
Department of Microbiology
Department of Immunology
Department of Medicine

Mycobacterium tuberculosis, the causative pathogen of human tuberculosis, is one of the most deadly infectious diseases to inflict man, having killed one-quarter of the population of Europe during the 19th century. The evolutionary success of this pathogen is dependent on its ability to cause disease in order to transmit. Disease symptoms are driven by the bacteria's ability to orchestrate the formation of immune cell aggregates, known as granulomas. Using the zebrafish model of mycobacterial infection, I have taken advantage of the optical transparency of the zebrafish larvae to intricately detail the cellular responses mediating granuloma development. I have identified both host-evasion and host-manipulation strategies used by mycobacteria to cause disease. Mycobacteria avoid detection by immune pattern recognition receptors that identify both pathogens and commensals. This evasion strategy fails in the presence of other bacteria and therefore provides an explanation for the longstanding observation that *M. tuberculosis* must initiate infection in the relatively sterile lower lung, as opposed to the upper airways, which are replete with commensals. Mycobacteria also manipulate the immune response by driving the expression of host chemokines to recruit bacterial permissive cells, which they must infect in order to cause disease. A finding that provides a mechanistic understanding for human studies where overexpression of these same chemokines were associated with developing active tuberculosis. Finally, my work identified a tissue resident macrophage population as being able to clear infection in unimmunized hosts, an epidemiologically documented process that is rarely represented in animal models. These data strengthen our understanding of mycobacterial pathogenesis and will help to guide future therapeutic and vaccine efforts.

Table of Contents

Acknowledgments

I want to extend my gratitude to those that enabled me to successfully survive and thrive throughout my graduate career. To begin with, I have to thank my parents for their never ending love and I support. Thanks for always making education a priority in my life. I also would like to thank Lalita Ramakrishnan for not only giving me a bench to call home but also for providing me with the intellectual training that has shaped my graduate career. I also want to thank all the members of the Ramakrishnan lab, past and present, you have made my work environment truly enjoyable. In particular, I want to thank David Tobin for taking me under his wing during my rotation through Lalli's lab. I also want to thank Chao-Tseung Yang for giving me the opportunity to help him identify the role neutrophils play during mycobacterial infection. I have to thank my classmates, may the bond we share never fade with time. I want to thank my committee members for their professional guidance: David Sherman, Kevin B. Urdahl, Ram Savan, and Daniel Campbell. Thanks to Ryan Larson for doing all of the mouse work that is presented here. I want to thank Michael Black for teaching me how to pipet and showing me the light that is molecular biology, and Laura Koth for introducing me to macrophage biology and giving me the opportunity to prove myself. Thank you OATs for giving me a much needed musical outlet. Thank you NAP for keeping me sane through this journey. And lastly, I have to thank my family and friends; I would not be where I am without you.

Chapter 1: An Introduction to Host Evasion and Exploitation Schemes of *Mycobacterium tuberculosis*

SUMMARY

Tuberculosis, an ancient disease of mankind, remains one of the major infectious causes of human death. We examine newly discovered facets of tuberculosis pathogenesis and explore the evolution of its causative organism *Mycobacterium tuberculosis* from soil dweller to human pathogen. *M. tuberculosis* has co-evolved with the human host to evade and exploit host macrophages and other immune cells in multiple ways. While the host can often clear infection, the organism can cause transmissible disease in enough individuals to sustain itself. Tuberculosis is a near-perfect paradigm of a host-pathogen relationship, and that may be the challenge to the development of new therapies for its eradication.

Introduction

Tuberculosis (TB) has afflicted humans for about 70,000 years and continues to take a huge toll on human life and health with 8.6 and 1.3 million cases and deaths, respectively, in 2013 (Zumla et al., 2013) (Comas et al., 2013). TB's timelessness in the face of significant human lifestyle changes over the millennia and the advances of modern medicine over the last century bespeaks the agility and toughness of its causative pathogen *Mycobacterium tuberculosis*. *M. tuberculosis* may be the paradigm for human host-pathogen adaptation.

TB's notoriety as one of the great bacterial terrors of humanity alongside plague, typhus, cholera, typhoid and diphtheria, has led to descriptors such as the "Great White Plague" and "The Captain of all those men of death". When compared to other major bacterial diseases, there are some interesting and potentially informative aspects of TB's pathogenesis. Human infection and disease is essential for the transmission and therefore the evolutionary survival of *M. tuberculosis*. This is in contrast to plague, which, despite its enormous impact on human history, is a zoonosis where human disease is essentially an accident with no bearing on the pathogen's subsequent survival. The same could be said for many commensal-pathogens, e.g. the pneumococcus, meningococcus, or the flesh-eating streptococci where human disease, while terrifying, is of marginal benefit to the long-term survival of the pathogen. Despite the inextricable connection between disease and transmission and thereby its survival, *M. tuberculosis* appears to lack the classical virulence factors that are the badges of honor of many of these pathogens - capsules to avoid phagocytosis, pili or other adhesins for adherence to host tissues, flagella for motility, enzymes and toxins to poison host cells. How does *M. tuberculosis* produce the disease so devastating to humans and so vital to the pathogen? The classical virulence factors of the mucosal commensal pathogens, many of which reside in the

nasopharynx, are really colonization factors that in the right host run amok to cause a disease that is of questionable benefit to the pathogens' evolutionary survival. These factors probably give the microbe a selective colonization advantage on mucosal surfaces where bacterial competition is rife. Not surprisingly, vaccines against individual virulence factors - be it a capsule of the pneumococcus or a toxin - sometimes eradicate colonization along with disease. As an example, the diphtheria toxin that has been responsible for countless million deaths in the past is likely a colonization factor that allows *Corynebacterium diphtheria* to compete effectively with other mucosal bacteria to establish a privileged niche in the tonsils. The diphtheria vaccine that is directed against this single toxin has wiped out colonization together with disease. These represent the more recently evolved 'crowd' diseases that emerged in the Neolithic age associated with the development of agriculture and the domestication of animals. In contrast, *M. tuberculosis* is an ancient companion of man since before the Neolithic age and its associated crowding (Comas et al., 2013), making TB a "heritage" disease for much of its history. We argue that *M. tuberculosis* and many of the other host-adapted mycobacteria have evolved a different strategy for insuring persistence in the host - they have honed their lifestyle to obviate the need for virulence (née colonization) factors like toxins and enzymes that break down anatomic barriers to outcompete other pathogens by simply traversing host mucosal barriers within host macrophages to sterile sites deep in the body. As we see it, *M. tuberculosis*' dirty little secret is to be hydrophobic and 'fly' more efficiently in a tiny droplet to bypass the innate immune system. Rather than jostling with other pesky microbes, *M. tuberculosis* can deal just with its host, and we suggest that host immune evasion, modulation and exploitation are the trump cards of the pathogenic mycobacteria. This recognition of *M. tuberculosis'* tactics brings

a new understanding of host and pathogen biology that can potentially be parlayed into new therapies and interventions.

This introduction will examine key new discoveries about TB pathogenesis against a backdrop of the natural history of infection and disease and its difficult treatment. We note that TB pathogenesis was last extensively reviewed in *Cell* in 2001 (Glickman and Jacobs, 2001), a time that marked the derivation of a complete basic molecular genetic tool kit and the ushering in of the postgenomic era of TB research following upon the complete genome sequence of *M. tuberculosis* (Cole et al., 1998). This review highlighted the problem of lengthy drug treatment as a factor that made global eradication of TB difficult, described new insights into the strategies used by *M. tuberculosis* to persist in macrophages, and discussed newly identified lipid effectors in virulence. Since then many additional mycobacterial genomes have been sequenced, enhancing our understanding of mycobacterial evolution. More sophisticated genetic approaches and new animal models have provided new and often surprising insights into how the pathogenic mycobacteria survive and replicate in macrophages and indeed orchestrate the formation of granulomas, macrophage aggregates, and exploit them for their expansion. We will discuss how the mechanisms used by mycobacteria to resist macrophages also renders them drug tolerant, a finding that has potential therapeutic implications. Finally, we will discuss how mycobacteria paradoxically can benefit from an over-exuberant host immune response to increase their numbers further and be transmitted to a new, susceptible host. The significance of these discoveries may be most fully appreciated in the context of both mycobacterial evolution and host adaptation. Where appropriate or interesting, we will compare or contrast mycobacterial pathogenic strategies to those of other pathogens. Many of our insights and ideas have come using *Mycobacterium marinum*, a close genetic relative of *M. tuberculosis* (Stinear et al., 2008),

which we have developed as a valid and tractable model for *M. tuberculosis* pathogenesis (Ramakrishnan, 2013; Tobin and Ramakrishnan, 2008). We will therefore use *M. marinum* as a stand-in for *M. tuberculosis*, as well as a comparator. We will organize our thoughts around the "pathogenic personality" of *M. tuberculosis* and its many facets as it goes through its pathogenic life cycle - entry into the host, attainment of a unique niche, multiplication within and exit from the host - all by avoiding, circumventing or manipulating host defenses with a unique "pathogenic signature" (Falkow, 2008) (Figure 1.1).

Stealth entry affords mycobacteria a privileged host niche

The optimal niche for a host-adapted pathogen within a host is the environment in which the pathogen is readily able to replicate. To arrive at, and replicate in, this niche, pathogens must circumvent host defenses, (Falkow, 2006), which are in turn substantially influenced by the commensal microflora that abundantly populate our skin and mucosal surfaces; the host-commensal alliance that forms the barrier to pathogens has recently been reviewed (Belkaid and Hand, 2014).

M. tuberculosis is known to initiate infection most efficiently in the lower lung through small aerosol droplets that can contain only 1-3 bacteria, a constraint that makes it less contagious than respiratory pathogens, such as the Group A streptococcus and *Corynebacterium diphtheriae* that initiate infection in the nasopharynx to respectively cause strep throat and scarlet fever, and diphtheria, that are spread though large, wet droplets. The insight that small droplets are most likely responsible for transmitting TB comes from human epidemiological studies examining transmission from index cases in confined spaces (Bates et al., 1965; Houk, 1980). Corroborating the human studies are studies that track infection serially in rabbits, demonstrating

that aerosol droplet size negatively correlates with infection burdens (Wells et al., 1948). When large aerosolized particles containing 10,000 bacteria were administered, they got stuck in the trachea and the rabbits got no or very little infection. In contrast, upon receiving small aerosols containing 1-3 bacteria that reached the alveolar spaces of the lung, the rabbits all got progressive infection.

A teleological explanation for why TB initiates in the lower lung at the cost of infectivity comes from the zebrafish larval model of TB (Cambier et al., 2014). The zebrafish larva is optically transparent so that infection with fluorescently labeled bacteria can be monitored in exquisite detail (Takaki et al., 2013). To examine the earliest interactions with the host, bacteria can be injected into the hindbrain ventricle, a microbiologically sterile neuroepithelium-lined cavity where macrophages and neutrophils are not present normally but migrate with the expected specificity in response to the microinjection of specific chemokines or bacteria (Takaki et al., 2013; Yang et al., 2012). The zebrafish work suggests that pathogenic mycobacteria have developed strategies to avoid the microbicidal macrophages that are the default recruits to keep mucosal commensal pathogens at bay. These macrophages already primed to be microbicidal are recruited through Toll-like receptor (TLR)-mediated signaling that is activated by the so-called pathogen-activated molecular patterns (PAMPs) present on bacterial surfaces. In mouse and zebrafish macrophages, the TLR-induced microbicidal activity is from reactive nitrogen species produced by the action of inducible nitric oxide synthase (iNOS)(Cambier et al., 2014); different microbicidal effectors may be induced in human macrophages (Liu et al., 2006). Mycobacteria, including *M. tuberculosis* and *M. marinum* are replete with PAMPs. Indeed, complete Freund's adjuvant that is used to prime immune responses is nothing but an oil emulsion containing dead *M. tuberculosis*. However these mycobacteria express a surface lipid

phthiocerol dimycocerosate (PDIM) that masks the PAMPs, so that they are not "seen" by the host innate immune system. Concomitantly, they use a related surface lipid, phenolic glycolipid (PGL) to induce the macrophage chemokine CCL2 to recruit and infect macrophages that are growth-permissive for them. However, this strategy of using a masking lipid to avoid the microbicidal macrophages, and a recruiting lipid to infect the permissive ones would be ineffective in the upper airway, an environment replete with an endless supply of TLR-stimulating commensal bacteria. On this battlefield, mycobacteria would be collateral damage caught in the crossfire; they would be killed by the microbicidal macrophages that are continually being recruited. Hence the need for the third component of their tripartite immune evasion strategy: small infection droplets that deliver them directly into the alveolar spaces of the lower lung, which harbors few, if any, commensals (Charlson et al., 2011) (Figure 1.2).

There is a growing appreciation for a commensal-primed barrier immunity that pathogens must evade, tolerate or interrupt. *Helicobacter pylori* a commensal pathogen that famously causes gastric ulcers is also a heritage pathogen, and has adapted to survive in the stomach, where competition from commensals is minimal (Monack, 2013). *H. pylori* too has evolved to avoid detection via TLRs: its flagellin is not recognized by TLR5 (Gewirtz et al., 2004) and its lipopolysaccharide (LPS) has a lower affinity for TLR4 than that of other bacteria (Moran, 2007). Therefore like *M. tuberculosis*, *H. pylori* has evolved to avoid pro-inflammatory host detection by initiating infection in anatomical locations where commensal competition is minimal. While *M. marinum* and *M. tuberculosis* have developed tactics to evade reactive nitrogen species, *Mycobacterium avium*, that causes TB-like disease in birds appears to have evolved a strategy to tolerate, and even benefit from them, and accordingly, does not express PDIM (Dhama et al., 2011; Dumarey et al., 1994; Gomes et al., 1999; Onwueme et al., 2005)

(Figure 1.3). The case of host-adapted Salmonella, another macrophage-dwelling class of pathogens may be illustrative as well. Salmonella infects via the terminal ileum that is replete with colonizing bacteria. To facilitate its transit through the commensal-laden gut, Salmonella appears to first drive an inflammatory response that generates the reactive nitrogen species to which the commensals are sensitive, but it, like *M. avium*, is tolerant at least early during infection (Fang, 2004; Henard and Vázquez-Torres, 2011). Upon reaching the terminal ileum the invading Salmonella enters into M cells, specialized cells of the follicle associated epithelium, a region that is again relatively free from commensal competition (Jones et al., 1994) and invade underlying macrophages. This multi-pronged strategy to interrupt the commensal barrier so as to reach the M cells affords Salmonella access to the systemic phagocytes of the host (called the reticuloendothelial system). The common theme emerging from these scenarios is that host-adapted pathogens must develop strategies to circumvent the host-beneficial commensal-primed immune barrier in order to reach their replicative niche. In turn, we emphasize that commensals exert a selective pressure that has shaped pathogen evolution.

Mycobacteria have to engage with the host to become phagocytosed by permissive macrophages by simultaneously using the surface lipid, PDIM, to dampen TLR signaling, and the related surface lipid, PGL, to induce CCL2 signaling. This finding has additionally provided an understanding of the role of these lipids in virulence (Siegrist and Bertozzi, 2014). PDIM is expressed only by pathogenic mycobacteria, is absolutely required for virulence, and is present in all *M. tuberculosis* clinical isolates (Onwueme et al., 2005). Yet PDIM synthesis is metabolically costly so that it is readily lost in axenic culture (Kirksey et al., 2011). PGL, in contrast, is not absolutely required for virulence; it is not present in all clinical *M. tuberculosis* isolates (Reed et al., 2004). However, it is present in many of the W-Beijing strains that have

predominated in outbreaks in North America, where TB is not prevalent. In the zebrafish, where low-dose infections can be examined longitudinally from the first instances of infection, PGL specifically increases infectivity of inocula of 1-3 bacteria (that mimic those of human infection) by enhancing the recruitment of mycobacterium-permissive macrophages. It is only in the context of examining the ability of the pathogen to establish infection, rather than sustain it, that the role of PGL is revealed. The presence of PGL on the bacterial surface substantially increases the organism's chances of reaching its preferred replicative niche. These findings may also serve to explain human studies showing an association between tuberculosis susceptibility and the high expression of CCL2, PGL's host partner in recruiting permissive macrophages (Flores-Villanueva et al., 2005). Further the finding that PGL increases virulence through enhanced infectivity provides an understanding of why PGL is in *M. cannetti* strains, ancestral to *M. tuberculosis* as well as in *M. marinum*, the closest genetic relative of the *M. tuberculosis* complex (Onwueme et al., 2005), suggesting its integral role in the evolution of mycobacterial pathogenicity. As noted before, TB is generally thought to have been present in humans for approximately 70,000 years, thus predating by ~ 60,000 years the Neolithic demographic transition and its resultant crowding (Bos et al., 2014; Comas et al., 2013). Thus, PGL may have been an essential virulence determinant for most of its history. Perhaps, the greatly increased transmission opportunities arising from human crowding made it dispensable.

Multiplication within the host - the macrophage niche

The strategy elaborated by *M. tuberculosis* to traverse host epithelial barriers within permissive macrophages is, of course, predicated upon its ability to survive within these highly-evolved phagocytic host cells. Indeed, macrophages comprise the replicative niche for most of the life cycle, not only of *M. tuberculosis* but of most other pathogenic mycobacteria (Figure

1.4). Accordingly, the ability to replicate in host cells is a defining feature of the pathogenic mycobacteria - be they human or animal pathogens - and reliably distinguishes them from their nonpathogenic soil-dwelling cousins like *Mycobacterium smegmatis* (SHEPARD, 1957)(Figure 1.3). A clue for how this ability to grow in host macrophages might have evolved comes from the remarkable finding that the ability of mycobacteria to replicate in macrophages tracks completely with their ability to grow in unicellular free-living amebae. Pathogenic mycobacterial species can replicate in amoebae whereas *M. smegmatis* cannot (Cirillo et al., 1997). Moreover, to the extent tested, the same mycobacterial determinants are required for growth in macrophages and amoebae (Alibaud et al., 2011; Hagedorn et al., 2009; Hagedorn and Soldati, 2007; Solomon et al., 2003). Thus predatory environmental amoebae, may have served as the ancient evolutionary training ground for mycobacterial pathogens to survive in the macrophages of their multicellular hosts. This has been postulated for *Legionella*, an accidental human pathogen that can cause serious pneumonia after being aerosolized from potable water sources where it is thought to be sustained through replication in environmental amoebae (Fields et al., 2002).

Any foreign particulate that is phagocytosed by macrophages is destined to be processed through the endocytic pathways. Thus, intracellular pathogens have evolved diverse ingenious signature strategies to thwart, modulate, exploit, or avoid host endocytic pathways. Broadly speaking, these pathogens can resist lysosomal fusion to reside in non-acidified endosome-like compartments, survive (or even require) acidification so as to be able to reside in acidified lysosome-like compartments, or break out of the phagosome altogether to reside in the cytosol (Alix et al., 2011)(Figure 1.4). Most such experimental studies on the virulence of intracellular mycobacteria have been conducted using either mouse or human cultured macrophages. For *M. tuberculosis,* observations in cultured macrophages have produced disparate results probably

because the cell lines, culture conditions and kinetics of infection differ considerably between different laboratories. *M. tuberculosis* is reportedly found localized to non-acidified early endosomes, or found in acidified lysosomes with a small proportion of the bacteria eventually breaking out of the phagosome to reside in the cytosol (Cosma et al., 2003) (van der Wel et al., 2007). Indeed, mycobacteria have specific virulence determinants that promote, at least in cultured cells, both the avoidance of acidification as well as acid resistance, suggesting that despite their best attempts, they might find themselves in acidified compartments (Rohde et al., 2007). In addition, the ability to break out into the cytosol is dependent on a specialized bacterial secretion system, ESX-1 (van der Wel et al., 2007), whose role we will elaborate upon in the context of the tuberculous granuloma in the following section.

The multiple subcellular compartments that *M. tuberculosis* can occupy within macrophages speak to the plethora of defenses with which they must contend even in the most permissive of macrophages. It is hardly surprising that diverse mycobacterial determinants are required for macrophage survival (Forrellad et al., 2013). What is surprising is that the obvious prediction that these determinants were acquired during mycobacterium's jump to becoming an amoeba-dweller does not stand scrutiny. While our search was not exhaustive, virtually all of the important *M. tuberculosis* virulence determinants that specifically promote intracellular growth are present in *M. smegmatis* (Forrellad et al., 2013)! What is more, in the cases tested the *M. smegmatis* gene can substitute for its *M. tuberculosis* gene in mediating macrophage growth and virulence, suggesting that no or few further modifications were needed to confer this function (Houben et al., 2009). For instance, the eukaryotic-like serine-threonine protein kinase PknG is secreted into the phagosomal lumen and promotes macrophage growth by inhibiting lysosomal fusion and thereby acidification of the mycobacterial phagosome (Walburger et al.,

2004). While the *M. smegmatis* PknG homologue is able to restore macrophage growth of the *M. tuberculosis pknG*, its function in the context of this saprophytic organism remains unknown. PknG is translationally repressed in *M. smegmatis* at least under axenic growth, suggesting that there is some specific "real-life" situation during life in the soil where it is induced presumably to perform some specific function (Houben et al., 2009).

Perhaps the most fascinating example of conservation across mycobacteria is that of the mycobacterial energy-dependent efflux pumps, that we recently discovered to be *M. tuberculosis* macrophage-growth factors by a circuitous route when looking for the basis of antibiotic tolerance (Adams et al., 2011; Rengarajan et al., 2005; Szumowski et al., 2013). In addition to developing genetic drug resistance through fixed mutations, *M. tuberculosis* famously develops what is called "phenotypic drug resistance" or "drug tolerance" where it becomes transiently resistant to antibiotics (in the absence of fixed genetic mutations) in the host. This necessitates long treatment periods to achieve clinical cures (Connolly et al., 2007). Mycobacterial drug tolerance has long been attributed to the bacteria being in a non-replicating or dormant state in the host (Chao and Rubin, 2010; Rittershaus et al., 2013). However, our recent work shows that when *M. tuberculosis* enters macrophages, it is, in fact, the actively-replicating bacteria within the macrophages that develop antibiotic tolerance through the induction of specific macrophage-induced efflux pumps (Adams et al., 2011; Schnappinger et al., 2003). These same efflux pumps that mediate macrophage-induced drug tolerance also promote intracellular mycobacterial growth (Adams et al., 2011; Schnappinger et al., 2003). This suggests that these pumps may have evolved in the soil-dwellers to defend against environmental toxins and inhibitors (including naturally occurring antibiotics), but came to be useful for the contemporary lifestyle of the pathogenic mycobacteria, facilitating intracellular survival, perhaps by protecting them

against the antimicrobial peptides made by these cells. With the advent of chemotherapy, their ancestral function to defend against antibiotics or other growth inhibitors affords added benefit in surviving within the host - the same pumps may efflux the natural macrophage defenses as well as the administered antibiotics (Adams et al., 2011; Schnappinger et al., 2003). These findings additionally have therapeutic implications because efflux pump inhibitors should prevent the replication of intracellular *M. tuberculosis*. Moreover, combining efflux pump inhibitors with standard antibiotic therapy should be a "double whammy" to intracellular *M. tuberculosis* because they should inhibit intracellular growth in their own right, and additionally allow the antibiotics to kill these bacteria better by preventing their efflux. Indeed, we have found this to be the case using inexpensive, well-tolerated approved human drugs that are currently used for other purposes (e.g. verapamil) (Adams et al., 2014; Adams et al., 2011; Gupta et al., 2013). Moreover, the addition of verapamil to standard antituberculous chemotherapy reduces relapse rates in *M. tuberculosis*-infected mice (Adams et al., 2014; Adams et al., 2011; Gupta et al., 2013). On the basis of all these findings, clinical trials of verapamil as a TB treatment-shortening agent are imminent.

In summary, returning to our comparative theme, it would appear that the environmental mycobacteria, e.g. *M. smegmatis*, had determinants that allowed them to survive in the soil even though they could not survive within unicellular predators. The selection for the ability to survive within unicellular amoebae, and eons later within the macrophages of multicellular creatures, required using these determinants together with acquiring new, as yet unknown ones possibly by horizontal gene transfer (Figure 1.4). One could argue that mycobacteria come 'pre-loaded' with the means to survive within a professional phagocytic cell. It is perhaps a general strategy for other soil organisms adapting to animal hosts as illustrated as well for *Rhodococcus*

equi, the horse and occasional human pathogen that diversified from soil-dwelling *Rhodococci* (Letek et al., 2010). In the case of mycobacteria, the pathogenic forbearer selected for growth in amoeba appears to have then followed different evolutionary branches to dwell in different hosts, sometimes involving the acquisition of plasmids, and as is so often the case, gene loss, so as to fine-tune adaptation to specific hosts (Boritsch et al., 2014; Wang and Behr, 2014)(Figure 1.3).

In the following section we will discuss the elaborate macrophage manipulation strategies used by *M. tuberculosis* to form the granuloma - the hallmark pathological structure of TB. We argue that it is as much a mycobacterial strategy for survival, as a host defense response.

Multiplication in the host - exploiting the granuloma

A granuloma is fundamentally an organized aggregate of macrophages whose membranes become tightly interdigitated like those of epithelial cells, leading them to be called epithelioid cells (Adams, 1976; Bouley et al., 2001). Granulomas can form in response to any number of persistent stimuli, both infectious and noninfectious, so that they are associated with myriad diseases (Ramakrishnan, 2012). They were first recognized as distinct structural entities in the context of human TB in the 17th century, preceding by some 200 years the discovery of *M. tuberculosis* as its cause, and even today, TB remains the commonest cause of granulomas worldwide (Ramakrishnan, 2012). For a very long time, the tuberculous granuloma, has been held to be an essential host protective structure - a fortress containing a complex mixture of diverse host cells that walls off bacteria (Saunders and Cooper, 2000) (Chao and Rubin, 2010; Rittershaus et al., 2013). Indeed, clinical and epidemiological studies clearly support the idea the granuloma can sterilize infection in many cases (Cosma et al., 2004; Feldman and Baggenstoss, 1938). Yet, we argue that there is an inextricable link between highly organized

granulomas and heavy bacterial burdens in TB, suggesting that in many cases, the granuloma can be at least conducive to high bacterial burdens if not downright supportive of them (Connolly et al., 2007). Indeed, our findings over the last decade suggest that mycobacteria actually enhance the formation of granulomas and have adapted to exploit these structures for their expansion and dissemination (Davis and Ramakrishnan, 2009). This modified view of the granuloma was made possible by studies in the zebrafish where we could visualize the earliest events of granuloma formation around the first infected macrophage that had arrived in the deep tissues. Bacterial expansion in granulomas is accomplished by the spread of bacteria from dying macrophages to newly arriving ones (Davis and Ramakrishnan, 2009). When mycobacterial numbers increase to a certain threshold in individual macrophages, they undergo an apoptotic death that leaves viable bacteria still encased within the dead cells (Figure 1.5). Concomitantly, multiple new uninfected macrophages are recruited to the nascent granuloma that engulf the bacterial contents of a given dead or dying macrophage, thus enabling them to fill up the new cells. This process of macrophage death and re-phagocytosis enables a tremendous expansion of the bacterial niche, all within macrophages (Davis and Ramakrishnan, 2009).

At a molecular level, this coordinated macrophage death and re-phagocytosis are mediated through a specialized mycobacterial secretion system called ESX-1, most likely through its secreted effector ESAT6 (Davis and Ramakrishnan, 2009; Volkman et al., 2004; Volkman et al., 2010)(Figure 1.5). ESAT6 has been shown to induce apoptosis of infected cells in culture through multiple pathways, one or more of which may be operant in the granuloma (Choi et al., 2010; Derrick and Morris, 2007; Keane et al., 1997; Mishra et al., 2010; Swaim et al., 2006). ESX-1/ESAT-6, also recruits macrophages by inducing host matrix metalloproteinase 9 (MMP9) in epithelial cells surrounding the nascent granuloma (Volkman et al., 2010). If host

MMP9 function is decreased, infection is attenuated, with reduced granuloma formation (Volkman et al., 2010). These discoveries, initially made in the zebrafish, are corroborated by findings in humans showing that MMP9 is induced in epithelial cells surrounding lung granulomas, and increased MMP9 secretion is associated with increased severity and mortality in tuberculous meningitis (Elkington et al., 2007; Price et al., 2001).

In summary, *M. tuberculosis* appears to use at least two distinct pathways to recruit macrophages. When a tubercle bacillus first enters the host animal, it uses its PGL surface lipid to recruit macrophages through the host CCL2 that then bring it across the host epithelium to deeper tissues (Cambier et al., 2014)(Figure 1.2). The intracellular bacteria then orchestrate the recruitment of additional macrophages to form the granuloma through their ESX-1 locus (Figure 1.5). Why the bacteria transition from using PGL to using ESAT6 to drive macrophage recruitment is unclear. What is clear is that in both phases, macrophage recruitment benefits the mycobacteria as much as the host! Thus, CCL2 and MMP9 may both represent host determinants that have been co-opted by mycobacteria for their benefit, and increased CCL2 and MMP9 expression are both linked to human susceptibility to TB (Elkington et al., 2007; Price et al., 2001); (Flores-Villanueva et al., 2005).

It is curious that while the growing granuloma supports *M. tuberculosis* expansion, the macrophages within this structure generally become more microbicidal suggesting that the bacterium should be put at a further disadvantage (Adams, 1976; Bouley et al., 2001). But it appears that the mycobacteria in turn rapidly adapt to the more hostile environment in the granuloma by transcriptionally inducing new genes (e.g. efflux pumps) upon entering a macrophage, which aid in intracellular survival. Moreover, when an infected macrophage forms or joins a granuloma, its intracellular bacteria rapidly induce additional genes that help it counter

the additional stresses of living within the cellular environment of the granuloma (Cosma et al., 2004; Davis et al., 2002; Ramakrishnan et al., 2000). If an infected animal with mature granulomas (frogs or zebrafish with *M. marinum*, or mice with *M. tuberculosis*) is superinfected with new mycobacteria, these bacteria enter new macrophages that preferentially migrate to existing granulomas rather than avoiding them as hostile sites (Cosma et al., 2004; Cosma et al., 2008). It is as if mycobacteria "know" that while the granuloma may not be a place where "the living is easy", it still does afford them a preferred and, paradoxically, a protected multiplication niche, and as we shall see in the following section, a transmission niche, as well.

Our proposed mycobacterial-centric view of granuloma biology and function returns us yet again to questions about how mycobacteria evolved to pathogenicity. We focus now on the ESX-1 secretion system and its effector, ESAT6. ESX-1/ESAT6, which like most other *M. tuberculosis* virulence factors, is also present in *M. smegmatis.* However, in *M. smegmatis,* this secretion system regulates bacterial conjugation (Coros et al., 2008; Parsons et al., 1998) (Figure 1.3). The *M. tuberculosis* and *M. smegmatis* homologs are functionally conserved (Converse and Cox, 2005; Flint et al., 2004), but the co-option of bacterial gene-exchange systems for virulence is not special to mycobacteria. In diverse bacterial pathogens like *H. pylori*, *Legionella*, and *Agrobacterium*, the type IV secretion system that is required for virulence also mediates DNA transfer or uptake. Equally interesting is the finding that ESX is not even mycobacterium-specific; an ESX homolog mediates virulence in *R. equi* while also being present in the soil *Rhodococci*, and indeed being widely distributed in GC-rich soil bacteria (Letek et al., 2010). The mechanistic details of how ESX-1/ESAT6 mediates granuloma formation and virulence remain to be understood. ESAT6 is reported to be associated with the ability of *M. tuberculosis* sub-populations to break out of the phagosome (De Leon et al., 2012; Hsu et al., 2003; van der

Wel et al., 2007)(Figure 1.4). In fact, prior to full-fledged phagosomal rupture, ESAT6 may permeabilize the phagosomal membrane enough to expose mycobacterial DNA to the host cytosolic DNA sensing pathway (Manzanillo et al., 2012). This results in the induction of Type I interferon, a cytokine that is best known for its antiviral activity; however mycobacteria appear to drive this cytosolic DNA sensing response in in their favor. Components of the cytosolic pathway and Type I interferon mediate host susceptibility in animal models. Type I interferon receptor knockout mice are more protected against TB, similar to the protection against TB afforded by knocking out MMP9 (Manzanillo et al., 2012; Mayer-Barber et al., 2014; Taylor et al., 2006; Watson et al., 2012). In humans too, a type I IFN transcriptional signature has been associated with active versus subclinical TB in humans, suggesting it is a host susceptibility factor for disease progression (Berry et al., 2010). Whether ESAT6 modulates host MMP9 activity and granuloma formation through its membrane permeabilization activity and/or by triggering the cytosolic DNA detection system still remains unclear. What is clear is that it represents another fascinating case where a ubiquitous bacterial determinant has been co-opted and fine-tuned through genetic selection, not just to modulate bacterial growth in macrophages, but, as well, to become integrated with other bacterial genes for a choreographed manipulation of macrophage migration and death to build the granuloma.

Of course, this initial phase of bacterial expansion in the granuloma is followed by the advent of an adaptive immune response which can often eradicate the tubercle bacilli, presumably by increasing the microbicidal capacity of the granuloma macrophages (Ramakrishnan, 2012). Epidemiological evidence would suggest that with a little help from adaptive immunity, the granuloma can sterilize infection in most cases (Cosma et al., 2004; Feldman and Baggenstoss, 1938). Conversely, the very large number of active TB cases with

full-fledged mature granulomas that are replete with lymphocytes, suggests that mycobacteria have evolved additional strategies to evade adaptive immunity. As we have detailed in prior reviews, many of these strategies have been elucidated recently and include delaying both T cell priming in the lymph nodes and their arrival and activity in the granuloma (Pagán and Ramakrishnan, 2014; Ramakrishnan, 2012). Thus, *M. tuberculosis* reduces macrophage responsiveness to signaling by gamma interferon, the main T cell cytokine (Banaiee et al., 2006). Finally, *M. tuberculosis* can synthesize its own tryptophan, so that unlike some other intracellular pathogens (e.g. Chlamydia), it is able to survive the intracellular tryptophan starvation brought on gamma interferon (Zhang et al., 2013). Thus, bacterial interactions with host adaptive immune system add layers of complexity to the host-pathogen interface. The tubercle bacillus first induces an innate inflammatory response to accelerate macrophage responses (recruitment, phagocytosis, apoptosis) that are normally protective to turn the granuloma response into a bacterial production factory. By then delaying T cell priming, arrival and activation together with macrophage responsiveness by what appears to be a highly orchestrated strategy, the bacteria buy themselves yet more time to establish a strong replicative niche in the granuloma.

Many diverse microorganisms induce granulomas and it will be interesting to compare the pathways and consequences of granuloma formation for each of them. Within the mycobacteria, a tantalizing difference in granuloma formation pathways is already apparent by comparing *M. marinum* and *M. tuberculosis* to *M. avium* (Figure 1.3). ESAT6/ESX1 is absent from *M. avium*, which is not a particularly successful pathogen in human hosts (Dhama et al., 2011; Dumarey et al., 1994; Gomes et al., 1999; Onwueme et al., 2005; Sørensen et al., 1995) (Figure 1.3). However, in birds, *M. avium* causes a full-blown granulomatous disease that is transmissible, usually by ingestion. So *M. avium* granulomas must form through a different

pathway. Meanwhile, *M. tuberculosis* ESAT6 has been recently revealed to have yet another function in supporting bacterial expansion in the granuloma - it induces immunosuppressive regulatory T cell populations that delay the migration of effector T cells into the granuloma (Shafiani et al., 2013; Shafiani et al., 2010). Thus, ESAT6 may prolong the phase of bacterial expansion in the innate granuloma that it orchestrates in the first place (Davis and Ramakrishnan, 2009). In this context, it is intriguing that birds, in contrast to mammals and zebrafish, appear to have lost the transcription factor FoxP3 that is required for regulatory T cell development (Andersen et al., 2012). Therefore a plausible explanation for *M. avium's* loss of ESX-1/ESAT6 is that it is superfluous for granuloma expansion in its bird hosts. In contrast, its retention in *M. tuberculosis* and *M. marinum* may reflect its central role in granuloma expansion in mammalian and fish hosts. The selective forces of the host's immune system are reflected in the array of expressed virulence genes seen in each host-adapted mycobacterial species. While our conjecture on the evolutionary connections may well be incorrect, our revised view of the role of the granuloma in the pathogenesis of tuberculosis can be tested further experimentally, and may have potential clinical relevance - we predict that the reduction of granuloma formation by pharmacological inhibition of the relevant host pathways (e.g. MMP9) should ameliorate infection.

Exit from the host - escaping the granuloma

A host-adapted pathogen's final step to ensure its evolutionary success is to exit the host and enter a new host for the infection cycle to start anew. In the case of *M. tuberculosis,* it must exit the granuloma of its infected host to enter and establish infection in a new host. Epidemiological evidence suggests that transmission occurs most efficiently from individuals

with organized granulomas that have undergone central necrosis (Sharma et al., 2005) (Reichler et al., 2002); (Bekker and Wood, 2010) (Huang et al., 2014). The necrotic areas rupture into the bronchial tree, thus exposing the mycobacteria to the airway whence they can be aerosolized in cough droplets. Recent work both from our laboratory and others takes a slightly modified view of the dynamics of cell death in a granuloma (Ramakrishnan, 2012). Broadly speaking, infected granuloma macrophages can die in two ways - by apoptosis or by necrosis. Apoptosis leaves the host cell membranes intact, so that the bacteria remain encased within the macrophage corpse, and are readily phagocytosed by new entering cells. In contrast, macrophage necrosis, or lysis, releases the intact bacteria into the extracellular milieu. This necrotic debris, or caseum, seems to be an ideal bacterial growth medium as the multiplying bacteria reach much higher numbers extracellularly and grow in characteristic serpentine cords. Thus, in our view, apoptotic death favors bacterial expansion or maintenance of the granuloma by providing new cells to grow in, albeit still restricted by macrophage defenses. Lysing out of the macrophages allows more exuberant growth probably because host defenses directed against extracellular bacteria like complement and antibodies seem to be ineffective against mycobacteria. Moreover, recent work suggests that these corded extracellular mycobacteria are not readily engulfed by new macrophages the way bacteria within apoptotic cells are (Bernut et al., 2014). It is not fully understood how the dynamics of the granuloma shift to favor necrosis but some interesting insights are emerging.

Our studies in *M. marinum*-infected zebrafish have uncovered two pathways that lead to macrophage necrosis, each through opposite dysregulation of TNF resulting in too little or too much TNF. TNF is required for macrophage microbicidal activity, although we do not

understand the specific mechanisms and effectors (Clay et al., 2008). Whereas host TNF deficiency causes mycobacteria to grow exuberantly within macrophages that then die and release them to the extracellular milieu (Clay et al., 2008), we have found that an excess of host TNF causes infected macrophages to undergo necrosis, through a programmed pathway called necroptosis (Roca and Ramakrishnan, 2013; Tobin et al., 2012). Host TNF excess causes the activation of the RIP1 and RIP3 kinases that then through a series of steps induce reactive oxygen species by the macrophage mitochondria (Roca and Ramakrishnan, 2013; Tobin et al., 2012). Reactive oxygen has dual effects: it kills both mycobacteria and macrophage. The net result is that just as the macrophage is on its way to killing its infecting mycobacteria, it dies. The few surviving mycobacteria that are released extracellularly can expand their numbers rapidly.

Perturbation of several pathways could lead to TNF dysregulation, and in turn granuloma necrosis. One that we identified in a zebrafish mutant screen for susceptibility to *M. marinum*, involves dysregulation of the leukotriene A4 hydrolase (LTA4H), a synthetic enzyme in the eicosanoid pathway that catalyzes the synthesis of the highly pro-inflammatory lipid leukotriene B_4 (Tobin et al., 2012; Tobin et al., 2010). LTA4H deficiency prevents the synthesis of this leukotriene and instead causes the accumulation of the anti-inflammatory lipid lipoxin A_4, which represses the TNF response to infection. In contrast, LTA4H excess causes an overproduction of leukotriene B_4 and an excess of TNF. In humans, a common *LTA4H* promoter variant regulates gene expression, and homozygotes for both the low- and high-expression variants, associated with low and high inflammation, respectively. Individuals with low- and high-expression variants of LTA4H get severe tuberculous meningitis with a high mortality. In contrast, the heterozygotes, with an intermediate (presumably optimal) level of LTA4H expression, are

protected. These findings in turn have therapeutic implications - in a Vietnamese tuberculous meningitis cohort, adjunctive treatment with the broadly immunosuppressive glucocorticoids which are now routinely administered along with antitubercular chemotherapy, only prevented mortality of the high LTA4H group while possibly increasing mortality of the low LTA4H individuals (Tobin et al., 2012; Tobin et al., 2010). These results suggest patient genotype-directed glucocorticoid treatment may optimize TB treatment.

Our detailed understanding of the two pathways through which excess TNF induced mitochondrial reactive oxygen causes macrophage necrosis also suggests new approaches to TB therapy (Roca and Ramakrishnan, 2013; Tobin et al., 2012). Reactive oxygen causes the translocation of the matrix mitochondrial protein cyclophilin D to participate in the formation of a pore on the mitochondrial membrane, thus causing leakage of mitochondrial contents. Additionally, the reactive oxygen also causes overproduction of a cellular lipid called ceramide that induces necrosis through mechanisms that are not yet clear. We have identified currently available oral drugs that can block each of these pathways. Alisporivir, a drug in phase 3 clinical trials for another disease blocks cyclophilin D, and desipramine, a tricyclic antidepressant, inhibits ceramide production. In the zebrafish, the combined use of these drugs allows the reactive oxygen to kill the bacteria without killing the macrophages, and thereby converts the hypersusceptible state of TNF excess to hyperresistant. It is possible that these drugs will have a similar effect in humans who induce excess TNF during infection.

Necrosis from excessive TNF may be further exacerbated by the participation of adaptive immunity, as much of the TNF induced in TB is produced by T cells (Roach et al., 2002; Saunders et al., 2004). Perhaps *M. tuberculosis* has co-opted T cells into producing the TNF that causes macrophage necrosis and thus encourages transmission. Indeed, T cell epitopes of all

known mycobacterial T cell antigens are reported to be hyperconserved across strains globally, even more so than those of essential genes (Comas et al., 2010). This finding suggests that T cell recognition favors the survival and transmission of mycobacteria, arguably by inducing TNF-mediated necrosis as described above. The hyperconservation of T cell epitope regions of expressed mycobacterial antigens highlights the close evolutionary relationship between T cell recognition and bacterial fitness. Epidemiological evidence suggests that individuals with diminished adaptive immunity (e.g. HIV-infected individuals or children) tend to have smaller and less necrotic granulomas than immunocompetent adults, and these former individuals while more susceptible to TB do not transmit it as well as the latter (Huang et al., 2014). The fact that at a global level, > 80% of TB occurs in individuals who are not HIV-infected (Zumla et al., 2013), is consistent with *M. tuberculosis* taking advantage of adaptive immunity for its transmission that the bulk of disease occurs in the context of an intact adaptive immune system.

In summary, our view is that *M. tuberculosis* and many other pathogenic mycobacteria are not innocent bystanders during the formation of granuloma. They can modulate the host response to infection to build and modify this complex immunological entity into a niche that can sustain infection, first through intracellular growth and then through extracellular growth that also favors transmission.

Concluding thoughts

The case of *M. tuberculosis* exemplifies how a series of genetic adaptations can convert a soil-dwelling microbe into one of the most successful and enduring pathogens of humanity. More people are thought to have died of TB than any other infectious disease throughout history, and more people are afflicted with active TB disease today than at any other time in history

(Lawn and Zumla, 2011). While marveling at the exquisite bacterial adaptations that have honed this microbe's success in its human niche, it is important to remember that most infected individuals (classically reported to be 90%) can successfully contain or clear the infection (Zumla et al., 2013). This occurs, either through an initial mobilization of innate immune mechanisms or, failing that, through adaptive immunity. In this introduction we have tried to point out how the outcome of each step of the host-pathogen interaction can represent 'success' for the host - infection can be suppressed or cleared at the first site of infection, in the innate granuloma or later when the granuloma is further re-enforced by adaptive immunity (Cambier et al., 2014; Lin et al., 2014) (Adams et al., 2011; Rengarajan et al., 2005; Szumowski et al., 2013).

Suppression of infection can result in a clinical latency where the bacteria persist indefinitely in the host and can produce active disease even decades later - a scenario that is emphasized in the literature (Chao and Rubin, 2010; Cosma et al., 2003; Rittershaus et al., 2013). However, careful longitudinal studies from the pre-antibiotic era suggest that most contemporary human disease manifests within a few months of infection or is cleared (Cosma et al., 2003). In today's world, it is these relatively recently infected individuals who transmit the bulk of the disease, rather than those in whom disease has recrudesced after many decades. From a medical perspective, this places the impetus on understanding how the majority of infected individuals progress to disease relatively rapidly. However, it is likely that clinical latency played an important place in sustaining the organism through the ~ 60,000 years before TB became a 'crowd' disease. The organism early on in its evolution did not have the advantage of large susceptible populations that resulted from the Neolithic revolution of domestication and the development of agriculture. It is hard to imagine how the early hunter-gathers living in small groups could have sustained *M. tuberculosis* without the benefit of activation of transmissible

disease in previously healthy infected individuals who were able to travel long distances. We speculate that in the latter part of its history, TB has shifted from being a heritage disease to a crowd disease, and the opportunities afforded by a growing susceptible host population may have led not only to increased transmission but to a more aggressive stance against innate immune defenses leading to epidemic spread rather than persistence.

It is interesting in this context that we may be witnessing a shift in transmission of another major mycobacterial disease leprosy. Leprosy is caused by *Mycobacterium leprae,* which appears to have also evolved from the common *M. tuberculosis* - *M. marinum* ancestor (Figure 1.3). *M. leprae* is particularly intriguing because it has undergone substantial gene reduction to the point where it has lost its capacity for axenic growth (Cole et al., 2001). At the same time, it has become specialized in its pathogenic niche, infecting Schwann cells of the peripheral nervous system through complex mechanisms (Masaki et al., 2013). For most of its pathogenic human history, *M. leprae* has been a strict human pathogen with transmission occurring only through prolonged contact with infected humans. Yet, in very recent times, the nine banded armadillo in the Southeastern United States became infected from humans and has now become a full-fledged reservoir for disease, so that leprosy is now mainly a zoonotic disease in this area (Truman et al., 2011). Albeit in a less dramatic way, *M. tuberculosis* must clearly have made adaptations to the very great changes in human lifestyles to retain its success. Understanding these changes may have more than academic value; they may help us better understand the disease itself and hence its treatment. The parallel evolution of pathogens to keep up with changing environments is hardly unique to mycobacteria but shared with many, many other pathogens.

Finally, our recent work has repeatedly confronted us with the fact that TB is not as much a disease of failed immunity as it is of co-evolution. At every step of infection, the bacterium appears to be inducing and benefitting from an over-exuberant response using the very inflammatory pathways that are thought to have evolved to thwart bacteria - CCL2 induction to enter the host, MMP9 induction to expand in the granuloma, and finally TNF and T lymphocytes to exit the granuloma for transmission. Despite all of this, both host and pathogen have prevailed. That is why we consider *M. tuberculosis* to be a paradigm of a host-adapted microorganism. It has co-evolved with the human immune system, discarding and gaining genes to be in tune with it. As an ancient disease agent adapting to humans, the microbe could not have anticipated that humans would be so successful. Yet, its stealth and subtlety have allowed it to thrive even in the face of modern medicine. While new therapeutic avenues will most likely be found, we must not undervalue the power of genetic selection for the survival of any microorganism. And based on past performance, particularly for *M. tuberculosis.*

Chapter 1 Figures

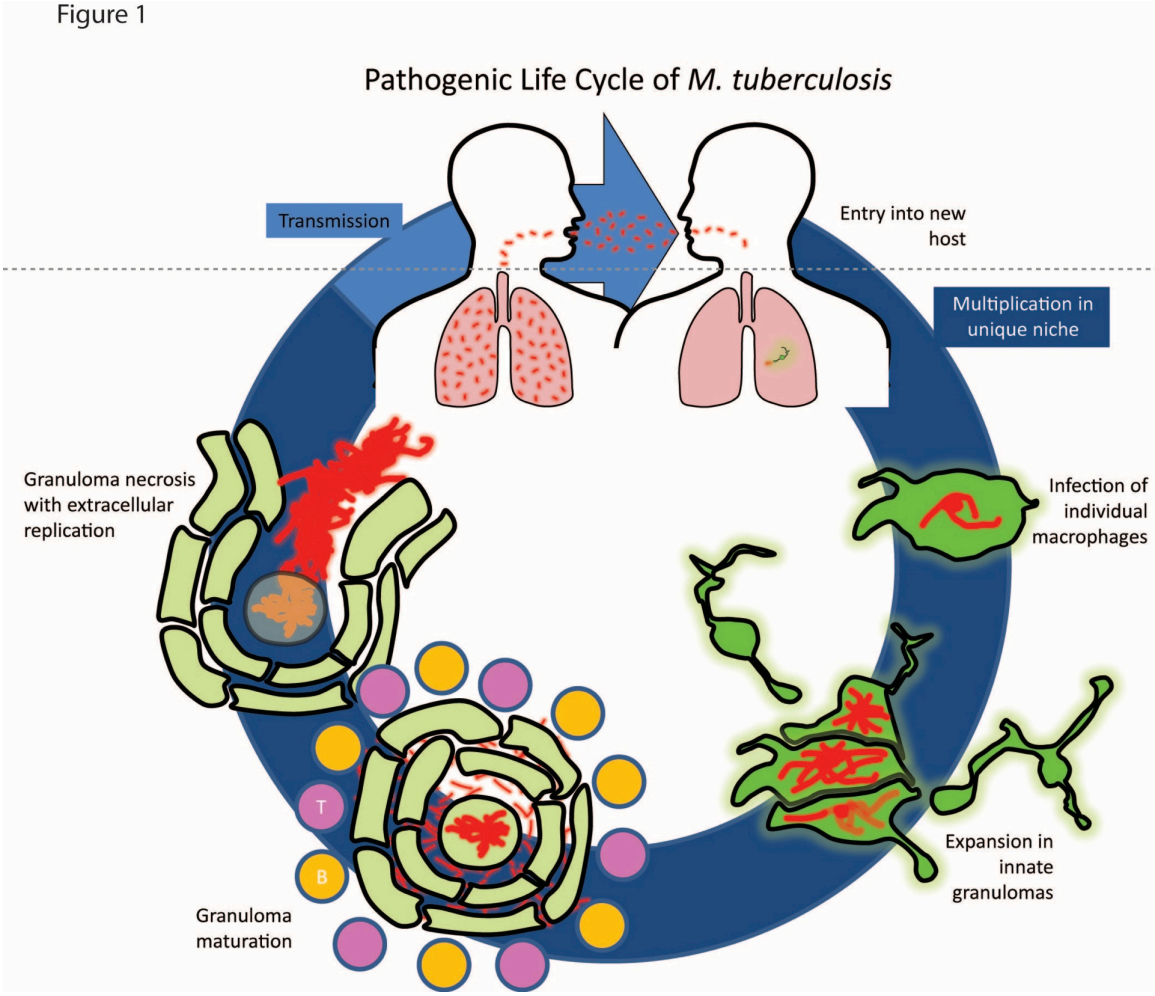

Figure 1.1: Pathogenic life cycle of *M. tuberculosis*. *M. tuberculosis* infection initiates when fine aerosol particles containing the bacteria coughed up by an individual with active disease are deposited in the lower lungs of a new host. The bacteria recruit macrophages to the surface of the lung, which become infected and serve to transport the bacteria across the lung epithelium to deeper tissues. A new round of macrophage recruitment to the original infected macrophage is initiated, forming the granuloma, an organized aggregate of differentiated macrophages and other immune cells. The granuloma in its early stages expands infection by allowing bacteria to spread to the newly arriving macrophages. As adaptive immunity develops, the granuloma can restrict bacterial growth. However, under many circumstances, the infected granuloma macrophages can undergo necrosis, forming a necrotic core that supports bacterial growth and transmission to the next host.

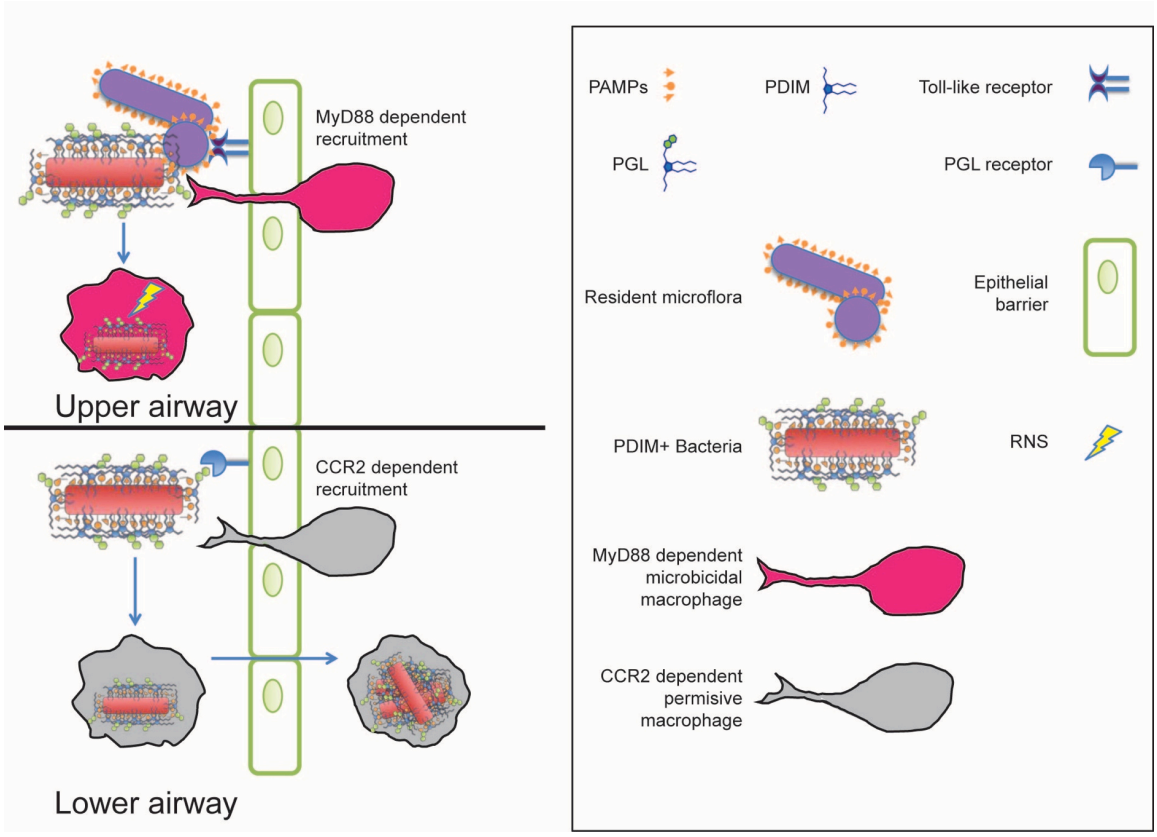

Figure 1.2: *M. tuberculosis* evades commensal bacteria to infect its host. *M. tuberculosis* avoids the recruitment of microbicidal macrophages to the site of infection by masking its PAMPs with the PDIM lipid. A related surface lipid PGL recruits permissive macrophages that can transport the bacteria into deeper tissues. However, the upper airways are colonized by resident microorganisms whose PAMPs recruit microbicidal macrophages. Therefore this mycobacterial strategy to evade microbicidal macrophages is only effective if infection is initiated in the relatively sterile lower lung.

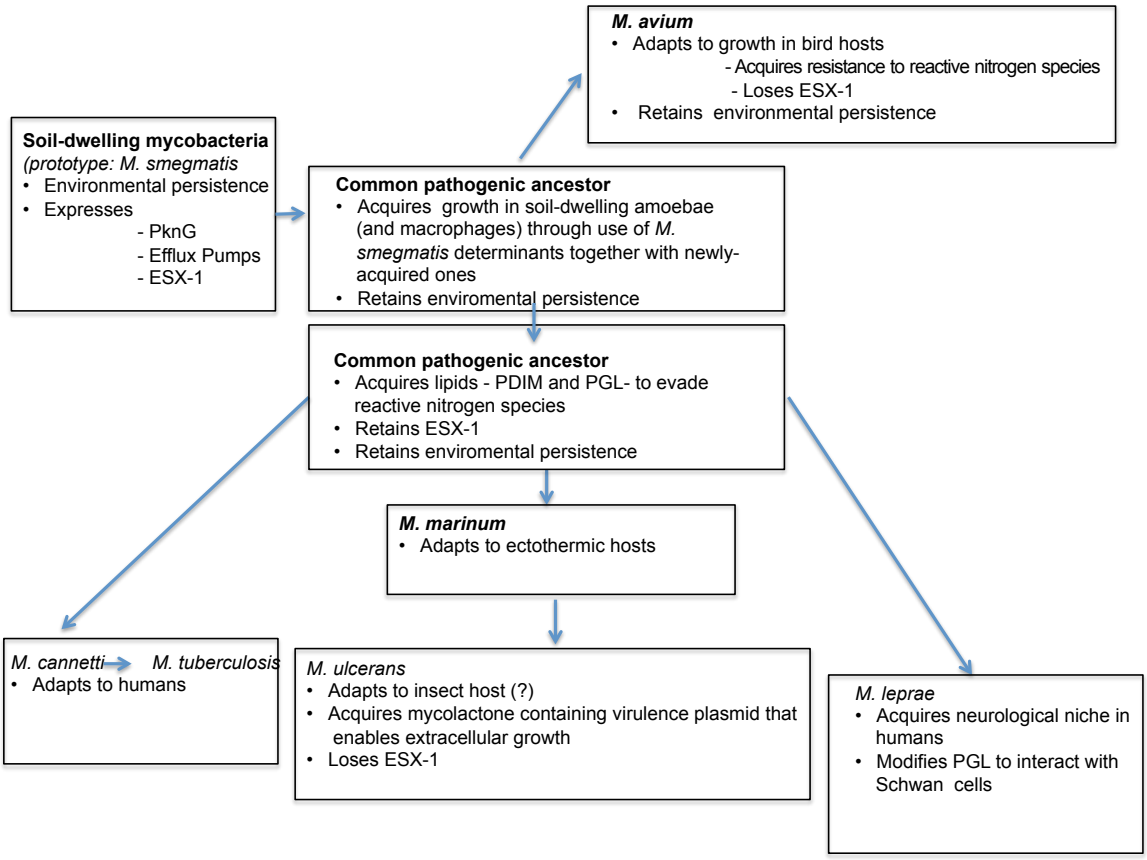

Figure 1.3: An evolutionary perspective of mycobacterial pathogenicity. An analysis of the pathogenic traits and preferred hosts of diverse mycobacterial species in relation to their genomes.

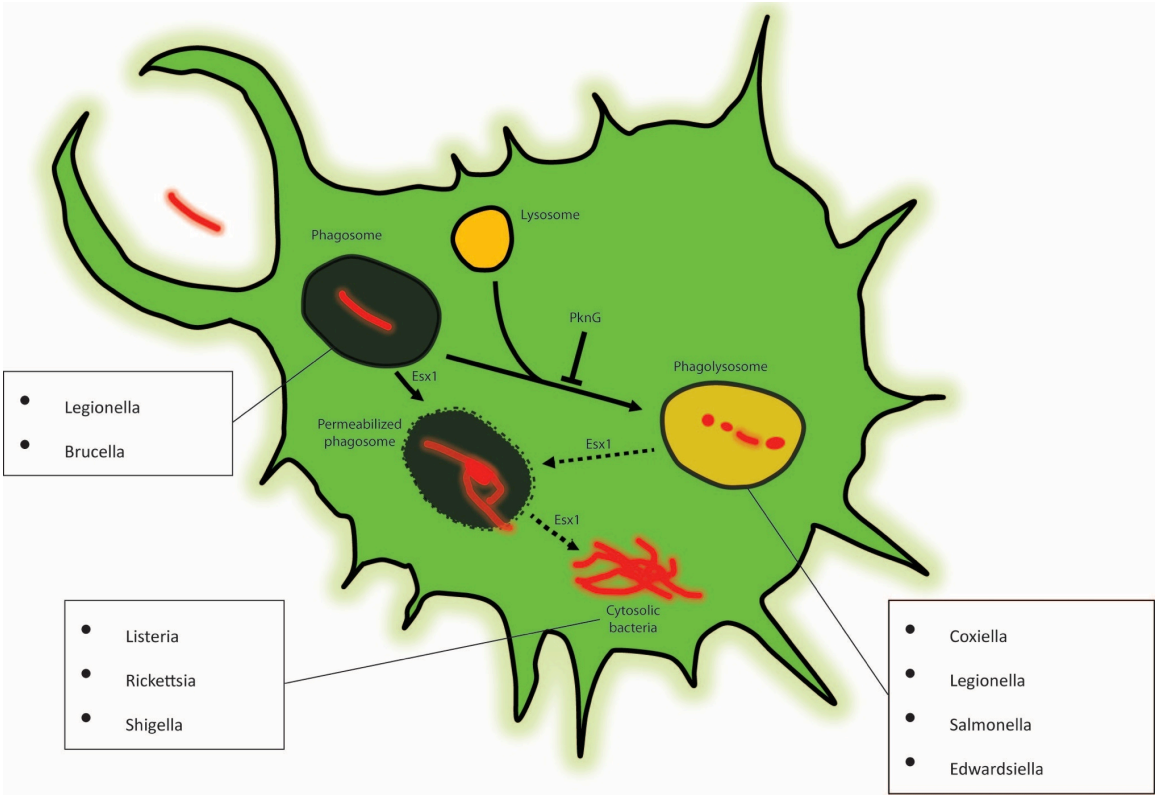

Figure 1.4: Intracellular niches of *M. tuberculosis.* The observed intracellular niches of M. tuberculosis within macrophages are shown with other pathogens occupying those niches indicated in connected boxes. Confirmed trafficking pathways are indicated with continuous arrows and putative ones with dashed arrows. Pathways dependent on the mycobacterial ESX1 secretion system are indicated.

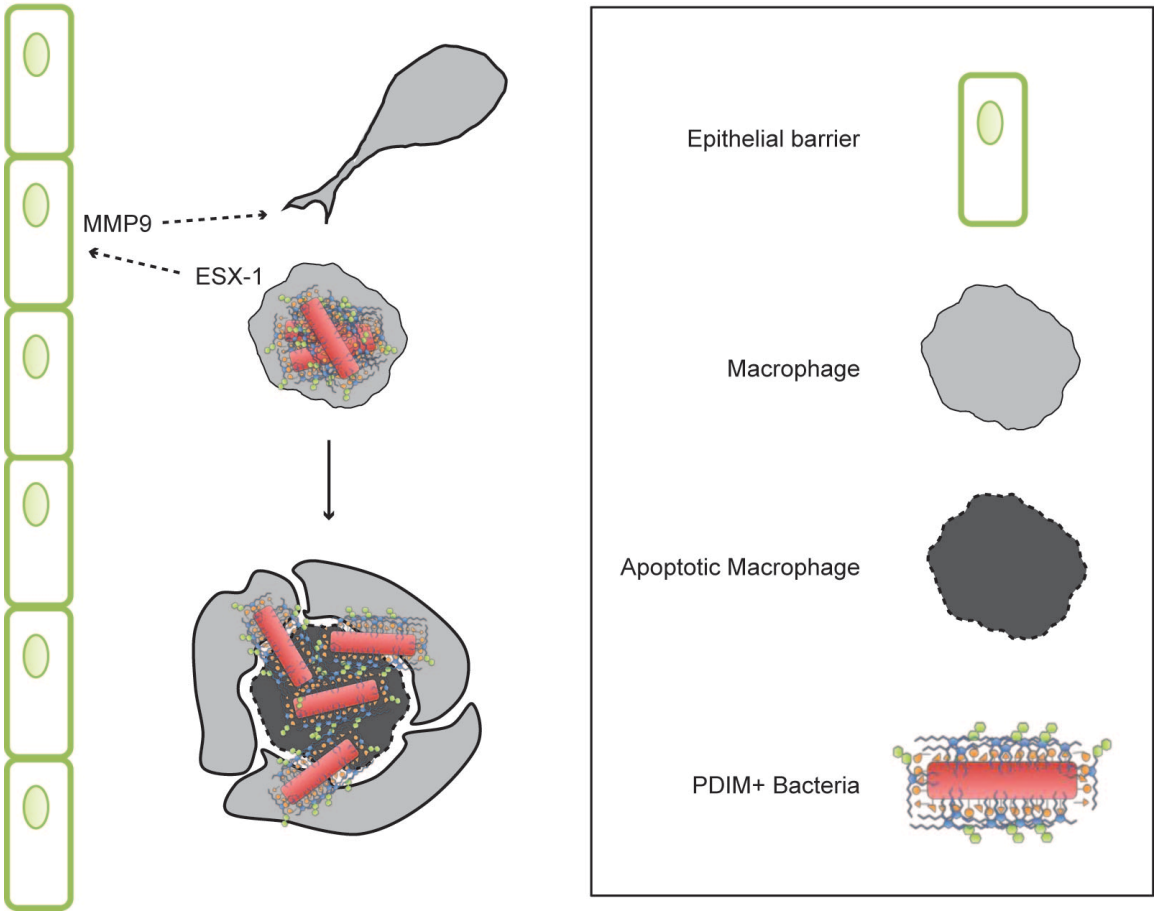

Figure 1.5: Mycobacteria exploit the granuloma to expand their numbers in early infection. Mycobacteria within infected macrophages induce, in an ESX1-dependent fashion, MMP9 expression in epithelial cells surrounding the nascent granuloma. MMP9 stimulates the recruitment of new macrophages to the granuloma. Multiple new arrivals phagocytose the bacterial contents of a given dying infected macrophage, thus spreading the bacteria to new macrophages and providing them new expansion niches.

Chapter 2: Neutrophils Exert Protection in the Early Tuberculous Granuloma by Oxidative Killing of Mycobacteria Phagocytosed From Infected Macrophages

SUMMARY

Neutrophils are typically the first responders in host defense against invading pathogens, which they destroy by both oxidative and nonoxidative mechanisms. However, despite a longstanding recognition of neutrophil presence at disease sites in tuberculosis, their role in defense against mycobacteria is unclear. Here we exploit the genetic tractability and optical transparency of zebrafish to monitor neutrophil behavior and its consequences during infection with *Mycobacterium marinum,* a natural fish pathogen. In contrast to macrophages, neutrophils do not interact with mycobacteria at initial infection sites. Neutrophils are subsequently recruited to the nascent granuloma in response to signals from dying infected macrophages within the granuloma, which they phagocytose. Some neutrophils then rapidly kill the internalized mycobacteria through NADPH oxidase-dependent mechanisms. Our results provide a mechanistic link to the observed patterns of neutrophils in human tuberculous granulomas and the susceptibility of humans with chronic granulomatous disease to mycobacterial infection.

INTRODUCTION

The crucial importance of neutrophils in host defenses is highlighted by the extreme susceptibility of patients with congenital or drug-induced neutropenia to a variety of bacterial and fungal infection (Amulic et al., 2012). These highly motile cells are rapidly recruited to infection sites and can destroy invading pathogens by both oxidative and nonoxidative mechanisms, whether through phagocytosis of the microorganisms themselves or through extracellular release of microbicidal granules (Amulic et al., 2012). In mycobacterial infections, the role of neutrophils remains poorly understood, despite a longstanding recognition of their presence at disease sites in tuberculosis (TB), for example in the cerebrospinal fluid of TB meningitis patients (Lowe et al., 2012; Thwaites et al., 2002). In the most common pulmonary form of TB, infected neutrophils are present together with the predominant macrophages, both in newly forming granulomas and in advanced cavitary lesions (Eum et al., 2010; Canetti, 1955), and a neutrophil-driven transcriptional signature has been identified in the blood of TB patients (Berry et al., 2010).

Studies on the mycobactericidal capacity of isolated human neutrophils are conflicting, perhaps because of the inherent variability of these terminally differentiated, short-lived cells in culture (Lowe et al., 2012). Some found that they kill *Mycobacterium tuberculosis* (Brown et al., 1987; Jones et al., 1990; Kisich et al., 2002), while others reported no effect (Corleis et al., 2012; Reyes-Ruvalcaba et al., 2008). Animal models have also yielded conflicting results. While earlier work identified a protective role for neutrophils in early infection (Pedrosa et al., 2000; Sugawara et al., 2004), recent work has focused on their pathological role, particularly with excessive neutrophil accumulation in advanced infection (Desvignes and Ernst, 2009; Eruslanov et al., 2005; Nandi and Behar, 2011).

Zebrafish larvae infected with their natural pathogen *Mycobacterium marinum,* a close genetic relative of *M. tuberculosis,* have proved a useful and relevant model for the mechanistic dissection of human TB (Tobin et al., 2012; Tobin et al., 2010; Volkman et al., 2010). Their genetic tractability and optical transparency have allowed dissection of mycobacterium-macrophage interactions not amenable in traditional animal models (Clay et al., 2007; Davis et al., 2002; Davis and Ramakrishnan, 2009). Here, we have sought to understand the role of neutrophils in mycobacterial infection using a zebrafish transgenic line with fluorescently labeled neutrophils (Hall et al., 2007). We show that zebrafish larval neutrophils share functional characteristics with human neutrophils and are rapidly recruited to *Pseudomonas aeruginosa,* against which they exert full protection. In contrast, they are rarely recruited to initial sites of Mm infection and even the few that are, seldom get infected. Neutrophil interactions with mycobacteria are initiated only when granulomas form. Signals from dead or dying granuloma macrophages recruit neutrophils, which then phagocytose infected macrophages. Using genetically engineered neutropenic zebrafish and zebrafish deficient in phagocytic oxidase activity, we show that neutrophils exert a protective effect through oxidative killing of the mycobacteria they phagocytose from dead granuloma macrophages.

RESULTS

Zebrafish lyz:EGFP *transgene specifically labels neutrophils*

lyz, encoding zebrafish lysozyme C, marks both neutrophils and macrophages at 32 hours post fertilization (hpf); at this developmental stage of exclusively primitive hematopoiesis from the yolk area, it is co-expressed with both the neutrophil-specific marker *myeloperoxidase* (*mpx*) and the macrophage-specific *csf1 receptor* (*fms*) (Figure 2.1A) (Herbomel et al., 1999; Liu and

Wen, 2002). Accordingly, zebrafish fluorescent transgenic lines using the *lyz* promoter were thought to label both phagocyte lineages (Hall et al., 2007). However, by 48 hpf when the site of hematopoiesis switches over to the caudal hematopoietic tissue (CHT) (Murayama et al., 2006), multiple lines of evidence led us to conclude that *lyz* exclusively marks neutrophils: 1) high resolution differential interference contrast (DIC) microscopy of the Tg*(lyz:EGFP)*^{nz117} (lyz-green) line showed that the GFP-positive cells contain the distinctive small motile granules specific for teleost neutrophils (Le Guyader et al., 2008)(Figure 2.1B), 2) the neutrophil-specific dye Sudan Black stained only and all GFP-positive cells in this line (Figure 2.1C) (Le Guyader et al., 2008), 3) in a double transgenic line, Tg*(lyz:DsRED2)*^{nz50} (lyz-red) and Tg*(mpx:GFP)*^{i114} (rendering neutrophils green fluorescent), all red fluorescent, lyz-expressing cells also expressed GFP (Renshaw et al., 2006)(Figure 2.1D), 4) in the lyz-green line, the GFP-positive cells did not stain with neutral red, a macrophage-specific dye (Figure 2.1E) (Herbomel et al., 1999)and 5) in the lyz-green line, whole mount in situ hybridization (WISH) revealed no overlap in macrophage-specific marker *fms* RNA expression and anti-GFP antibody staining (Figure 2.1F). Thus, the *lyz* promoter is a reliable and specific marker for neutrophils in zebrafish larvae from 48 hpf on. The combination of DIC and fluorescence microscopy using the *lyz* fluorescent lines allows the visualization of both neutrophils and macrophages as illustrated in Figure 2.1E.

Zebrafish larval neutrophils and macrophages respond to distinct signals

In zebrafish larvae, neutrophil migration to the ear and macrophage migration to the hindbrain ventricle (HBV) in response to injected compounds or bacteria can be readily assessed (Tobin et al., 2010). Using these two phagocyte recruitment assays, we found that recombinant human interleukin 8 (IL-8 or CXCL8), a neutrophil-specific chemotactic cytokine (Stillie et al.,

2009), recruited neutrophils but not macrophages (Figure 2.1G and 2.1H). In contrast, human leukotriene B_4 (LTB_4) recruited neutrophils and macrophages, consistent with its activity as a dual neutrophil and macrophage chemoattractant in humans (Crooks and Stockley, 1998)(Figure 2.1G and 2.1H). Finally, the synthetic N-formylated peptide N-formyl-methionine-leucine-phenylalanine (fMLP), a potent neutrophil chemoattractant (Schiffmann et al., 1975), recruited neutrophils but not macrophages (Figure 2.1I and 2.1J). Neutrophil recruitment by fMLP was abolished by modified antisense oligonucleotide (morpholino) knockdown of its predicted receptor (*formyl peptide receptor 1*) (Williams et al., 1977) while leaving baseline macrophage recruitment unchanged (Figure 2.1I and 2.1J). These findings suggest functional conservation of neutrophil chemotaxis between zebrafish and humans, and that larval zebrafish neutrophils and macrophages already have distinct chemotactic responses.

Neutrophils do not interact with Mm at initial sites of infection.

Previously we had observed very few infected neutrophils at 1 day post infection (dpi) into the caudal vein upon staining infected larvae with an Mpx antibody (Clay et al., 2007). This finding suggests either that neutrophils do not phagocytose mycobacteria or that neutrophils destroy mycobacteria rapidly upon phagocytosis. To distinguish between these possibilities, we injected red fluorescent Mm into the caudal vein of 48 hpf lyz-GFP line and monitored infection serially by DIC and fluorescence microscopy. At 10 minutes post infection, we observed several infected macrophages but no infected neutrophils (Figure 2.2A). Again at one-hour post infection (hpi), no infected neutrophils were found despite many uninfected neutrophils being clustered around the injection site, probably reflecting its proximity to the CHT site of their origin (Figure 2.2B) (Hall et al., 2007). To rule out the possibility that zebrafish neutrophils are

developmentally immature at 48hpf, similar experiments were conducted in 5 dpf larvae and no infected neutrophils were observed at 1 dpi (Supplementary Figure 2.1A). Thus, neutrophils do not phagocytose extracellular mycobacteria, even when in close proximity.

Mycobacterial infection is characterized by rapid macrophage recruitment (Dannenberg, 1993); in the zebrafish larva, phagocyte recruitment is readily observed by injection of bacteria into the HBV (Figure 2.1A), a site that is normally devoid of phagocytes (Clay et al., 2007). Injection of red fluorescent Mm into the HBV of 48 hpf lyz-green fish consistently produced a significant influx of macrophages, but not neutrophils (Figure 2.2C). In contrast, Pa, a pathogen that interacts with both neutrophils and macrophages in humans and zebrafish (Brannon et al., 2009; Cheung et al., 2000; Lyczak et al., 2000), recruited similar numbers of both cell types (Figure 2.2D). In the rare case where a few neutrophils were recruited to the HBV following Mm infection, only macrophages were infected (Figure 2.2E). This finding is consistent with our observations during caudal vein infection (Figure 2.2A). In contrast, both neutrophils and macrophages became infected with Pa (Figure 2.2E). The differential phagocytic capacity of macrophages and neutrophils for Mm was further highlighted in time-lapse DIC images showing a macrophage actively moving towards and phagocytosing Mm in the HBV (Movie S1A); in contrast the few neutrophils arriving in the HBV did not interact with Mm even when in close proximity; they continued their rapid migration past the bacteria (Movie S1B).

We explored the possibility that mycobacteria actively inhibit neutrophil recruitment. If so, the presence of Mm should reduce neutrophil migration to Pa. However, neutrophil recruitment in response to co-injection of Mm and Pa into the HBV was indistinguishable from Pa infection alone (Figure 2.2F). Strikingly, the recruited neutrophils did not phagocytose Mm even while retaining their capacity to phagocytose Pa (Figure 2.2G and 2.2H).

In vitro, complement-mediated opsonization of mycobacteria increases their phagocytosis by neutrophils (Jones et al., 1990; Majeed et al., 1998). We asked if complement opsonization facilitated the phagocytosis of Mm by the neutrophils brought into proximity to the mycobacteria by co-infection with Pa. Opsonization with fetal bovine serum or fresh adult zebrafish serum did not increase neutrophil phagocytosis of Mm (Supplementary Figure 2.1B –2.1E). In sum, mycobacteria appear to be invisible to neutrophils in terms of both chemotaxis and phagocytosis.

Neutrophils become infected in early granulomas through phagocytosis of infected macrophages

While no infected neutrophils were observed at the initial infection site, serial monitoring of infection in the lyz-green larvae consistently revealed infected neutrophils within the granulomas that form by 2-4 dpi (Figure 2.3A and 2.3B)(Davis et al., 2002). High-resolution spinning disc confocal microscopy of individual granulomas over two hours showed uninfected neutrophils trafficking into granulomas and moving rapidly amongst its infected macrophages (Figure 2.3C and 2.3D). Many interacted closely with infected macrophages that were static, therefore probably dying (Davis and Ramakrishnan, 2009), and eventually engulfed their bacterial contents (Figure 2.3C and 2.3E). We also observed neutrophils that migrated through the granuloma and left without becoming infected. Since most granuloma neutrophils at any given time were infected (Figure 2.3A), infected neutrophils may be preferentially retained within these structures. In sum, neutrophils arriving in the granuloma become infected through phagocytosis of dying infected macrophages, similar to newly arriving macrophages (Davis and Ramakrishnan, 2009).

Neutrophil recruitment into granulomas is mediated by cell death signals from infected macrophages

Why might neutrophils be attracted to *Mycobacterium*-containing granulomas but not directly to the infecting mycobacteria? We observed that the number of infected neutrophils increased with granuloma size (Figure 2.4A), representing a constant proportion of the total number of infected cells (15-18%), and of the total bacterial volume in granulomas over a range of sizes (1.27 +/- 0.12 $x10^{-4}$ / mm^3). Given that larger granulomas contain more dying infected macrophages, we wondered if these were providing the signals for neutrophil recruitment. To test this possibility, we infected fish with Mm that lack the RD1 locus (*Δrd1)*, one of whose encoded secreted proteins, ESAT-6 promotes the apoptotic death of macrophages (Davis and Ramakrishnan, 2009; Derrick and Morris, 2007; Volkman et al., 2004). Owing to its reduced ability to form granulomas, 5-fold more *Δrd1* bacteria were required to create similar sized granulomas to wildtype (WT) (Davis et al., 2002). A 4.5-fold reduction of recruited neutrophils in *Δrd1* was accompanied by a 5.2-fold reduction of infected neutrophils within them (Figure 2.4B and 2.4C and Supplementary Figure 2.2A). In contrast, granulomas formed by an Mm mutant defective in the secreted protein Erp that specifically mediates intramacrophage mycobacterial growth (Clay et al., 2007; Cosma et al., 2006), had no reduction in infected neutrophils despite being slightly smaller (Supplementary Figure 2.2B and 2.2C). Together, these results suggested that neutrophils respond to signals emanating from dead cells in granulomas. To test this directly, we treated Mm-infected larvae with Q-VD-OPH, a pan-caspase inhibitor that blocks apoptosis in zebrafish (Walters et al., 2009). Q-VD-OPH treatment produced a 7.2-fold reduction in the number of TUNEL (terminal deoxynucleotidyl transferase dUTP nick end labeling)-positive cells (Figure 2.4D). Q-VD-OPH-treated fish had a 3.5-fold

reduction in neutrophil recruitment to granulomas corresponding to a similar (3.7-fold) reduction in infected granuloma neutrophils (Figure 2.4E and 2.4F, and Supplementary Figure 2.2D). Thus signals from dying macrophages appear to recruit neutrophils.

Neutrophils play a protective role in the early granuloma

We next asked if neutrophil recruitment to granulomas influences the course of infection. We took advantage of the zebrafish WHIM transgenic line, Tg(-*8mpx:cxcr4.1-EGFP)*^{uwm3} developed to model the human WHIM (warts, hypogammaglobulinemia, infections, and myelokathexis) syndrome caused by mutations in the neutrophil chemokine receptor, CXCR4, and characterized by chronic neutropenia owing to neutrophil retention in the hematopoietic tissues (Walters et al., 2010). In the zebrafish WHIM line, a mutated zebrafish *cxcr4* is under control of the *mpx* promoter. Its neutrophils are retained in the CHT and pronephros, and neutrophil migration to wound sites is impaired (Figure 2.5A and 2.5B) (Walters et al., 2010).

We found WHIM fish to display the expected neutrophil migration defect in response to Pa infection: HBV infection of 48 hpf fish revealed a drastic reduction in neutrophil recruitment that resulted in increased susceptibility of these animals (Supplementary Figure 2.3A and 2.3B). Only neutrophil migration was defective; macrophage migration to both Pa and to Mm was normal (Supplementary Figure 2.3A and 2.3C).

WHIM granulomas created by HBV injection had 4-fold fewer infected neutrophils than WT (Figure 2.5C-2.5E), accompanied by a 1.7-fold increase in bacterial burdens (Figure 2.5C, 2.5D and 2.5F). This increased bacterial burden in individual WHIM granulomas was confirmed at the whole animal level by injection of Mm into the caudal vein. An increase in bacterial burdens in the WHIM fish became apparent at 2 dpi coincident with granuloma formation and

progressed to a 2.3 fold difference at 5 dpi (Figure 2.5G). These results confirm a protective effect of neutrophils during early infection, which is temporally linked to the granuloma formation that allows them access to the mycobacteria.

A subpopulation of neutrophils can kill their phagocytosed mycobacteria

The most parsimonious explanation for our findings was that granuloma neutrophils directly kill the bacterial contents of the macrophages they phagocytose. To determine if this was the case, we first characterized the motility dynamics of infected neutrophils by real-time, high resolution imaging at 3-5 minute intervals over 5-8 hours. Two discrete populations were discerned based on velocity, 80% were relatively nonmotile (speed < 0.01mM/second) and 20% moved through the granuloma at speeds comparable to infected macrophages (mean speed 0.026 mM/second) (Davis and Ramakrishnan, 2009). Representative motile and nonmotile cells are shown in Figure 2.6A. The nonmotile cells were more spherical, as a consequence of being more highly infected than the motile cells (Figure 2.6B and 2.6C); this relationship is exemplified in Figure 2.3B. The inverse correlation between motility and infection level has also been observed for granuloma macrophages (Davis and Ramakrishnan, 2009). These findings posed the following questions: does the progression of infection reduce the motility of all neutrophils so that infected motile cells all progress to become heavily infected, nonmotile cells? Alternatively, do the less infected cells represent a discrete subset of neutrophils with increased mycobactericidal activity?

To address these questions, we quantified neutrophil bacterial burdens every 3-5 minutes for at least one hour. In the motile neutrophils, there was a reduction in intracellular bacterial fluorescence over time, indicative of bacterial killing; the example in Figure 2.6D and 2.6E

shows a 50% reduction in bacterial fluorescence over 50 minutes. Furthermore, motile neutrophils could phagocytose and kill bacteria multiple times as exemplified in Figure 2.6F and 2.6G. From the time it was first visualized, the bacterial fluorescence inside this neutrophil decreased over the first 30 minutes. While in the process of killing its intracellular bacteria, this neutrophil moved into close proximity to an infected macrophage forming membrane protrusions that wrapped around it (Figure 2.6F, 30 minute time point). After the resolution of the tethering between the infected neutrophil and macrophage, we observed increased bacteria in the neutrophil (Figure 2.6F, 40 minutes). A second close encounter with the same infected macrophage at 55 minutes resulted in another increase in bacterial fluorescence at 60 minutes, followed by a 60% decrease at 85 minutes.

Only motile infected neutrophils appeared to have this microbicidal capacity. The nonmotile cells did not kill their bacteria over a seven-hour observation period and even appeared to support intracellular bacterial replication (Supplementary Figure 2.4 and data not shown). Thus, a minority of neutrophils can kill mycobacteria effectively through repeated rounds of phagocytosis.

Neutrophils kill intracellular mycobacteria through oxidative mechanisms

To determine if neutrophils depend on the production of reactive oxygen species (ROS) to kill their internalized mycobacteria, we used morpholino knockdowns to create larvae doubly deficient in two key subunits of NADPH oxidase, *gp91*^{phox} and *p22*^{phox} (Niethammer et al., 2009). These *phox* morphants exhibited the expected increase in susceptibility to Pa infection (Supplementary Figure 2.5A) (Speert et al., 1994). With Mm, similar numbers of infected neutrophils were present in *phox* morphant and WT granulomas, suggesting that recruitment and

phagocytosis were unaffected (Supplementary Figure 2.5B). However, the morphant neutrophils had a greatly reduced capacity to kill their internalized mycobacteria (Figure 2.7A-2.7C). Thus, neutrophils appear to play a protective role by intracellular killing through NADPH-dependent mechanisms.

DISCUSSION

From early in development, zebrafish have functionally mature neutrophils that share several key characteristics with adult human neutrophils. They are highly motile and exhibit the expected specific responses to chemotactic signals. They are recruited to Pa infection, against which they protect by oxidative killing. Thus validating the zebrafish larval model for the study of neutrophils, we have explored their role in mycobacterial infection. We find that, like many other serious human pathogens, mycobacteria initially evade neutrophil phagocytic mechanisms. However, tuberculous granuloma formation later circumvents this mycobacterial evasion strategy by cloaking the pathogen within macrophages. Signals from dying granuloma macrophages appear to beckon neutrophils, which upon arrival can collect mycobacteria from macrophages by phagocytosis and kill them by oxidative mechanisms.

The mechanism of neutrophil function in granulomas revealed here provides a possible explanation for longstanding observations of the susceptibility of chronic granulomatous disease (CGD) patients to mycobacterial infection. CGD is characterized by decreased respiratory burst production owing to genetic deficiencies in phagocytic NADPH oxidase (Amulic et al., 2012). Along with well-documented susceptibilities to other catalase-producing organisms, susceptibility to TB in highly endemic areas has been documented (Doğru et al., 2010; Lee et al., 2008), and is likely underreported given the improbability of diagnosing CGD in these areas. What is striking is the widely documented susceptibility of CGD sufferers to disseminated disease following vaccination with the live attenuated Bacille Calmette Guerin (BCG) strain, derived from *Mycobacterium bovis* (Movahedi et al., 2003; Reichenbach et al., 2001). BCG lacks the RD1 locus and we find that granulomas formed by RD1-deficient bacteria recruit fewer neutrophils, presumably because they contain fewer dead macrophages. Given the convincing

role of an intact phagosomal oxidase in human BCG infection, we speculate that even the fewer neutrophils in RD1 mutant granulomas are capable of clinically significant mycobacterial killing.

How do our findings relate to the published findings on neutophils in TB? While recent studies have focused on the pathological role caused by excessive neutrophil accumulation in late disease (Desvignes and Ernst, 2009; Nandi and Behar, 2011), some older work supports our finding of an early protective role for them (Martineau et al., 2007; Pedrosa et al., 2000). Several in vitro and in vivo models have been proposed for the protective mechanism of neutrophils during mycobacterial infection. Collectively these models attribute the beneficial nature of neutrophils to their indirect enhancement of macrophage microbicidal activity, either via cytokine production or by macrophages acquiring neutrophilic granules upon phagocytosis of apoptotic neutrophils (Silva et al., 1989; Tan et al., 2006). These models are based on indirect or in vitro evidence and our observations do not rule them out as additional mechanisms of protection by neutrophils. Importantly, our results suggest direct oxidative killing as a substantial protective mechanism.

Then, contrary to our findings, direct phagocytosis of mycobacteria by mammalian neutrophils has been reported. Many of these studies used isolated neutrophils (Majeed et al., 1998; Persson et al., 2008), or animals with high infection doses that may not represent the low bacterial numbers thought to result in human infection (Abadie et al., 2005). In the zebrafish too, we found that very high inocula (> 250 bacteria per animal) did produce a low level of direct neutrophil infection, < 5% of the total infected phagocytes at the initial infection site. Conversely, with low infection doses in mice, the earliest infected neutrophils were observed only at 2 weeks post infection (Pedrosa et al., 2000; Tsai et al., 2006). Importantly, our data are in accordance with extensive observations of tuberculous lesions in the human lung, where

neutrophils were seldom found to be directly infected, except after what appeared to be an unusually high inoculum that produced tuberculous bronchopneumonia (Canetti, 1955).

Our findings place mycobacteria among the group of notorious pathogens that cause severe systemic disease, particularly meningitis, by evading neutrophil phagocytosis at least partially (Tunkel and Scheld, 1993). These organisms often use their capsule or the functional capsular equivalents in their cell wall to avoid phagocytosis, and mycobacterium may similarly employ one or multiple components of its complex cell wall (Brennan, 2003).

Finally our data suggest a role for neutrophils as macrophage scavengers, a reversal of the well-recognized arrangement in which macrophages act as scavengers that efficiently remove apoptotic neutrophils and cell debris to resolve inflammation (Amulic et al., 2012; Mosser and Edwards, 2008; Serhan, 2007). Previous studies in a lipopolysaccharide-induced lung inflammation model in the mouse have reported a similar scavenger behavior of neutrophils and proposed it as a back-up mechanism when the scavenging capacity of macrophages is insufficient (Rydell-Törmänen et al., 2006). While our data suggest that caspase-mediated cell death recruits neutrophils, the precise viability status of the cells phagocytosed by neutrophils awaits deeper examination.

A teleological consideration of our findings may serve as a useful perspective on the host-mycobacterium interface. Mycobacteria may have evolved to avoid neutrophils while possessing multiple mechanisms to gain macrophage entry (Ernst, 1998). The macrophage may provide mycobacteria a safe haven, sheltering them from other immune cells, while transporting them into deeper tissues, potentially as a means to minimize competition with mucosal organisms (Clay et al., 2007). Once within the host tissues, mycobacteria additionally benefit from inducing macrophage death and recruitment to promote granuloma expansion through

phagocytosis of dead macrophages by multiple newly arriving ones (Davis and Ramakrishnan, 2009). However, macrophage death—the very mechanism mycobacteria use to promote their expansion in granulomas—also causes neutrophil recruitment that results in mycobacterial killing. Identification of mycobacterial neutrophil evasion strategies should be of interest and may be useful in the context of vaccination strategies. Moreover, in terms of therapeutic strategies, further investigation is warranted into how the dichotomous mycobactericidal capacity of granuloma neutrophils can be tipped to favor the host.

METHODS

Zebrafish and bacterial strains

The wild-type zebrafish AB line from the Zebrafish International Resource Center (ZIRC), along with transgenic lines, Tg(*lyz:EFGP*)^{nz117}, Tg(*lyz:DsRED2*)^{nz50}, Tg(*mpx:GFP*)^{i114}, and Tg(*-8mpx:cxcr4.1-EGFP)*^{uwm3} (Hall et al., 2007; Renshaw et al., 2006; Walters et al., 2010) were maintained, infected and imaged as described (Cosma et al., 2006). Fluorescent derivatives of Mm strain M (ATCC #BAA-535) and mutants derived from it were used (Clay et al., 2008; Cosma et al., 2006). Pa PAO1 strain and the fluorescent derivatives used have been previously described (Brannon et al., 2009). Pa burdens were determined by plating lysed larvae for colony-forming units (CFU) and Mm burdens were determined by bacterial fluorescent pixel counts (FPC) in live animals (Adams et al., 2011).

Quantification of phagocyte recruitment and phagocytosis of bacteria

15-25 pg of IL-8 (rhIL-8, R&D Systems, Inc.), 5-15 pg of LTB_4 (Cayman Chemicals), 10-15 nl of 0.2 mM fMLP (Sigma) and/or specified bacterial doses were injected into the HBV of 44-52 hpf larvae. Six hours after injection, the identity and quantity of phagocytes and their infection status per larvae was determined using DIC and fluorescence microscopy on Nikon's Eclipse E600. Objectives used in this assay included 20x Plan Fluor 0.5 NA and 40x Plan Fluor 0.75 NA (Davis and Ramakrishnan, 2009).

Opsonization of bacteria

A mixture of Mm and Pa was incubated at room temperature for 20 minutes in 70% FBS (heat-inactivated at 56^{o}C for 30 minutes or not), or in 70% adult zebrafish serum. Zebrafish

adult serum was obtained using a protocol modified from (MacCarthy et al., 2008) as follows: blood was collected from the aorta of 8-12 month old adults using a capillary tube, transferred to a glass tube, allowed to clot at room temperature for 2 hours, and then incubated at 4^{o}C for 4 hours to contract the clot. Serum was collected by centrifugation.

Morpholino injection

Splice blocking morpholinos purchased from Gene Tools, LLC (Eugene, OR, USA) were injected into one to eight cell stage embryos and the efficacy of gene knockdown confirmed by reverse transcription polymerase chain reaction (RT-PCR). Morpholino concentrations that achieved maximal gene knockdown with low toxicity were chosen. The *fpr1* (XM_003200188) morpholino sequence is 5'- GATCCATCATTGTACCTTCAAACCT-3'. Morpholinos targeting zebrafish *gp91^{phox}* and *gp22^{phox}* were used as described (Niethammer et al., 2009).

Whole mount in situ hybridization and antibody staining

Whole-mount *in situ* hybridization (WISH) with the *fms* probe was combined with fluorescence detection of GFP with an anti-GFP antibody as described (Clay and Ramakrishnan, 2005; Clay et al., 2008).

Analysis of cellular dynamics of neutrophils in granulomas

For single time point static assessment of neutrophil recruitment to, and infection in, granulomas, lyz-green larvae infected with red fluorescent Mm were imbedded in 1% agarose (low melting point) for imaging (Davis and Ramakrishnan, 2009). A series of z-stack images with a 2.5 mm step size was generated of the granuloma, using the galvo scanner (laser scanner)

of the Nikon A1 confocal microscope with a 20x Plan Apo 0.75 NA objective. The size of the given granuloma was evaluated by its bacterial burden determined by the 3D surface rendering feature of Imaris (Bitplane Scientific Software).

Cellular dynamics of neutrophils in granulomas were monitored by time-lapse confocal imaging. A series of z-stack images with a 2.5 mm step size was taken at 3-5 minute intervals over 5-8 hours using the high-speed scanner (resonant scanner) with a 20x Plan Apo 0.75 NA objective. Neutrophils were tracked using the 3D-tracking feature and their bacterial burdens determined using the 3D surface rendering feature, both in Imaris.

Q-VD-OPH Treatment and TUNEL staining

Larvae were incubated for 24 hours in 50 mM of Q-VD-OPH (R&D Systems, Inc.) dissolved in DMSO or the corresponding concentration of 0.5% DMSO as a control (Walters et al., 2009)after which TUNEL staining was performed as described (Volkman et al., 2004).

STATISTICS

Statistical analyses were performed using Prism 5.01 (GraphPad).

Chapter 2 Figures

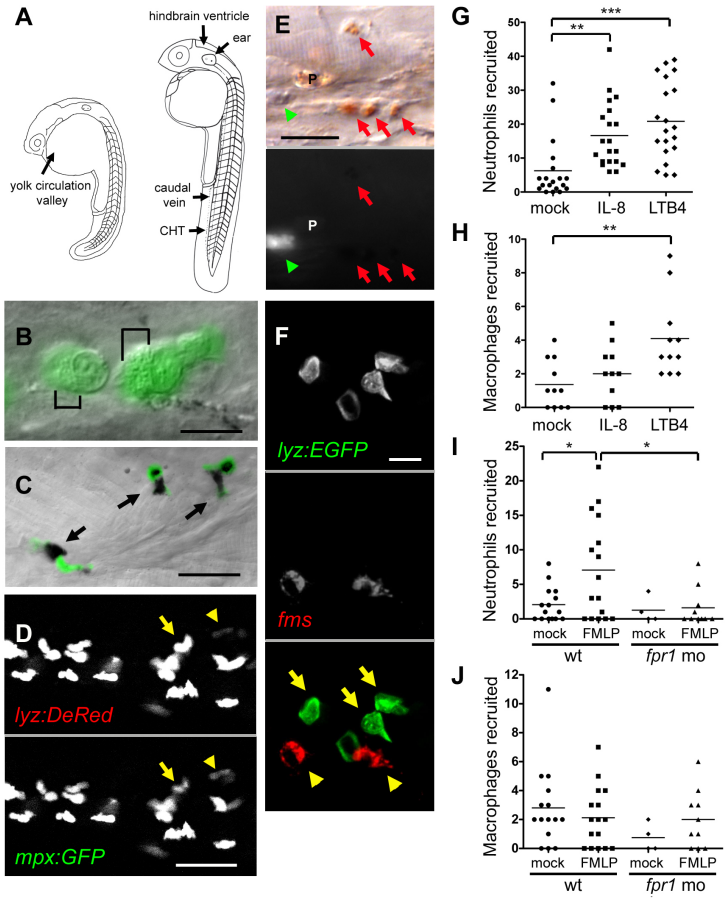

Figure 2.1: Zebrafish neutrophils are marked by GFP expression in the lyz-green line and are functionally similar to mammalian neutrophils

(A) Cartoon of the zebrafish at two developmental stages showing sites of primitive and definitive hematopoiesis (black arrows) and injection sites used in this study (red arrows). CHT: caudal hematopoietic tissue. (B) GFP positive cells in lyz-green fish showing well defined granules (black brackets). Scale bar, 10 mm. (C) Co-localization of GFP-expressing cells (black arrows) with Sudan Black. Scale bar, 20 mm. (D) Individual fluorescence channels of a single image of the lyz-red - mpx:gfp double transgenic larvae. Arrow identifies a cell with differential expression of the two transgenes. Scale bar, 20 mm. (E) DIC (top) and GFP fluorescence channel (bottom) of a single image of a lyz-green larva stained with neutral red. Macrophages, red arrows; neutrophil, green arrowhead; pigment cell, P. Scale bar, 20 mm. (F) Whole-mount *in situ* hybridization analysis of 48 hpf lyz-green larva with *fms* probe (red fluorescence) combined with GFP antibody staining (green fluorescence). Macrophages, yellow arrowheads; neutrophils, yellow arrows. Scale bar, 10 mm. (G-J) Median phagocyte recruitment into the ear (G) or hindbrain ventricle (HBV) (H-J) of 48 hpf larvae in response to injection of vehicle (mock), IL-8, LTB_4, or fMLP. In I and J, *fpr1* mo refers to larvae with morpholino knockdown of the *formyl peptide receptor 1*. Results in G-J representative of two experiments. Significance testing performed by Kruskal-Wallis test with Dunn's posttest in G-J. *$p < 0.05$; **$p < 0.01$; ***$p < 0.0001$.

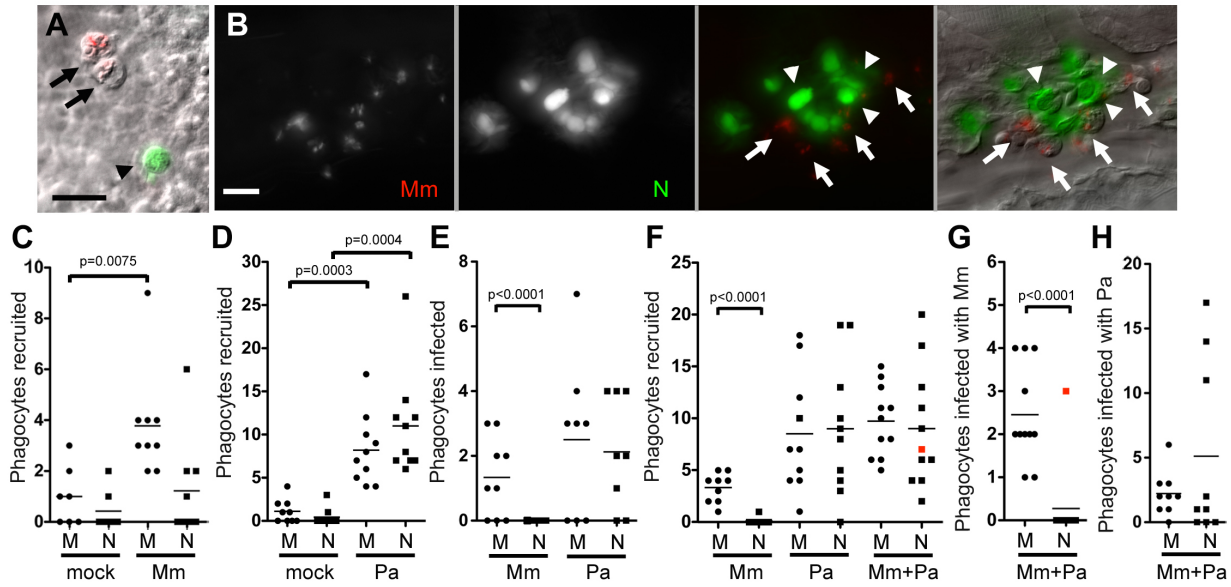

Figure 2.2: Neutrophils are poorly recruited to the initial site of mycobacterial infection and do not phagocytose mycobacteria

(A) Fluorescence and DIC overlay of macrophages infected with red fluorescent Mm, (arrows) and a green fluorescent neutrophil (arrowhead) 10 minutes after caudal vein injection of 48 hpf larva. Scale bar, 10 mm. (B) Infected macrophages (arrows) and uninfected neutrophils (arrowheads) 24 hours after Mm injection into caudal vein of 48 hpf larva. Scale bar, 20 mm. (C-H). Median number of phagocytes recruited to, and infected in, the HBV of 48 hpf larvae 6 hours post infection of vehicle (mock), (C) 108 Mm, (D) 45 Pa, (E) 108 Mm or 18 Pa, and (F-H) 27 Mm and 22 Pa together. M, macrophage, N, neutrophil. Results in C –H each representative of more than three experiments. p value determined by Mann-Whitney rank test. (Also see Supplementary Figure 2.1).

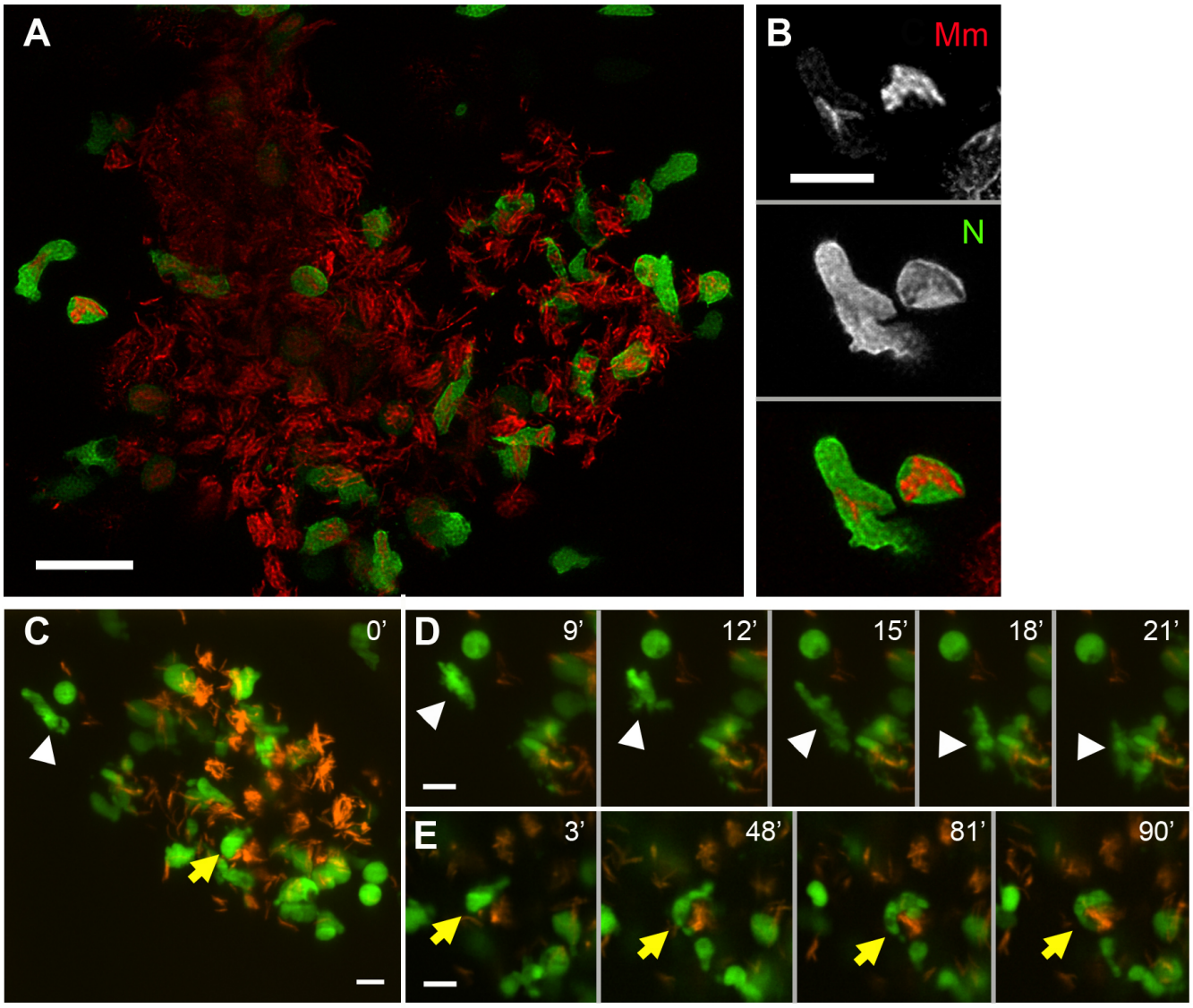

Figure 2.3: Neutrophils are present in the early granuloma
(A) High-resolution laser-scanning confocal image showing a mycobacterial granuloma containing uninfected and infected neutrophils. Scale bar, 20 mm. (B) Two GFP positive neutrophils infected with red fluorescent Mm from granuloma in A. Scale bar, 10 mm. (C-E) Series of time-lapse spinning disc confocal images highlighting cellular dynamics of neutrophils of the early granuloma. (C) A snapshot of a granuloma with the two neutrophils (arrowheads) monitored by time-lapse imaging. (D) Uninfected neutrophil (white arrowhead) arriving at the granuloma shown in (C). (E) Uninfected neutrophil (yellow arrowheads) engulfing infected macrophage to become infected. Elapsed minutes indicated in upper right corner of D and E. Green, neutrophil (N); red, Mm. Scale bars in C, D and E, 15 mm.

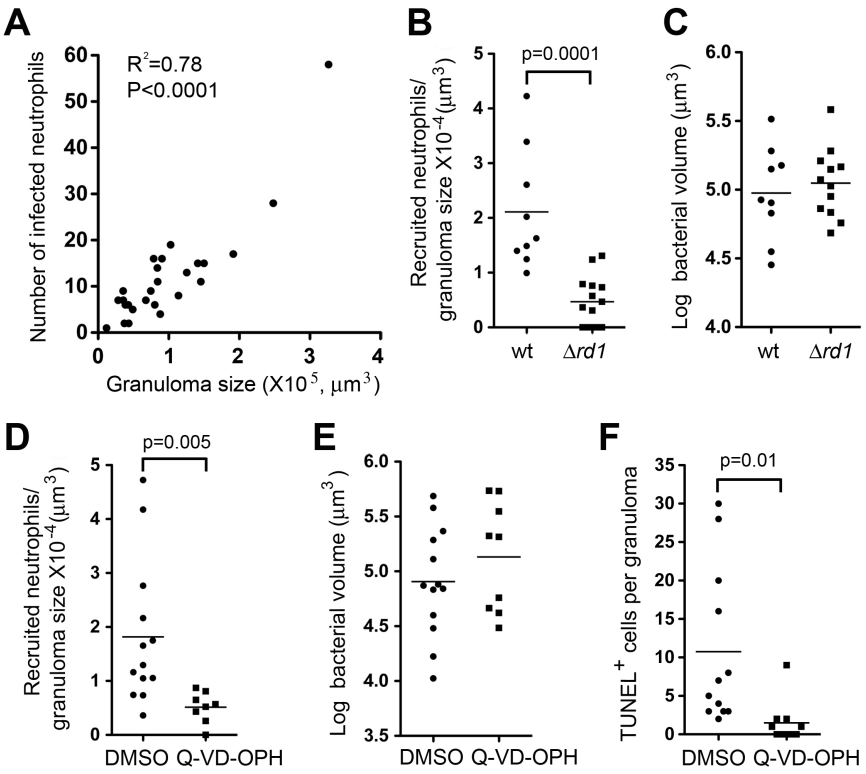

Figure 2.4: Neutrophil recruitment to granulomas is mediated by death signals
(A) Number of infected neutrophils in granuloma vs. granuloma size as determined by log bacterial volume (mm^3). $R^2 = 0.78$; two-tailed $p<0.0001$, Pearson correlation (B) Median neutrophils recruited to wild-type (from 9 animals) and D*rd1* Mm granulomas (from 12 larvae) in the HBV at 3 dpi, normalized to granuloma size. (C) Mean size of WT and D*rd1*Mm containing granulomas in B. Results in (B) and (C) representative of two experiments. (D) Median TUNEL+ cells in WT Mm containing granulomas treated with DMSO (vehicle control) or Q-VD-OPH, normalized to granuloma size, 9 larvae per treatment. (E) Median neutrophils recruited to granulomas in D, normalized to granuloma size. (F) Mean size of granulomas in D. Results in D-F representative of two experiments. Recruited neutrophils in (B) and (E) represent the sum of infected and uninfected neutrophils within or closely surrounding the granuloma. p value by Student's unpaired t test (B and E), and by Mann-Whitney rank test (B, D and E). Also see Supplementary Figure 2.2.

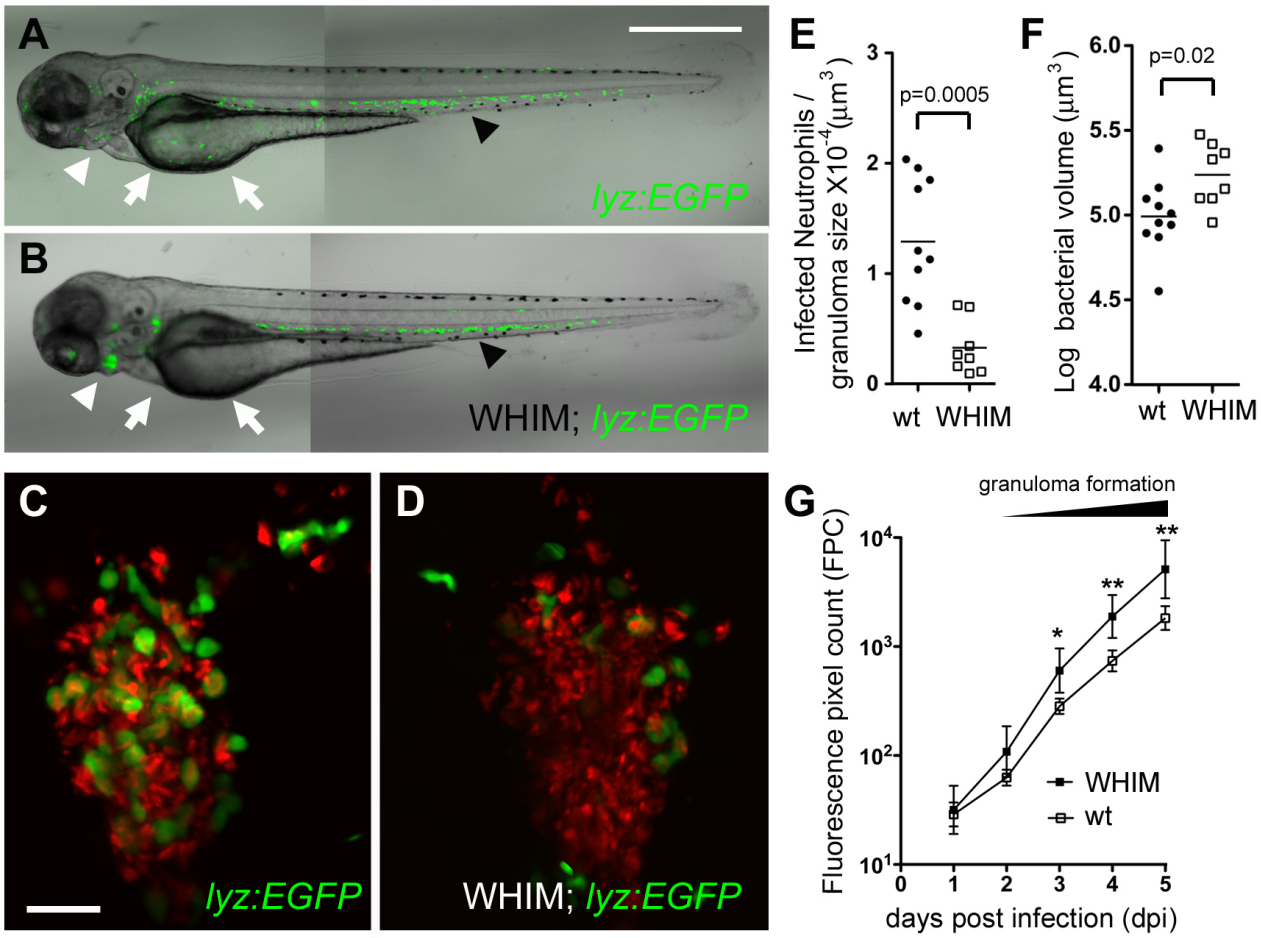

Figure 2.5: Neutrophils play a protective role upon granuloma formation
(A and B) Fluorescence and DIC overlay of 3 dpf WT (A) and WHIM (B) zebrafish showing neutrophil distribution. Arrows, yolk; white arrowheads, pronephros; black arrowheads, CHT. Scale bar, 300 mm. (C and D) High-resolution laser confocal images of representative 3 dpi granulomas in wild-type (C) and WHIM (D) larvae. Green, neutrophil (N), red, Mm. Scale bar, 30 mm. (E) Median infected neutrophils per granuloma, normalized to granuloma size. Granulomas were from 10 WT and 7 WHIM larvae. p value by Mann-Whitney rank test. (F) Mean size of granulomas in (E). p values determined by Student's unpaired t test. (G) Serial bacterial burdens (mean+/-SEM) of 2 dpf wild-type (n=13) or WHIM (n=10) fish infected by caudal vein with 189 Mm measured by fluorescent pixel count (FPC). Representative of three experiments. *p < 0.05; **p < 0.01. (one-way ANOVA with Bonferroni's multiple comparison test; all other comparisons not significant). Also see Supplementary Figure 2.3.

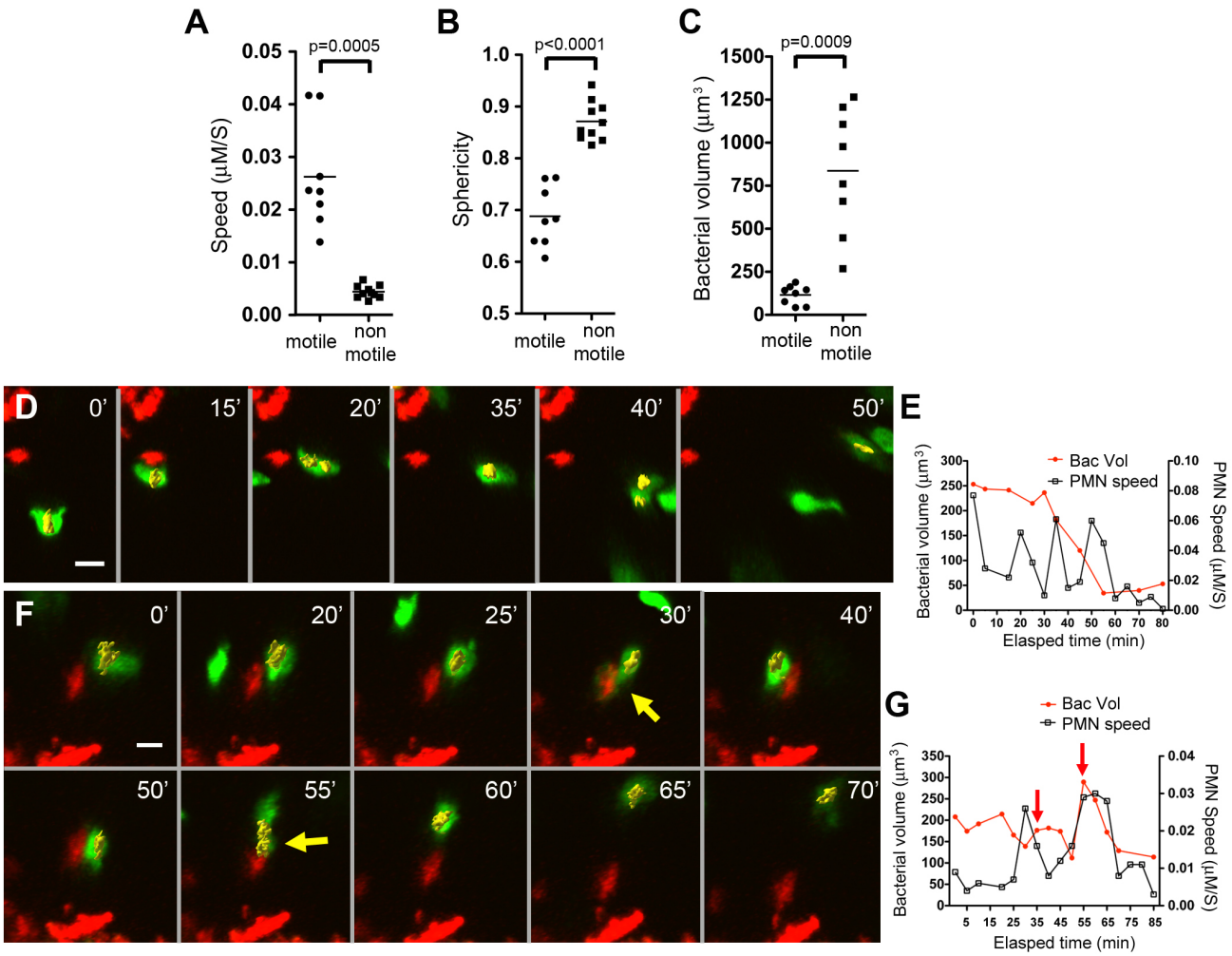

Figure 2.6: Neutrophils phagocytose and kill mycobacteria from infected granuloma macrophages.

(A-C) Mean speed (A), sphericity (B) and bacterial volume (C) of infected neutrophils in 3 dpi granulomas, sampled from 3 granulomas each from different larvae. p value by Student's unpaired t test (B) and by Student's unpaired t test with Welch's correction (A and C). (D) Representative frames of time-lapse laser confocal images of infected motile neutrophils in larva showing a neutrophil (white arrowhead) phagocytosing bacteria from a granuloma macrophage. (E) Bacterial burden over time and interval speed of neutrophil in D. (F) Representative frames of time-lapse laser confocal images of infected motile neutrophil in larva showing neutrophil (white arrowhead) repeatedly phagocytosing bacteria (yellow and blue arrows) from a granuloma macrophage. (G) Bacterial burden over time and interval speed of neutrophil in F with yellow and blue arrowheads indicating respective phagocytic events in F. In D and F, Green, neutrophil (N); red, Mm, minutes in upper right corner. Yellow objects (white arrowheads) showing bacteria within neutrophils are built by 3D surface rendering with Imaris. Also see Supplementary Figure 2.4.

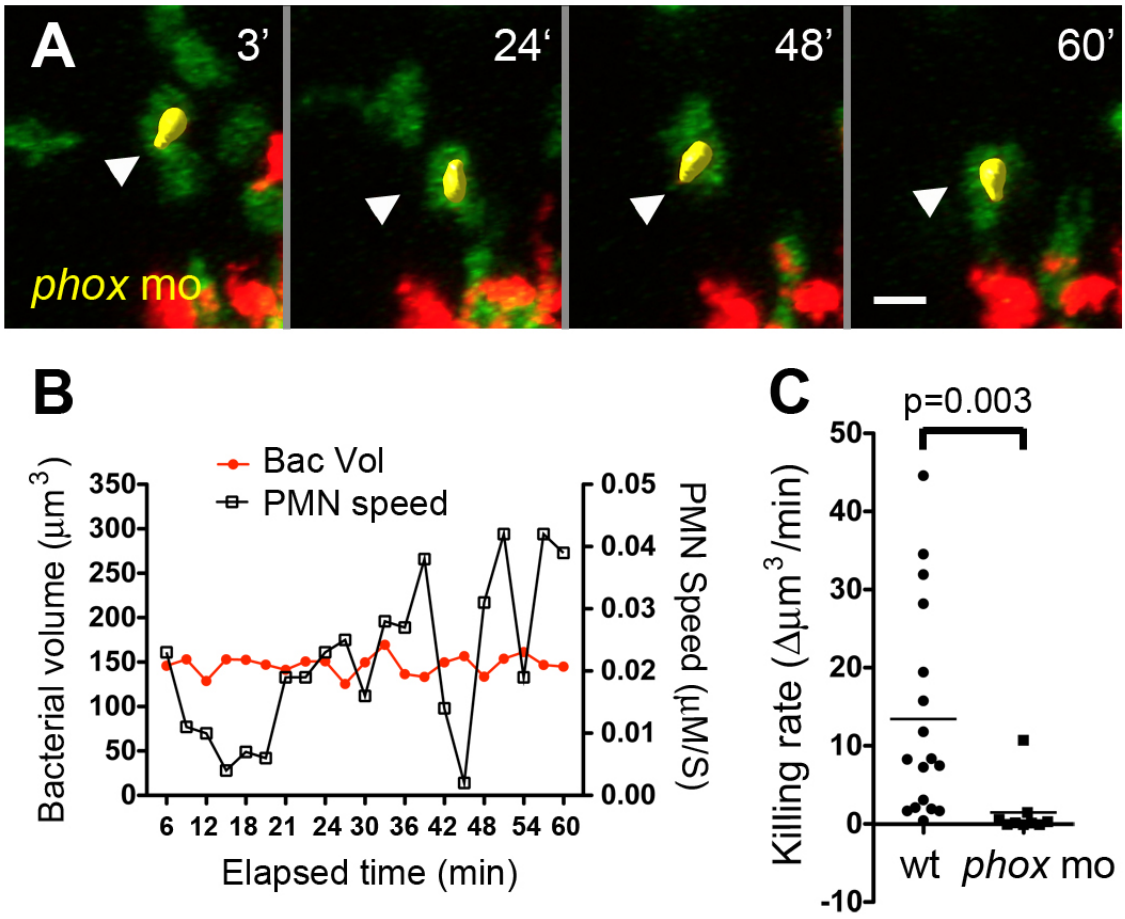

Figure 2.7: Neutrophil killing of intracellular mycobacteria is mediated by NADPH oxidase.
(A) Representative frames of time-lapse laser confocal images of a motile infected neutrophil (white arrowhead) in phox morphants (*phox* mo). Green, neutrophil (N), red, Mm. Elapsed minutes in upper right corner. (B) Bacterial burden over time and interval speed of neutrophil in A. (C) Median killing rate (decrease in bacterial volume of infected neutrophil over time) of WT and *phox* morphant neutrophils. Infected neutrophils were sampled from 3 granulomas in 3 different infected larvae for each group. p values by Mann-Whitney rank test. Also see Supplementary Figure 2.5.

Chapter 2 Supplementary Figures

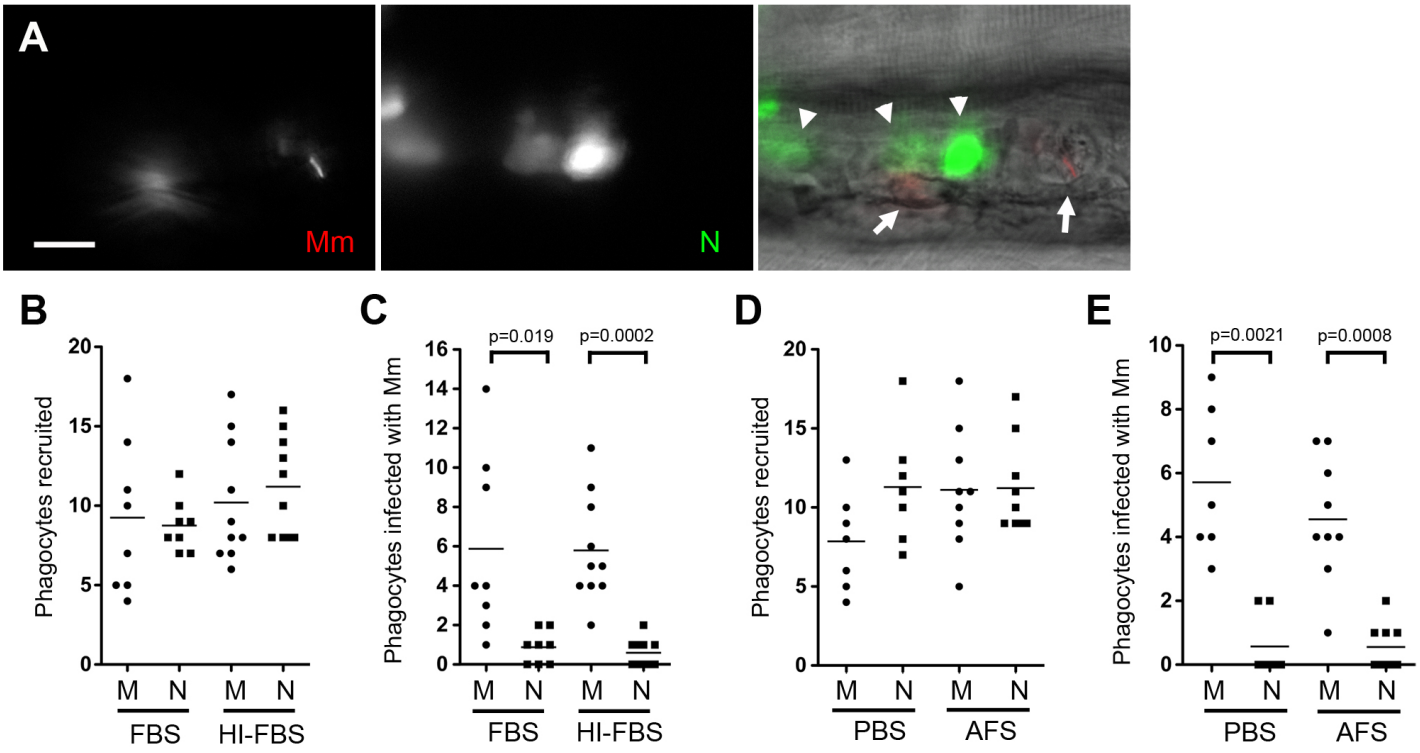

Supplementary Figure 2.1: Poor phagocytosis of mycobacteria by neutrophils at the initial infection site at late developmental stages or in the presence of serum
(A) Fluorescence and DIC overlay of red *M. marinum* (Mm) (arrows) and green neutrophils (N) (arrowhead) in 5 dpf larva 24 hours after caudal vein injection. Scale bar, 10 mm. (B and C) Mean phagocyte recruitment and phagocytosis per larva at 6 hpi of 80-120 *M. marinum*, and 30-40 *P. aeruginosa* incubated with fetal bovine serum (FBS) or heat-inactivated (HI) FBS prior to injection. (D and E) Mean phagocyte recruitment and phagocytosis per larva at 6 hpi of 90 *M. marinum*, and 30-40 *P. aeruginosa* incubated with phosphate buffered saline (PBS) or adult fish serum (AFS) prior to injection. M, macrophage; N, neutrophil. p value determined by Student's unpaired t test (C) and Mann-Whitney rank test (B, D, E).

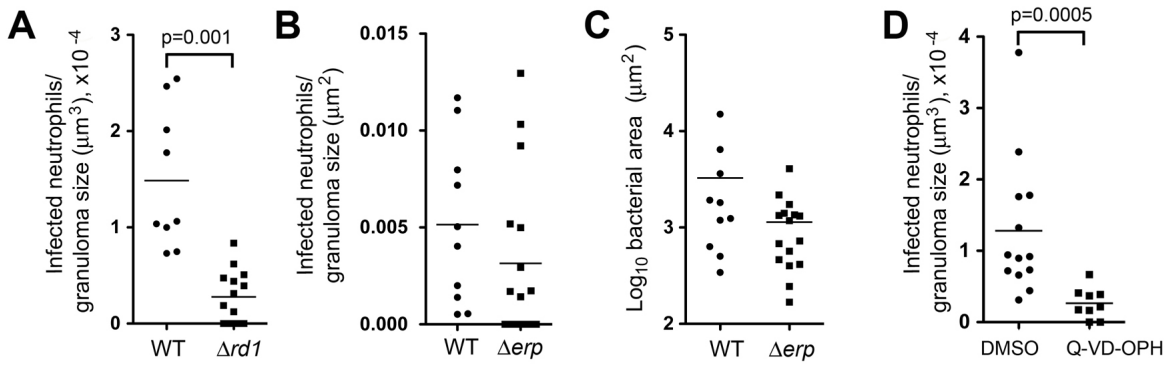

Supplementary Figure 2.2: Infected neutrophils in D*rd1*, D*erp* and Q-VD-OPH-treated granulomas.

(A) Mean infected neutrophils in WT and Δ*rd1 M. marinum* containing hindbrain ventricle (HBV) granulomas at 3 dpi. Granulomas are the same samples as in Figure 2.4B and 2.4C. p value determined by Student's unpaired t test. Representative of two experiments. (B) Mean neutrophils recruited to WT (from 10 animals) and D*erp M. marinum* (from 16 animals) containing HBV granulomas at 3 dpi, normalized to granuloma size, as determined by bacterial fluorescence area (mm^2) and previously described (Davis and Ramakrishnana, 2009). (C) Mean size of granulomas in (B). Five to seven times more D*erp M. marinum* was injected into the HBV to generate granulomas with similar sizes as WT *M. marinum* generated granulomas. (D) Mean infected neutrophils in the WT *M. marinum* containing granulomas in fish treated with DMSO (vehicle control) or Q-VD-OPH. Granulomas are the same samples as in Figure 2.4D, 2.4E and 2.4F. p value determined by a Mann-Whitney rank test.

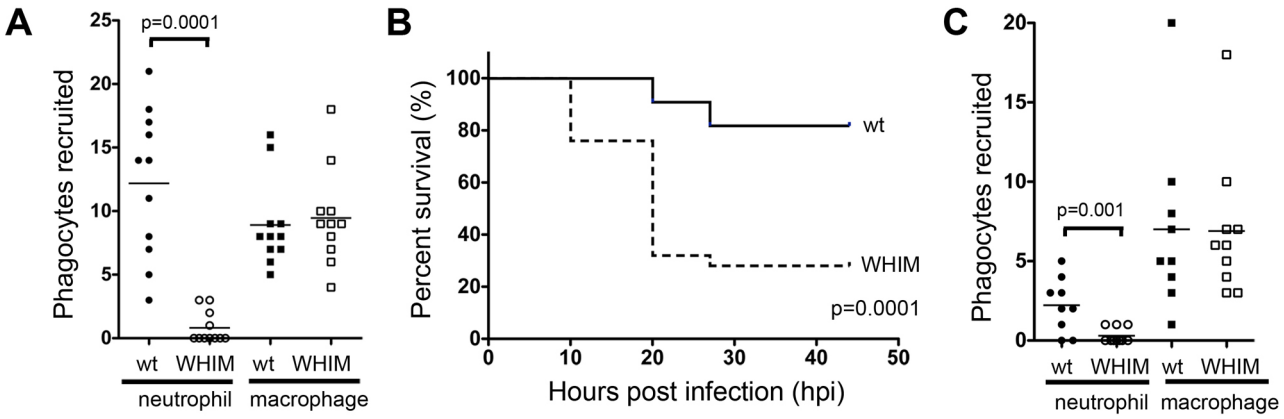

Supplementary Figure 2.3: Defective neutrophil migration in WHIM fish
(A) Mean phagocyte recruitment to the HBV after injection of 20 *P. aeruginosa* in wild-type (wt) and WHIM fish. (B) Survival of wild-type and WHIM fish (n=25 each) infected with 2,643 CFU of *P. aeruginosa*. Median survival for WHIM fish was 20 hpi, whereas 80% of wild-type fish survived through the end of the experiment. p value determined by log-rank test. Representative of two experiments. (C) Mean phagocyte recruitment to the HBV after injection of 113 *M. marinum* in wild-type and WHIM fish. p values determined by a Mann-Whitney rank test (A and C).

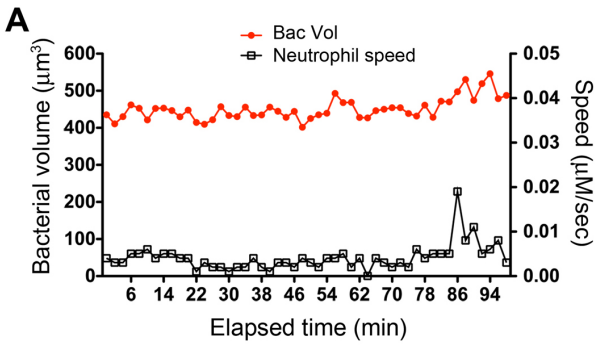

Supplementary Figure 2.4: Bacterial burden in nonmotile neutrophils remains relatively constant over time
Bacterial volume and speed of a representative infected nonmotile neutrophil in a granuloma.

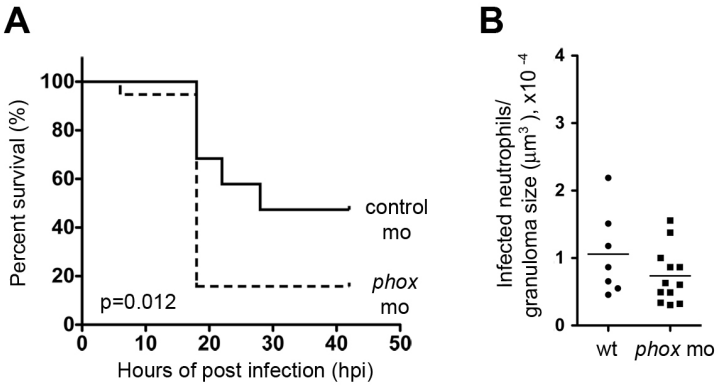

Supplementary Figure 2.5: Functional characterization of *phox* morphants in the context of bacterial infection
(A) Survival of control- and *phox* morpholino (mo)-injected fish (n=19 each) infected with 4,080 CFU of *P. aeruginosa*. Median survival for *phox* morphants was 18 hpi, whereas control morphants was 28 hpi. p value determined by log-rank test. Representative of two experiments. (B) Mean infected neutrophils in WT *M. marinum* containing granulomas in wild-type (wt, n=7) and *phox* morphants (n=12).

Chapter 3: Mycobacteria manipulate macrophage recruitment through coordinate use of membrane lipids

SUMMARY

The evolutionary survival of *Mycobacterium tuberculosis*, the cause of human tuberculosis (TB), depends on its ability to invade the host, replicate, and transmit infection. At its initial peripheral infection site in the distal lung airways, *M. tuberculosis* infects macrophages which transport it to deeper tissues (Philips and Ernst, 2012). How mycobacteria survive in these broadly microbicidal cells is an important question. Here we show that *M. tuberculosis,* and its close pathogenic relative *Mycobacterium marinum,* preferentially recruit and infect permissive macrophages while evading microbicidal ones. This immune evasion is accomplished by using cell surface associated phthiocerol dimycoceroserate (PDIM) lipids (Onwueme et al., 2005) to mask underlying pathogen-associated molecular patterns (PAMPs). In the absence of PDIM, these PAMPs signal a toll-like receptor (TLR)-dependent recruitment of macrophages that produce microbicidal reactive nitrogen species. Concordantly, the related phenolic glycolipids (PGL) (Onwueme et al., 2005), promote recruitment of permissive macrophages via a host chemokine receptor 2 (CCR2)-mediated pathway. Thus, we have identified coordinated roles for PDIM, known to be essential for mycobacterial virulence (Murry et al., 2009) and PGL, which (along with CCR2) is known to be associated with human TB (Flores-Villanueva et al., 2005; Reed et al., 2004). Our findings also suggest an explanation for the longstanding observation that *M. tuberculosis* initiates infection in the relatively sterile environment of the lower respiratory tract, rather than in the upper respiratory tract, where resident microflora and inhaled environmental microbes may continually recruit microbicidal macrophages through TLR-

dependent signaling.

RESULTS & DISCUSSION

Pattern recognition receptors (PRRs) such as the TLRs enable host recognition of diverse microbes through their PAMPs (Medzhitov, 2007). Macrophages recruited through TLR signaling pathways can eradicate organisms invading the oropharyngeal mucosa, e.g. *Streptococcus pneumoniae* (Weiser, 2009). In contrast, pathogenic mycobacteria appear to use macrophages and myeloid dendritic cells for transport across epithelial barriers to their infection niche (Philips and Ernst, 2012;Yang et al., 2012). Mycobacteria are replete with TLR PAMPs, such as lipoproteins and bacterial cell wall peptidoglycan, that have been shown to activate cytokine responses in cultured macrophages (Philips and Ernst, 2012). Yet in vivo studies find TLR signaling to be dispensable in the early stages of infection (Mayer-Barber et al., 2010), suggesting that mycobacteria have evolved mechanisms to circumvent the bactericidal consequences of TLR signaling.

To explore these mechanisms, we used zebrafish larvae infected with *M. marinum*, a close genetic relative of *M. tuberculosis*, and the causative agent of TB in ectotherms. This model has yielded important insights into the pathogenesis and genetics of human TB (Ramakrishnan, 2012). In humans, the earliest interactions between mycobacteria and phagocytes occur at the lung epithelial surface. Such interactions can be modeled in the larva by injection of bacteria or other chemical stimuli into the hindbrain ventricle (HBV), a neuroepithelium-lined cavity to which phagocytes are recruited (Yang et al., 2012) (Fig.1a). We used morpholino knockdown to create zebrafish deficient in MyD88, a common downstream adaptor molecule for TLR signaling pathways (Medzhitov, 2007). As expected, MyD88 morphants had decreased macrophage recruitment to *Staphylococcus aureus* and *Pseudomonas*

aeruginosa, mucosal bacteria that can be commensal or pathogenic (Eddens and Kolls, 2012; Rosenthal and Tager, 1975; Wertheim et al., 2005) (Fig. 3.1b). Similarly, macrophage recruitment to the nonpathogenic *Mycobacterium smegmatis* was MyD88-dependent. In contrast, macrophage recruitment to *M. marinum* was MyD88-independent (Fig. 3.1c). This finding suggested that pathogenic mycobacteria have the ability to mask PAMPs that would otherwise induce TLR signaling during the initial infection phase. We hypothesized that such a factor would be a cell surface associated virulence determinant. In this light, PDIM seemed a likely candidate, particularly because it is present only in the pathogenic mycobacteria, including *M. tuberculosis* and *M. marinum,* but absent in *M. smegmatis* (Onwueme et al., 2005). We created a *M. marinum* mutant that lacks PDIM on its surface by knocking out the PDIM transporter, encoded by the *mmpL7* gene, and confirmed that it was attenuated in zebrafish larvae (Fig. 3.1d and Supplementary Fig. 3.2). If PDIM is masking PAMPs, then macrophage recruitment to Δ*mmpL7* bacteria should be MyD88-dependent, and this was the case (Fig. 3.1e). In contrast, macrophage migration remained MyD88-independent in response to *M. marinum* deficient in another cell surface-associated virulence determinant, Erp (Δ*erp*) (Fig. 3.1d, e and Supplementary Fig. 3.2) (de Mendonça-Lima et al., 2003). This result was consistent with *M. smegmatis* possessing a functional *erp* (de Mendonça-Lima et al., 2003), and suggested further that the evasion of MyD88-dependent immune detection was mediated specifically by PDIM.

Our model posits that pathogenic mycobacteria use PDIM to evade recruitment of MyD88-dependent macrophage populations detrimental to their survival. Therefore, we predicted that wild-type mycobacteria should be unaffected in MyD88 morphants, whereas the attenuation of Δ*mmpL7* should be reversed. We found both to be the case (Fig. 3.1f). For these assays, ~ 80 *M. marinum* were injected into the HBV. However, MyD88 morphants were

previously reported to be susceptible to higher *M. marinum* inocula delivered intravenously (van der Vaart et al., 2013). We confirmed these findings, showing that MyD88 deficiency increased susceptibility at later time points after intravenous administration of >300 CFU (Supplementary Fig. 3.3). It is likely that MyD88 exerts its protective responses at these later stages through mechanisms distinct from the ones we have uncovered, such as through IL-1-mediated responses (Mayer-Barber et al., 2010). Indeed, IL-1 expression was undetectable 3 hours following infection when we observed MyD88-dependent macrophage recruitment (data not shown) suggesting an IL-1 independent role for MyD88 in mediating recruitment towards PDIM-deficient mycobacteria.

Further characterization of wild-type versus PDIM-deficient bacteria revealed that both strains recruited cells expressing the macrophage-specific marker mpeg1(Yang et al., 2012) (Supplementary Fig. 3.4a). We next asked whether these macrophages possessed differential microbicidal potential. We examined the expression of inducible nitric oxide synthase (iNOS) in these recruited cells because: 1) it is induced in macrophages upon TLR signaling (Medzhitov, 2007), and can be expressed by zebrafish (Tobin et al., 2010), mouse (Chan et al., 1992) and human (Kröncke et al., 1998) macrophages following mycobacterial infection and 2) mycobacteria are known to be susceptible to reactive nitrogen species (RNS) in both murine (Chan et al., 1992) and human (Kröncke et al., 1998) macrophages. We found very few iNOS-positive macrophages arriving to wild-type *M. marinum*, whereas the majority of those arriving in response to Δ*mmpL7* bacteria were iNOS-positive (Fig. 3.2a-c, and Supplementary Fig. 3.4b). Δ*erp* bacteria elicited very few iNOS-expressing macrophages (Fig. 3.2c and Supplementary Fig. 3.4b), further showing that this early manipulation of macrophage recruitment and/or activation is a specific characteristic of PDIM. We confirmed that RNS were the major mediators of

MyD88-dependent macrophage microbicidal activity by showing that the iNOS inhibitors CPTIO and L-NAME reversed growth attenuation of the Δ*mmpL7* mutant (Fig. 3.2d and Supplementary Fig. 3.4c).

Together our findings suggested that PDIM mediates an immune evasion strategy, whereby mycobacteria evade detection by TLRs so as to avoid recruitment of iNOS-expressing, microbicidal macrophages. To test this idea, we co-infected red fluorescent wild-type bacteria with green fluorescent wild-type or Δ*mmpL7* bacteria. We found that wild-type bacteria were attenuated in the presence of Δ*mmpL7* bacteria, and that this attenuation transfer was specifically caused by co-infection with Δ*mmpL7* and not with wild-type or Δ*erp* bacteria (Fig. 3.2e and Supplementary Fig. 3.5a, b). Furthermore, this transfer of attenuation from Δ*mmpL7* to wild-type bacteria was dependent on macrophages; no attenuation was observed when macrophages were depleted prior to infection using a morpholino against the myeloid transcription factor, PU.1 (Fig. 3.2f) (Tobin et al., 2010). Attenuation transfer was similarly dependent on MyD88 signaling, as well as on RNS production (Fig. 3.2g, h and Supplementary Figure 3.5c).

Since PDIM is not the only substrate for the MmpL7 transporter, we confirmed that the effects were due to the lack of PDIM *per se* by using a PDIM synthesis mutant, Δ*mas,* showing it to both recruit macrophages in a MyD88-dependent fashion and to transfer attenuation to wild-type bacteria (Supplementary Fig. 3.6). Finally, to rule out the possibility that the PDIM-deficient mutants simply had increased expression of the culpable PAMP(s), we co-injected heat-killed, crushed wild-type bacteria together with live wild-type bacteria. If the culpable PAMP(s) are expressed by wild-type bacteria, then they should become exposed by crushing the bacteria and cause attenuation of the live bacteria. We found this to be the case (Fig. 3.2i). Altogether,

these results suggest that PDIM physically masks underlying mycobacterial PAMPs, thereby preventing mycobacterial delivery into microbicidal macrophages.

To corroborate our findings in a second model, we infected mice via aerosol with wild-type *M. tuberculosis* (H37Rv) or with an isogenic strain (Δ*drrA*) defective for proper PDIM surface localization and virulence in mice (Murry et al., 2009). At 21 DPI, we found substantially greater proportions of iNOS-producing cells among the $CD11b^{+}Ly6C^{hi}$ inflammatory monocyte population in the lungs of mice infected with the Δ*drrA* mutant compared to mice infected with the wild type strain (Fig. 3.3 and Supplementary Fig. 3.7). Thus PDIM-mediated evasion of TLR-dependent immune recognition is shared by *M. tuberculosis* in the context of the mammalian lung, consistent with its central role in avoidance of TLR-dependent anti-microbial mechanisms such as iNOS and antimicrobial peptides (Medzhitov, 2007).

We next sought to understand the mechanism by which mycobacteria recruit the permissive macrophages that are essential for their transport into host tissues. Given our prior finding that *M. marinum* recruits only macrophages (and not neutrophils) to the HBV (Yang et al., 2012), we considered macrophage-specific chemokines as candidates for mediating this recruitment. We investigated CCR2, which has been implicated in macrophage migration to bacterial pathogens in mice (Serbina et al., 2008), including macrophages that are permissive to *M. tuberculosis* replication after aerosol infection (Antonelli et al., 2010). We identified the functional zebrafish CCR2 orthologue (see methods section) and confirmed that its knockdown resulted in reduced macrophage migration in response to recombinant human chemokine ligand 2 (hCCL2) and not to the closely related human macrophage chemokines CCL4 and CCL5 (Supplementary Fig. 3.8a). The specificity of CCL2-mediated macrophage migration was

revealed by the following findings: 1) human and mouse CCL2 induced macrophage but not neutrophil migration (Supplementary Fig. 3.8b, c) 2) recombinant human IL-8, a neutrophil chemokine, induced neutrophil but not macrophage migration (Supplementary Fig. 3.8b, c) 3) human LTB_4 induced recruitment of both neutrophils and macrophages (Supplementary Fig. 3.8b, c), as expected (Tobin et al., 2010) and 4) Myd88 knockdown did not diminish CCL2-mediated macrophage migration, ruling out TLR-mediated migration in response to any endotoxin that might be contaminating the chemokine preparations (Supplementary Fig. 3.8b).

CCR2 morphants had reduced macrophage migration in response to wild-type *M. marinum*, confirming the role of this pathway in recruitment (Fig. 3.4a). Recruitment to PDIM-deficient *M. marinum* was unaffected showing that TLR PAMPs trigger recruitment through a CCR2-independent pathway (Fig. 3.4a). Accordingly, we found that *M. marinum* infection induced CCL2, and that CCL2 morphants also had reduced macrophage recruitment in response to infection (Fig. 3.4b and Supplementary Fig. 3.9).

Turning to the question of which bacterial determinant induced the CCR2 pathway, we considered PGL, a molecule closely related to PDIM in both *M. marinum* and *M. tuberculosis* (Onwueme et al., 2005). While many clinical *M. tuberculosis* isolates have lost PGL, its presence has been linked to increased virulence (Reed et al., 2004). Moreover, among *M. tuberculosis* clinical isolates, PGL expression was linked to *ccl2* expression in a mouse lung infection model (Ordway et al., 2007). Similarly, we found that PGL was required for *ccl2* induction in the larva; deletion of the *M. marinum pks15* locus specifically abrogates PGL, but not PDIM, production (data not shown) and resulted in loss of *ccl2* induction. Δ*mmpL7* bacteria, which lack surface expression of both PGL and PDIM, similarly failed to induce *ccl2,* highlighting that this chemokine is not induced through TLR interactions, but rather is specifically induced through

PGL-mediated interactions (Fig. 3.4b). Furthermore, Δ*pks15* bacteria recruited fewer macrophages upon infection of wild-type larvae, and this reduction was similar to that seen in CCR2 morphants infected with wild-type bacteria (Fig. 3.4c). There was no additional reduction in recruitment when CCR2 morphants were infected with PGL-deficient bacteria, suggesting that PGL recruits macrophages solely through the CCR2 pathway (Fig. 3.4c).

Our findings implicate PGL in bacterial virulence and correspondingly, the CCR2 pathway in host susceptibility. Globally, a large proportion of *M. tuberculosis* isolates are PGL deficient due to a frameshift in *pks15* (Onwueme et al., 2005). However, the importance of PGL in mediating virulence and/or transmission is underscored by its presence in many of the W-Beijing strains, which are becoming rapidly enriched among *M. tuberculosis* isolates globally (Reed et al., 2004), and have predominated in outbreaks in North America where TB is not prevalent (Reed et al., 2004). Infectivity is a key requirement for transmission, and our data suggested that PGL may enhance infectivity through CCR2-mediated recruitment of permissive macrophages at the earliest stages of infection. This enhancement may be particularly relevant in the context of human infections, in which the infectious dose is thought to be as low as 1-3 bacteria (Bates et al., 1965; Wells et al., 1948). To test the hypothesis that PGL enhances infectivity at low doses, we compared the ability of wild-type and PGL-deficient strains to establish infection. Confocal microscopy was used five hours after HBV injection to select those animals that had received 1-3 bacteria (Supplementary Fig. 3.10), and then again at 5 DPI to identify which animals were still infected. We found that 89% of the wild-type but only 18% of the Δ*pks15* infections were successful (Fig. 3.4d). Concurrent administration of recombinant CCL2 restored the infectivity of Δ*pks15* bacteria, provided the CCR2 pathway was intact (Fig. 3.4d). Correspondingly, we found that wild-type bacteria had a lower infectivity rate in CCR2

morphants (Fig. 3.4d). Consistent with our finding that PGL recruits macrophages solely through CCR2, there was no further decrease in infectivity in CCR2 morphants infected with the PGL mutant (Fig. 3.4d). Finally, the infectivity of wild-type bacteria in MyD88 morphants was undiminished (90% for wild-type vs. 83% for morphants), consistent with our finding that TLR signaling is not involved in macrophage recruitment to wild-type bacteria.

These findings highlight the interdependency between bacterial PGL and host CCR2 signaling in driving bacterial infectivity under the low inoculum conditions relevant to human infection. Prior investigations into the role of PGL and CCR2 may have failed to reveal these mechanisms because those studies used higher inocula (Sinsimer et al., 2008) and, in the study of CCR2 signaling, a PGL-deficient strain (Scott and Flynn, 2002). Indeed, our finding that CCR2 signaling is a host susceptibility factor is reinforced by human studies showing an association between the high expression of CCL2 and TB susceptibility (Flores-Villanueva et al., 2005). Furthermore, the association appears to be stronger in East Asian populations (Feng et al., 2012), where clinical isolates are enriched for the predominantly PGL-expressing, W-Beijing strains (Gagneux, 2006). In light of our findings, we propose that the enrichment of PGL expression among these strains is influencing this association, as the CCR2 pathway would be most relevant in the context of bacterial PGL stimulation.

Finally our data suggested an explanation for why *M. tuberculosis* must reach the alveolar surfaces of the distal lung in order to initiate infection (Wells et al., 1948) (Supplementary Fig. 3.1). It is well established that TB results from inhalation of small aerosol droplets containing ~1-3 bacteria, which are capable of reaching the alveolar surfaces of the distal lung; in contrast, large droplets harboring ~10^4 bacteria are trapped in the upper bronchial passages and are far less successful at establishing infection (Bates et al., 1965; Wells et al.,

1948). These observations have led to the idea that the alveolar surfaces of the distal lung offer a more favorable environment for mycobacterial proliferation. We hypothesized that commensal microbes from the oropharyngeal surfaces as well as inhaled environmental organisms, might lead to continual TLR signaling in the upper respiratory tract that would then override the mycobacterial PDIM-dependent immune evasion strategies we identified. In contrast, the lower respiratory tract, which is relatively sterile (Charlson et al., 2011), would favor recruitment of *Mycobacterium*-permissive macrophages. To test this hypothesis we co-infected animals with *M. marinum* together with bacterial colonizers of the pharynx that induce TLR signaling - either *S. aureus*, a common Gram-positive colonizer of the nasopharynx in both adults and children (Wertheim et al., 2005) or the Gram-negative bacterium *P. aeruginosa,* also reported to colonize the pharynx of asymptomatic adults and children (Rosenthal and Tager, 1975). Co-infection with *P. aeruginosa* resulted in the attenuation of wild-type mycobacteria even by 1 DPI, and continuing into 3 DPI (Fig. 3.5a). Mycobacterial growth was attenuated despite rapid clearing of *P. aeruginosa*: 56% of the animals had cleared the co-infected *P. aeruginosa* by 1 DPI, and 76% by 3 DPI, with only a few residual bacteria in the remaining animals. Thus, it was not the physical presence of, but rather the detrimental immunological milieu induced by *P. aeruginosa* that was responsible for the attenuation of *M. marinum*. Consistent with our hypothesis, we found that the detrimental effect of *P. aeruginosa* on mycobacterial survival was MyD88-dependent (Fig. 3.5b). *S. aureus* co-infection also had a MyD88-dependent detrimental effect on *M. marinum* survival (Fig. 3.5c)

Our prior work identified strategies by which intracellular mycobacteria manipulate host pathways after having traversed epithelial barriers; these involve a bacterial protein secretion system that expands the bacterial niche through macrophage recruitment to the nascent

granuloma (Ramakrishnan, 2012). We now describe what may be the first contact between mycobacteria and their hosts, and the manner in which mycobacteria manipulate recruitment, and potentially influence the differentiation or activation state, of the first responding macrophages so as to gain access to their preferred niche (Supplementary Fig. 3.1). The choreographed entry involves two related mycobacterial lipids acting in concert to avoid one host pathway while inducing another. Our findings link PDIM, recognized as an absolutely essential mycobacterial virulence factor, to the evasion of TLR detection and thus explain the dispensability of TLR-mediated immunity in protection against *M. tuberculosis* infection in both human and animal studies (Mayer-Barber et al., 2010; von Bernuth et al., 2012). In contrast, PGL is dispensable for virulence, being variably present among clinical isolates. Yet, its presence in the ancestral *M. cannetti* strains as well as in *M. marinum,* the closest genetic relative of the *M. tuberculosis* complex (Onwueme et al., 2005), suggests its integral role in the evolution of mycobacterial pathogenicity. TB is an ancient disease and the enhanced infectivity conferred by PGL may have been essential for most of its history before human crowding, with its greatly increased opportunities for transmission, made it dispensable (Comas et al., 2013).

Our findings suggest that commensal flora may play a central role in choreographing mycobacterial entry. Not only must pathogenic mycobacteria possess a physical barrier to prevent host TLR-mediated detection, but they must also evade TLR signaling initiated by other organisms, by entering through the distal lung (Supplementary Fig. 3.1). Our work may also explain the paradox that smaller *M. tuberculosis* droplets are more infectious than larger ones. However the requirement placed on mycobacteria to gain entry through the distal lung makes TB less contagious than most other respiratory infections, thus assigning a protective role to the commensal flora. Conversely, the persistence of human TB for over 70,000 years (Comas et al.,

2013) attests to the effectiveness of the mycobacterial evolutionary survival kit (masking lipid, recruiting lipid and small infection droplets) to simultaneously evade and manipulate the host and its commensal flora.

METHODS

Bacterial Strains and Methods. *M. marinum* strain M (ATCC BAA-535) and the Δ*erp* mutant have been described(Cosma et al., 2006). The Δ*mmpL7* and Δ*pks15* mutants were generated as described in the following section. Fluorescently labeled bacterial strains were generated by transformation with the pTEC15 or pTEC27 plasmids (deposited with Addgene, plasmids 30174 and 30182 respectively), resulting in *msp12*-driven expression of the wasabi or tdTomato fluorescent proteins, respectively. Mycobacteria were grown at 33˚C in Middlebrook 7H9 broth or on 7H10 agar (both by Difco) supplemented with 0.5% bovine serum albumin, 0.005% oleic acid, 0.2% glucose, 0.2% glycerol, 0.085% sodium chloride and 0.05% Tween-80 (broth culture only). 50 μg/mL hygromycin was added as appropriate. For sucrose counter-selection, 7H10 agar was supplemented with 10% sucrose. Single-cell suspensions of bacteria were prepared as described(Takaki et al., 2012). To prepare heat-killed crushed *M. marinum,* bacteria were incubated at 80°C for 20 minutes and then homogenized in a Biospec Bead Beater together with 0.1 mm silica spheres for 1 minute. The *P. aeruginosa* PAO1 fluorescent strain used in this study has been described(Brannon et al., 2009). The *S. aureus* Newman strain expressing pOS1-SdrC-mCherry #391 was a gift from Dr. Juliane Bubeck Wardenburg.

Targeted Deletion of *mmpL7* and *pks15*. A 2638 bp PstI fragment containing part of the *mmpL7* (MMAR_1764) ORF was cloned into a pBluescript-derived vector, pBSXKpn.2 (CLC,

unpublished). A 1124 bp KpnI fragment internal to *mmpL7* was then excised and replaced with the *aph* cassette, conferring kanamycin resistance. The sucrose counter-selectable marker, *sacB*, and an additional marker *hygA*, conferring hygromycin resistance, were then added to create pJENK7.1::Hyg. This construct was transformed into the wild-type reference strain, M, and kanamycin-resistant colonies were selected. Subsequent screening for sucrose-sensitivity identified merodiploids that were verified by southern blotting. One such merodiploid was then grown in liquid culture for ten days and plated on sucrose-containing medium. Sucrose- and kanamycin-resistant, hygromycin-sensitive colonies were then verified by southern blotting to identify the *ΔmmpL7* mutant, KT15. This strain was verified to be deficient in surface localization of PDIM (data not shown), and exhibited colony morphology defects previously reported for *M. marinum* PDIM mutants(Yu et al., 2012). The *pks15* (MMAR_1762) locus was deleted as follows. Flanking regions upstream and downstream of *pks15* were amplified by PCR using primers 5'pks15F (5'CCGCTCGAGGGTGCGATGCGTGGTATC3'), 5'pks15R.2 and (5'CGACTAGTTCAGTTGCTCCTGTTCATG3'), 3'pks15F , and (5'GGAGCAACTGAACTAGTACCATCCGACACCGACTG3') and 3'pks15R.2 (5'CCGTCTAGAGTGGTGCTGTTCGGCGTC3'), respectively. These fragments were sequentially inserted, directly adjacent to each other into pBluescriptSK+::SacBHyg.1 (CLC, unpublished), a pBluescript derivative which contains *sacB* and *hygA* external to the MCS. The resulting construct, pPKS15KO, bears an unmarked deletion of the *pks15* ORF, and was used to transform strain M, and hygromycin resistant colonies were selected. Putative merodiploids were verified by Southern blotting and then counter-selected on sucrose as above, to produce the sucrose-resistant, hygromycin-sensitive isolate (KT21) which was then verified by Southern blotting. Additional verification by thin layer chromatography determined that PGL was absent,

while PDIM production was retained (data not shown), consistent with deletion of *pks15* in *M.tuberculosis*(Reed et al., 2004).

Zebrafish Husbandry and Infections. Wild-type AB zebrafish were maintained as described(Takaki et al., 2013). Larvae (of undetermined sex given the early developmental stages used) were infected at 36–48 hours post-fertilization (hpf) via caudal vein or hindbrain ventricle injection using thawed single-cell suspensions of known titer(Takaki et al., 2012; Takaki et al., 2013). Number of animals to be used for each experiment was guided by past results with other bacterial mutants and/or zebrafish morphants. Larvae were randomly allotted to the different experimental conditions. Zebrafish husbandry and all experiments performed on them were in compliance with Institutional Animal Care and Use Committee approved protocols.

Microscopy and Image-Based Quantification of Infection Level. Wide-field microscopy was performed using a Nikon Eclipse Ti-E equipped with a C-HGFIE 130W mercury light source, Chroma FITC (41001) filter, and 2x/0.10 Plan Apochromat objective. Fluorescence images were captured with a CoolSNAP HQ2 Monochrome Camera (Photometrics) using NIS-Elements (version 3.22). Quantification of fluorescent *M. marinum* infection using images of individual embryos using Fluorescent Pixel Count (FPC) was performed as previously described(Takaki et al., 2012). For confocal imaging, larvae were imbedded in 1.5% agarose (low melting point)(Davis and Ramakrishnan, 2009). A series of z-stack images with a 2 μm step size was generated through the infected HBV, using the galvo scanner (laser scanner) of the Nikon A1 confocal microscope with a 20x Plan Apo 0.75 NA objective. Bacterial burdens were determined

by using the 3D surface-rendering feature of Imaris (Bitplane Scientific Software)(Yang et al., 2012).

Hindbrain Assays. Macrophage recruitment assays were performed as previously described(Takaki et al., 2013). For determination of hindbrain ventricle infection burdens, 1 and 3 DPI larvae were mounted in 1.5% agarose and confocal z-stacks of 2 μm were obtained.

iNOS Staining. Antibody staining of larvae was performed as described(Clay et al., 2007). Larvae were then imaged using confocal microscopy and the number of infected macrophages that were positive for iNOS staining was determined for each larva.

iNOS Scavengers. Fish were treated as previously described(Lepiller et al., 2007). CPTIO or L-NAME (Sigma) were used at a final concentration of 500 μM and 1 mM, respectively in 0.1% DMSO in fish water. Fish were incubated immediately following infection and fresh inhibitor was added every 24 hours until bacterial burden was determined.

Morpholinos. Morpholinos described in Table S1 were injected at the 1-4 cell stage as previously described(Tobin et al., 2010).

RT-PCR to verify efficacy of Myd88 MO. RNA was extracted from pools of 15-40 embryos using TRIzol reagent (Life Technologies), treated with Turbo DNA-Free Kit (Life Technologies) and cDNA synthesized with PrimeScript (Takara). Primers used for PCR were as follows: *actin* FWD 5'-ACCTGACAGACTACCTGATG, REV 5'-TGAAGGTGGTCTCATGGATAC, *myd88* FWD 5'-ATGGCATCAAAGTTAAGTATAGACC, REV 5'-AGGGCAGTGAGAGTGCTTTG.

Identification of candidate CCR2 orthologue in zebrafish

BLAST searches of the zebrafish genome (www.ensembl.org) identified two closely-related CCR-like genes on Chromosome 16, ENSDARG00000079829 and ENSDARG00000062999. In BLAST comparisons to the human genome ENSDARG00000079829 was found to have the highest homology to human CCR2 (E value 8.8e-112), while ENSDARG00000062999 was most highly homologous to human CCR4 (E value 2e-90). In addition, annotation of the zebrafish genome from NCBI annotates ENSDARG00000079829 as a CCR-2-like gene. We confirmed expression of the mRNA and identified the short 5' upstream exon ATGTCGGCGACACAAAACAGTA via 5'-RACE(Maruyama et al., 1995).

Identification of zebrafish CCL2 orthologue. Protein sequences of human and mouse CCL2 were used to interrogate the zebrafish genome by BLAST. Expression levels of the four most closely-related zebrafish proteins was then examined at 3 HPI to identify the likely functional orthologue (Supplementary Fig. 3.9a). Of the four candidates, only ENSDARG00000041835 was significantly induced at 3 HPI. Knockdown of ENSDARG00000041835 resulted in a decrease in macrophage recruitment into the HBV at 3 HPI (Supplementary Fig. 3.9b).

Quantitative Real-time PCR (qRT-PCR). cDNA was synthesized from pools of 20-40 larvae as previously described(Clay et al., 2007). Quantification of ccl2 RNA levels were determined using SYBR green and the following primer pair; 5'GTCTGGTGCTCTTCGCTTTC3' and 5'TGCAGAGAAGATGCGTCGTA3'.

Infectivity Assay. 2 DPF larvae were infected via the HBV with an average of 0.8 bacteria per injection. Fish harboring 1-3 bacteria were then identified at 5 HPI by confocal microscopy. These infected fish were then evaluated at 5 DPI and were scored as infected or uninfected, based on the presence or absence of fluorescent bacteria.

Mice, aerosol infections, and flow cytometry. C57BL/6 mice were purchased from Jackson Laboratories. All mice were housed under specific pathogen free conditions at Seattle Biomedical Research Institute, and all experiments were performed in compliance with the respective Institutional Animal Care and Use Committee approved protocols. Ten-week old female mice were randomized to the different experimental groups. The number of mice to be used to adequately power the experiment was guided by the results of the corresponding zebrafish experiments. A stock of *M. tuberculosis* strain H37Rv or the isogenic PDIM-deficient *ΔdrrA* strain was sonicated before use and mice were infected in an aerosol infection chamber (Glas-Col) with approximately 200 colony forming units (CFUs) of H37Rv or 1000 CFUs of *ΔdrrA* to achieve similar bacterial burdens at 21 days post infection. The infectious dose in each experiment was determined by plating lung tissue of two mice from each group. Colonies on 7H10 agar plates were counted after 21 days of incubation at 37°C. Lung tissue was perfused with 5 ml of PBS administered through the right ventricle of the heart, finely chopped using a gentleMACS Octo Dissociator (Miltenyi Biotec) and incubated at 37°C for 30 minutes in HEPES buffer containing Liberase Blendzyme 3 (Roche Applied Science). Following digestion, single cell suspensions were prepared by passing tissue through a cell strainer. Single cells suspensions were then stained for flow cytometric analysis. Lung single cell suspensions were surface stained at 4°C for 20 minutes in the presence of Fc block (24G2) with the following antibodies from eBioscience: PE-Cy7 labeled anti-CD4 (GK1.5, eBioscience), anti-CD8α (53-6.7, eBioscience), anti-CD11c (N418), and FITC-labeled anti-Ly6G (1A8) to exclude T cells, DCs, and neutrophils. Alveolar macrophages were excluded based on their high CD11c expression and autofluorescence. PerCPCy5.5 labeled anti-Ly6C (HK1.4) and APC-efluor 780 labeled anti-CD11b (M1/70) were used to identify CD11b+Ly6C^{HI} monocytes. Intracellular

staining was done following fixation and permeabilization following manufacturer recommendations (eBioscience). Cells were fixed and permeabilized using eBioscience's Fix/Perm buffer for 1 hour at 4°C, followed by staining for iNOS with anti-NOS2 Alexa Fluor 405 (C-11, Santa Cruz Biotechnology) or mouse IgG1 isotype control for 30 minutes at 4°C. Samples were analyzed on an LSR-II (BD Biosciences) and FlowJo Software (Treestar).

Statistics. Statistical analyses were performed using Prism 5.01 (GraphPad). For data sets requiring $\log_{10}$ transformation prior to ANOVA, embryos with no detectable fluorescence above background were assigned a value of 0.9, with 1 being the limit of detection, prior to $\log_{10}$ transformation. Post-test *P* values are as follows: $*P < 0.05$; $**P < 0.01$; $***P < 0.001$.

Chapter 3 Figures

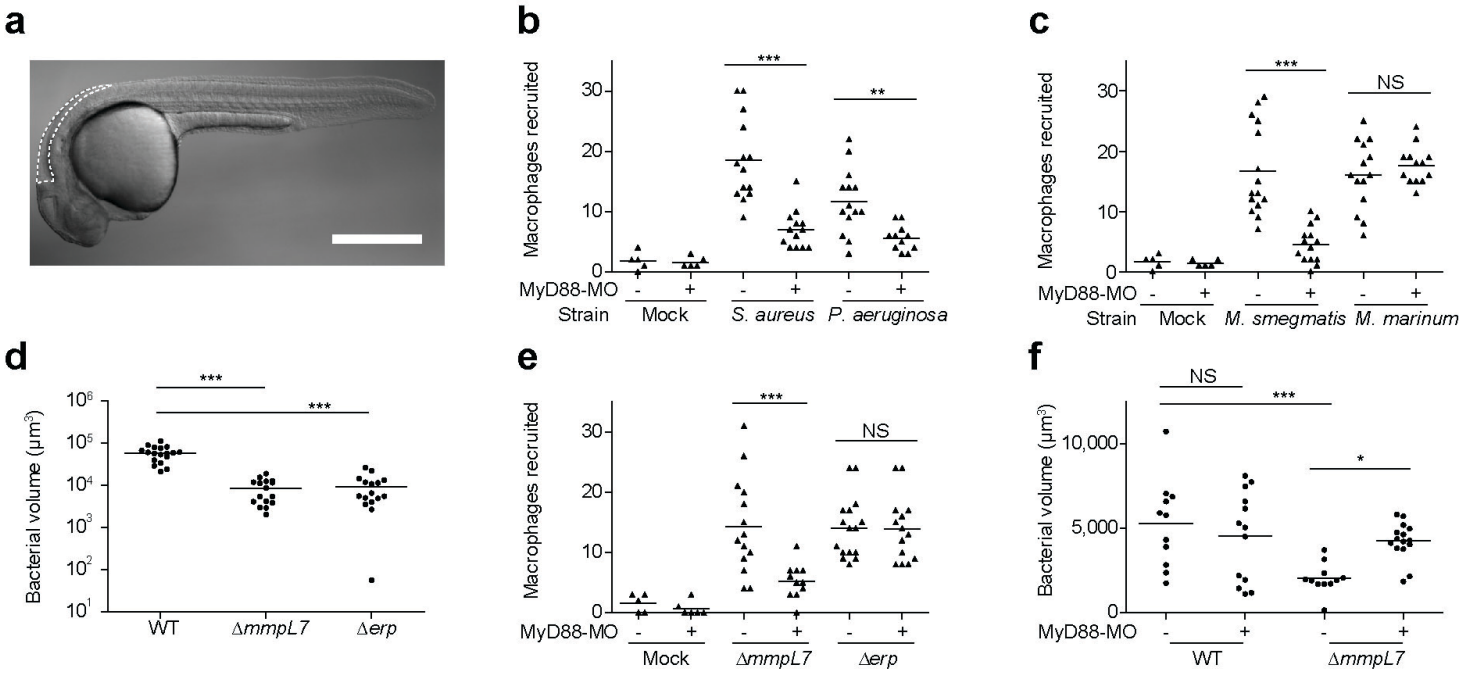

Figure 3.1: PDIM mediated evasion of MyD88 dependent macrophage recruitment. **a**, Schematic of a 2dpf zebrafish showing the hindbrain ventricle (HBV) injection site outlined with dashed white line. Scale bar = 500 µm. **b-c**, Mean macrophage recruitment at 3 HPI into the HBV of wild-type or MyD88-morphant (MO) fish following infection with 150 *S. aureus*, 200 *P. aeruginosa* (**b**), 80 *M. marinum* or 85 *M. smegmatis* (**c**). Representative of three separate experiments. **d**, Mean bacterial burdens at 3 DPI following HBV infection of wild-type fish with 80 wild-type, Δ*mmpL7,* or Δ*erp M. marinum*. Representative of three separate experiments. **e**, Mean macrophage recruitment at 3 HPI into the HBV of wild-type or MyD88 MO fish following infection with Δ*mmpL7* or Δ*erp M. marinum*. Representative of four separate experiments. **f**, Mean bacterial burdens of wild-type or MyD88 MO fish at 3 DPI following HBV infection with wild-type or Δ*mmpL7 M. marinum*. Representative of three separate experiments. Significance testing for all panels done using one-way ANOVA, with Bonferroni's post-test for comparisons shown.

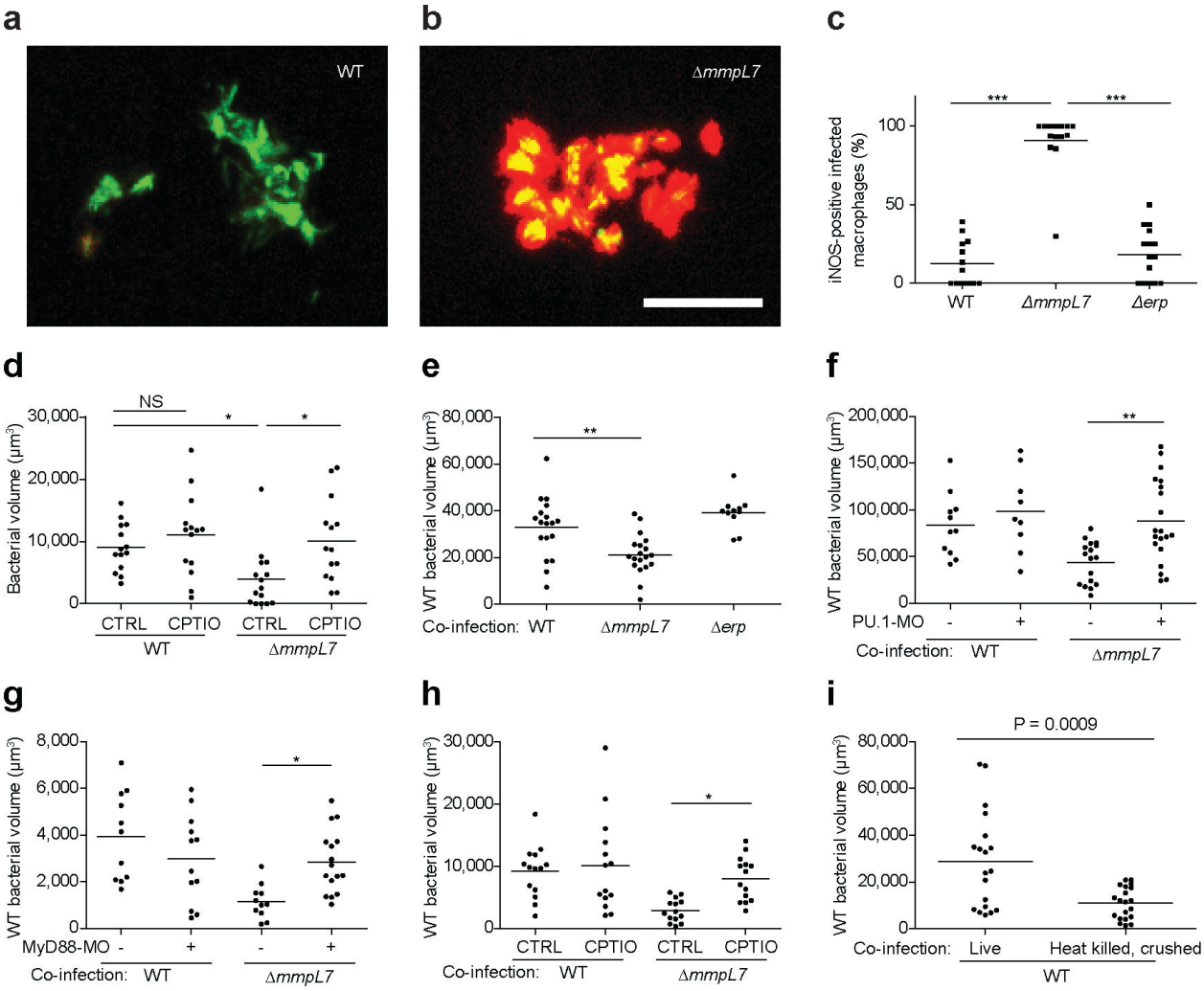

Figure 3.2: Increased iNOS-dependent microbicidal activity of macrophages recruited to PDIM-deficient mycobacteria. a, b, Representative images of wild-type (**a**) and Δ*mmpL7* (**b**) *M. marinum*-infected fish from (**c**). Scale bar = 50μm. **c**, Percent of infected macrophages that were iNOS-positive, in the HBV at 3 DPI with 80 wild-type, Δ*mmpL7*, or Δ*erp M. marinum*. Representative of three separate experiments. **d**, Mean bacterial burdens of 2dpf control (CTRL) or RNS scavenger (CPTIO) treated fish following HBV infection with 80 wild-type or Δ*mmpL7 M. marinum*. Representative of two separate experiments. **e-h**, Mean bacterial volume of red fluorescent wild-type *M. marinum* (infection inoculum 30-40) when co-infected with 30-40 green fluorescent wild-type, Δ*mmpL7*, or Δ*erp M. marinum* at 3 DPI in wild-type (**e**), pu1 MO (**f**), myd88 MO (**g**), or CPTIO-treated (**h**) larvae. **e, g**, Co-infection of wild-type Mm and Δ*mmpL7 M. marinum* in wild-type or myd88 MO fish is representative of at least three separate experiments, and co-infection with Δ*erp* is representative of two separate experiments. **f, h,** Representative of two separate experiments. **a-h,** Significance testing done using one-way ANOVA, with Bonferroni's post-test for comparisons shown. **i,** Mean bacterial volume of red fluorescent wild-type *M. marinum* at 3 DPI (infecting inoculum 30-40) when co-infected with the volume equivalent of 30-40 heat-killed, crushed wild-type *M. marinum*. Representative of two separate experiments. Student's unpaired *t* test.

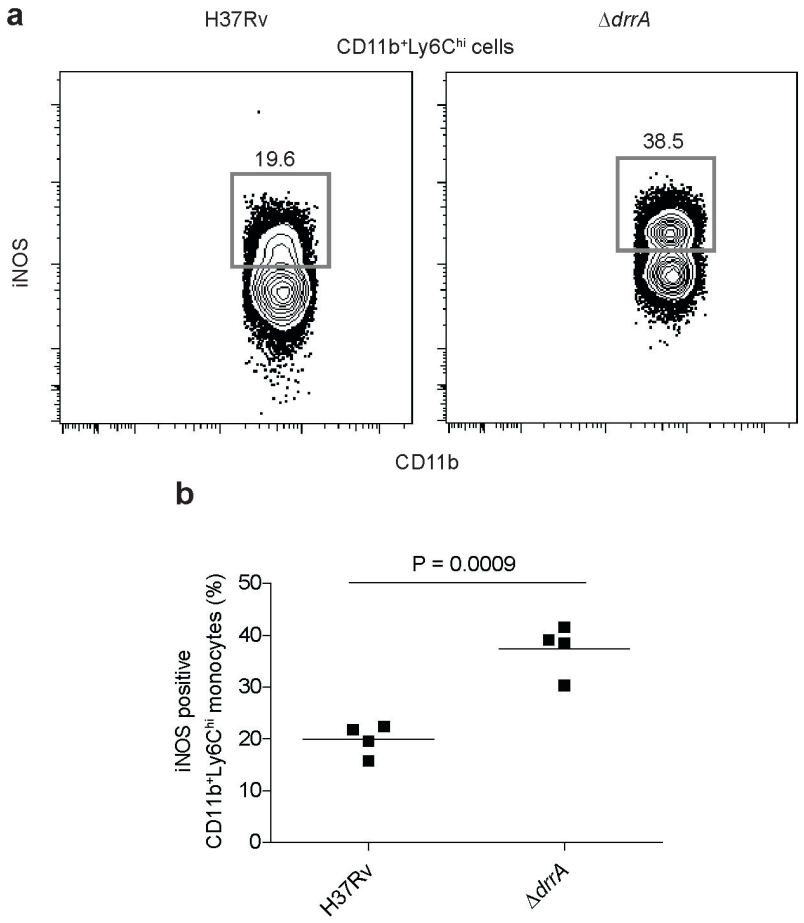

Figure 3.3: Elevated frequencies of iNOS expressing inflammatory monocytes in mice infected with PDIM-deficient *M. tuberculosis*. C57B6 mice were infected via the aerosol route with H37Rv or an isogenic PDIM-deficient mutant (Δ*drrA*). Lung tissue was harvested on 21 DPI and iNOS (protein expression was measured via flow cytometry. Representative FACS plots (**a**) and graphical depiction (**b**) of frequencies of iNOS expressing cells within the $Ly6C^{+}CD11b^{+}$ inflammatory monocyte population. Representative of two separate experiments. Student's unpaired *t* test.

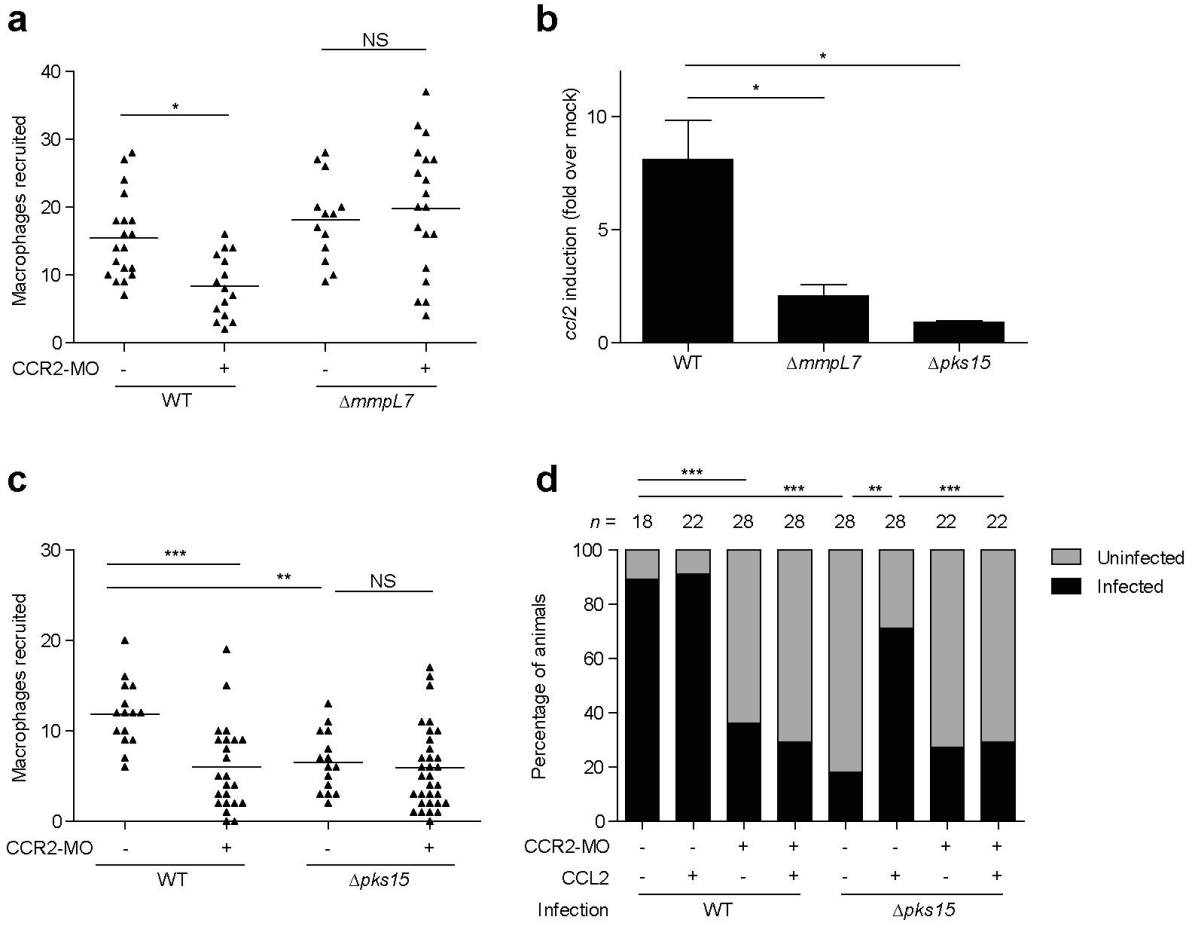

Figure 3.4: Macrophage recruitment and subsequent infectivity is mediated by mycobacterial PGL and host CCR2. **a**, Mean macrophage recruitment at 3 HPI into the HBV of wild-type or CCR2 MO fish following infection with 80 wild-type or Δ*mmpL7 M. marinum*. Representative of three independent experiments. One-way ANOVA, with Bonferroni's post-test for comparisons shown. **b**, CCL2 mRNA levels (mean +/- SEM of four individual experiments) induced at 3 hours post caudal vein infection of 2dpf larvae with 250-300 wild-type, Δ*pks15*, or Δ*mmpL7 M. marinum*. One-way ANOVA with Tukey's post-test for comparisons shown. **c**, Mean macrophage recruitment at 3 HPI into the HBV following infection with 80 wild-type or Δ*pks15 M. marinum*. Representative of three separate experiments. One-way ANOVA with Bonferroni's post-test for comparisons shown. **d**, Wild-type and CCR2 MO fish, with or without the addition of 5 µg/mL CCL2, were infected in the HBV with 1-3 wild-type or Δ*pks15 M. marinum*. Graph shows the percent of fish that were infected (black) or uninfected (gray) after five days. n=number of larvae per group. Representative of two separate experiments. Significance was evaluated using Fisher's exact test for each comparison.

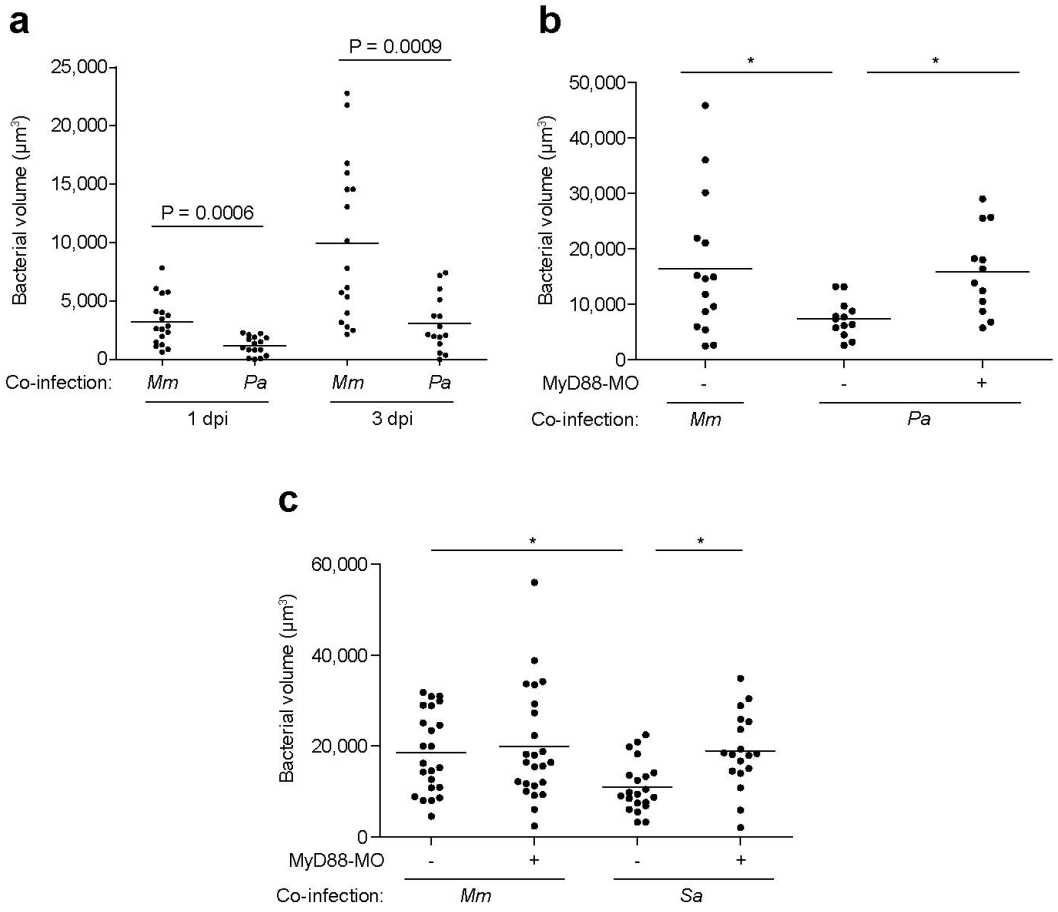

Figure 3.5: MyD88-dependent macrophage recruitment elicited by other bacterial pathogens and commensals attenuates pathogenic mycobacteria. **a,** Mean bacterial volume of red fluorescent *M. marinum* (infecting inoculum 30-40) following co-infection with either 30-40 green fluorescent *M. marinum* or 300 *P. aeruginosa* at 1 and 3 DPI. Representative of three separate experiments. Significance assessed using Student's *t* test. **b-c**, Mean bacterial volume of 30-40 red fluorescent wild-type *M. marinum* (infecting inoculum 30-40) following co-infection with either 30-40 green fluorescent wild-type *M. marinum* or 300 *P. aeruginosa* (**b**) or 300 *S. aureus* (**c**) at 3 DPI, in wild-type or MyD88 MO larvae. Significance tested by one-way ANOVA with Bonferroni's post–test for comparisons shown.

Chapter 3 Supplementary Figures

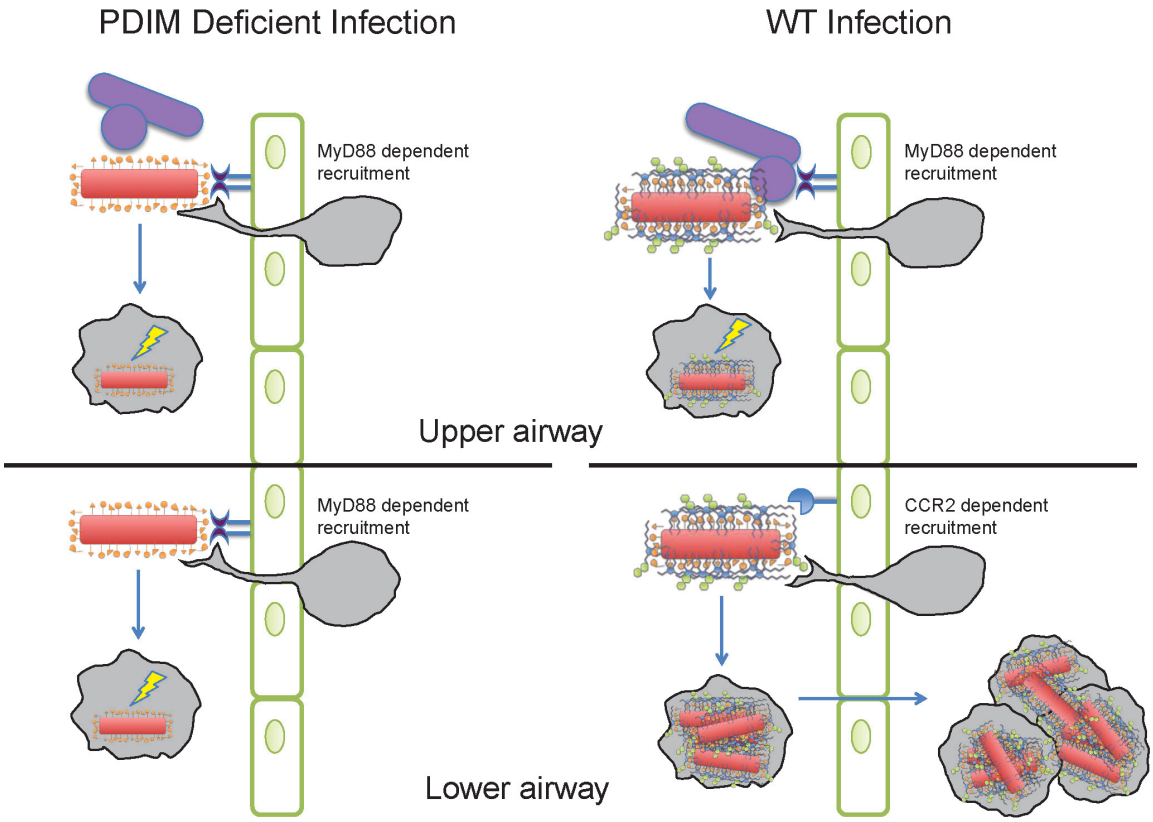

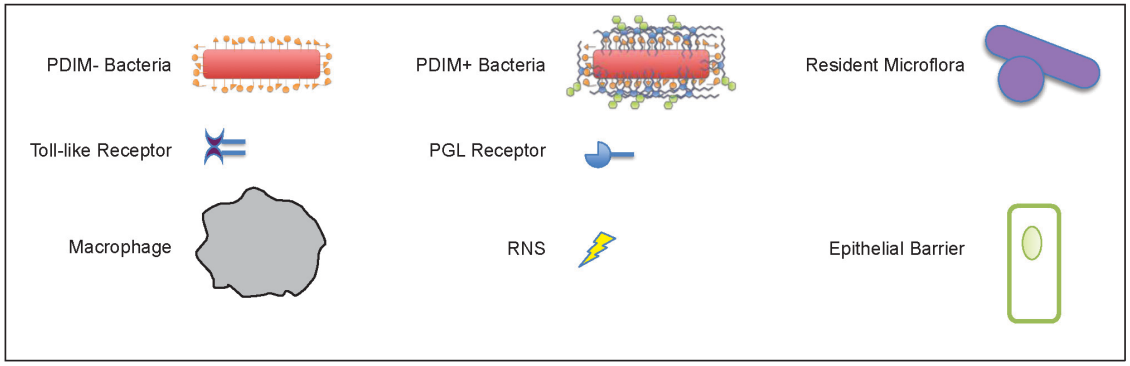

Supplementary Figure 3.1: Coordinate use of PDIM-mediated immune evasion and PGL-mediated recruitment by pathogenic mycobacteria. Model for infection with wild-type (WT) and PDIM-deficient mycobacteria are shown in the context of the relatively sterile lower airway versus the upper airway, with its higher levels of resident microflora and inhaled environmental organisms.

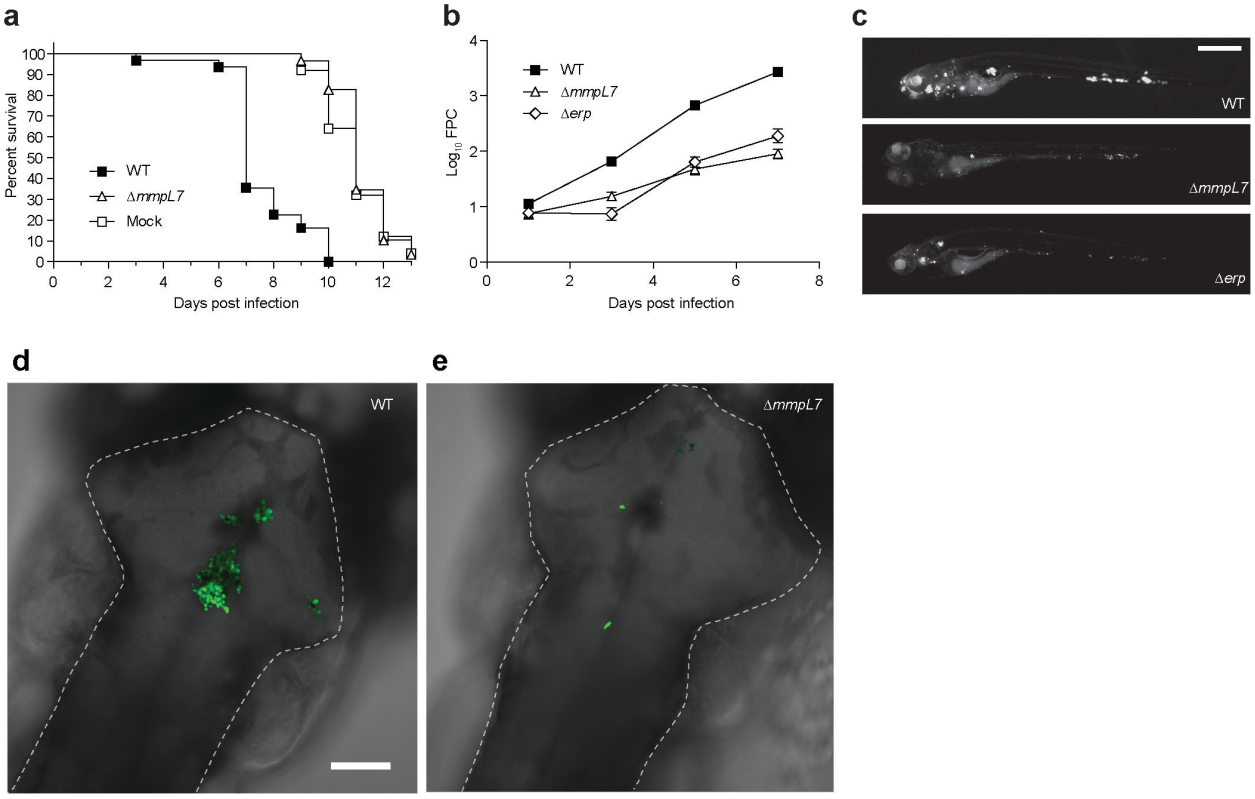

Supplementary Figure 3.2: *ΔmmpL7* bacteria are attenuated in zebrafish larvae. a, Kaplan-Meier graph showing daily survival of larvae infected via caudal vein injection with medium (mock), 29 wild-type or 70 Δ*mmpL7 M. marinum*. N=25 (mock), 31 (wild-type), or 29 (Δ*mmpL7*) larvae per group. Mean time to Death (days): Mock (11), wild-type (7.6) and Δ*mmpL7* (11.2). Survival was compared by log-rank test: wild-type vs. mock and wild-type vs. Δ*mmpL7,* p<0.0001; mock vs. Δ*mmpL7*, p=0.5601. **b, c,** Larvae were infected via caudal vein injection 1 DPF with 550 wild-type, 650 *ΔmmpL7*, or 700*Δerp,* fluorescent *M. marinum*. **b,** Infection burdens were measured by Fluorescent Pixel Count (FPC). **c,** Representative images at 7 DPI. Scale bar = 500 μm. At 3, 5 and 7 DPI, Log_{10} FPC was compared by ANOVA, with Dunnett's post-test. ***, p<0.001. **d,e,** Representative images from wild-type (**d**) and Δ*mmpL7* (**e**) *M. marinum* HBV infections quantified in Figure 1d. HBVs are outlined with a dashed white line. Scale bar = 100μm.

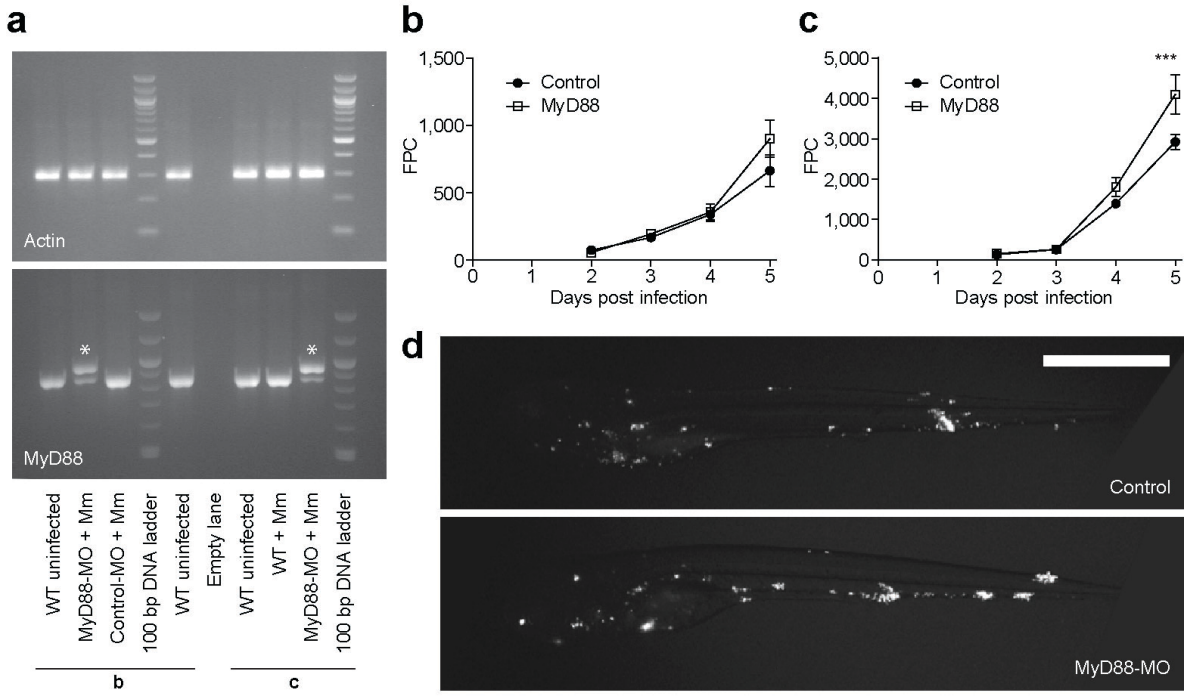

Supplementary Figure 3.3: Knockdown of MyD88 results in a late, dose dependent hypersusceptibility to *M. marinum* systemic infection. **a**, RT-PCR for *actin* (upper panel) and *myd88* (lower panel) demonstrating that that the majority of *myd88* transcripts at 7 DPF are abnormal in MyD88 morphants. Lanes marked 'b' and 'c' correspond to morphants from the same experiments depicted in panels **b** and **c** respectively. The abnormal larger transcript (indicated by *) results from the inclusion of intron 2 in the final transcript, incorporating a premature stop codon that truncates the protein prior to the TIR (Toll/Interleukin Receptor) domain. (**b, c)** Caudal vein infection of MyD88 morphants with 141 (b) or 325 (c) CFU *M. marinum*/larva. Bacterial burden was assessed by FPC and each time point was compared by one-way ANOVA and Bonferroni's post-tests, *** $p<0.001$. **d**, Representative images of larvae at 5 DPF from experiment in (c).

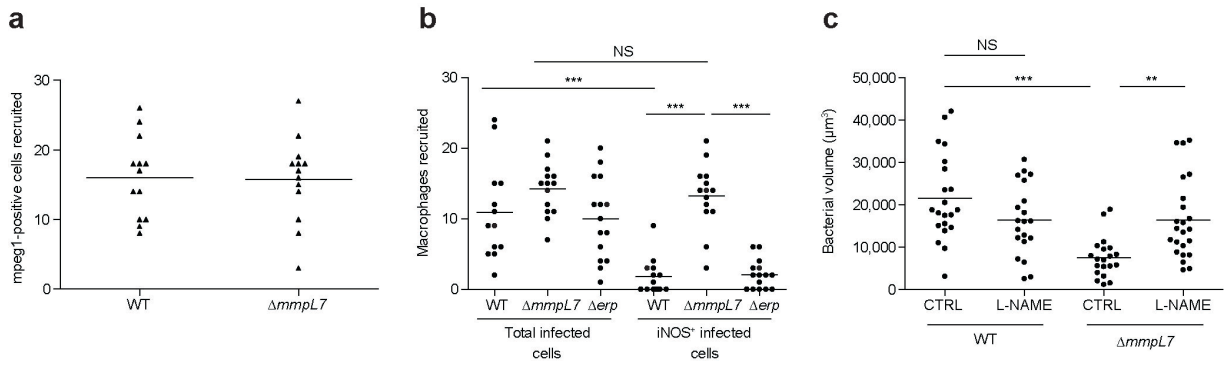

Supplementary Figure 3.4: Characteristics of macrophages recruited to wild-type and PDIM-deficient bacteria. a,. Mean mpeg1 positive macrophages recruited at 3 HPI into the HBV of wild-type fish following infection with 80 wild-type or Δ*mmpL7 M. marinum*. **b,** Data from Figure 2C expressed as mean numbers of total infected macrophages and iNOS expressing infected macrophages following HBV infection with 80 wild-type, Δ*mmpL7*, or Δ*erp M. marinum*. **c, bacterial burdens after L-NAME treatment.** Mean bacterial burdens of 2 DPF control (CTRL) or iNOS inhibitor (L-NAME) treated fish following HBV infection with 80 wild-type or Δ*mmpL7 M. marinum*.

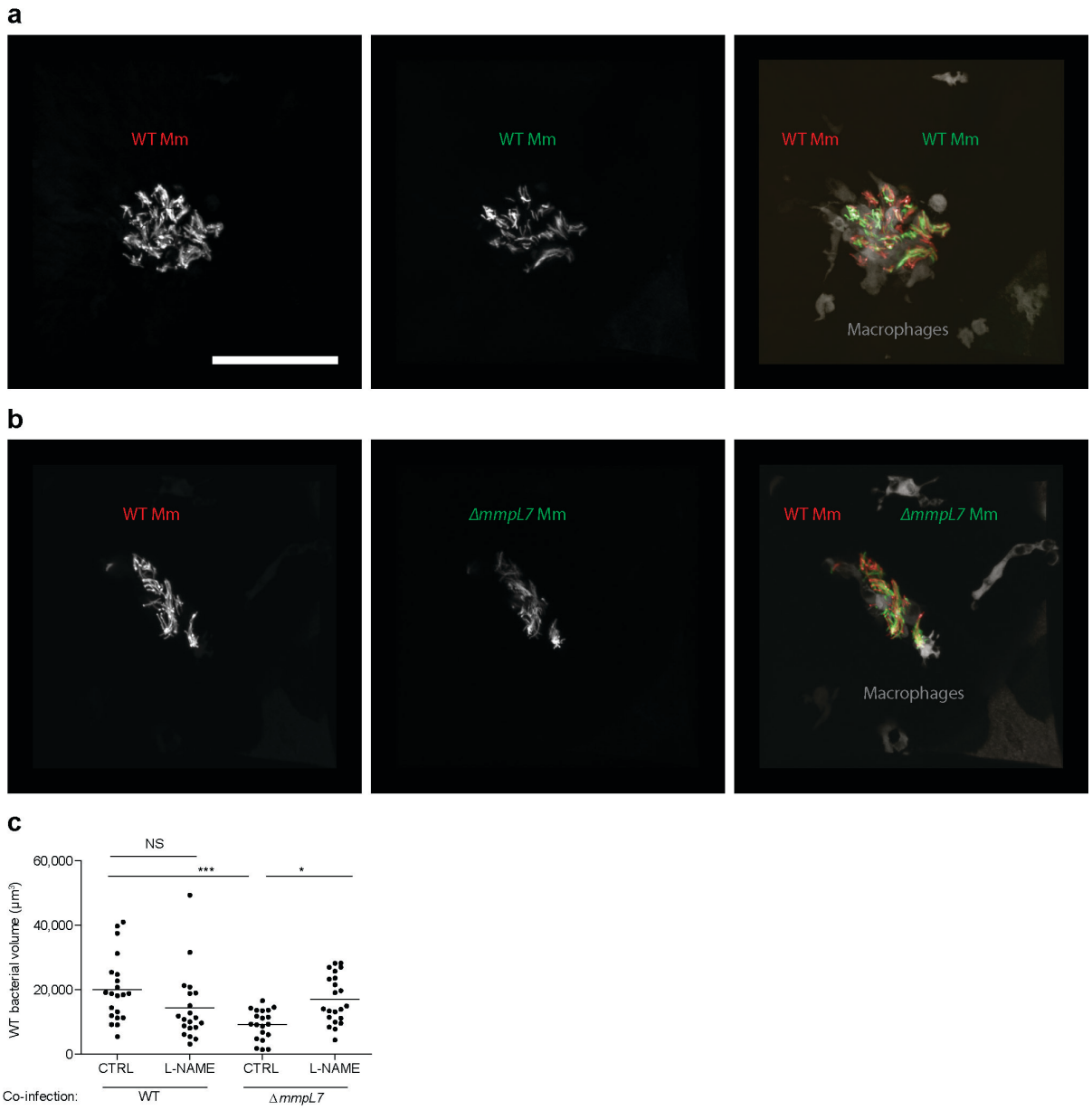

Supplementary Figure 3.5: Wild-type bacterial burdens after co-infection with wild-type or Δ*mmpL7* bacteria. Representative images from the HBV co-infections quantified in Figure 3.2f. **a-b**, Red fluorescent wild-type (WT) *M. marinum* co-infected with green fluorescent wild-type (**a**) or Δ*mmpL7* (**b**) *M. marinum*. Scale bar = 50 µm. **c,** Wild-type bacterial burdens after co-infection with wild-type or Δ*mmpL7 M. marinum* with and without L-NAME treatment.

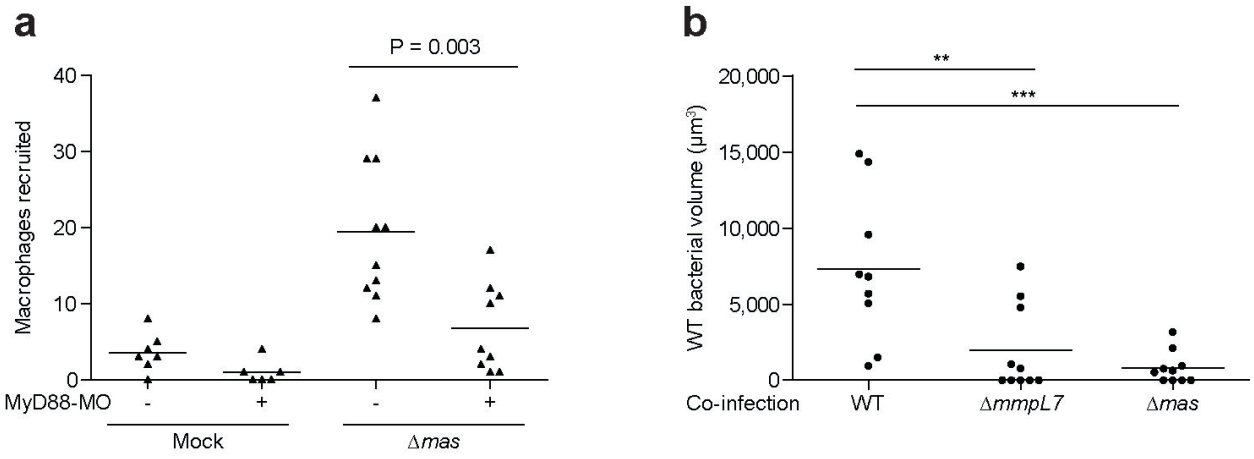

Supplementary Figure 3.6: MyD88-dependent macrophage recruitment occurs in response to PDIM deficiency rather than due to a loss of another MmpL7 exported product. a, Mean macrophage recruitment at 3 HPI into the HBV of wild-type or MyD88 MO larvae following infection with 80 Δ*mas M. marinum*. **b**, Mean surviving bacterial volume of red fluorescent wild-type *M. marinum* (initial infection dose of 30-40 CFU) when co-infected with 30-40 green fluorescent wild-type, Δ*mmpL7* or Δ*mas M. marinum* at 3 DPI. Representative of two separate experiments.

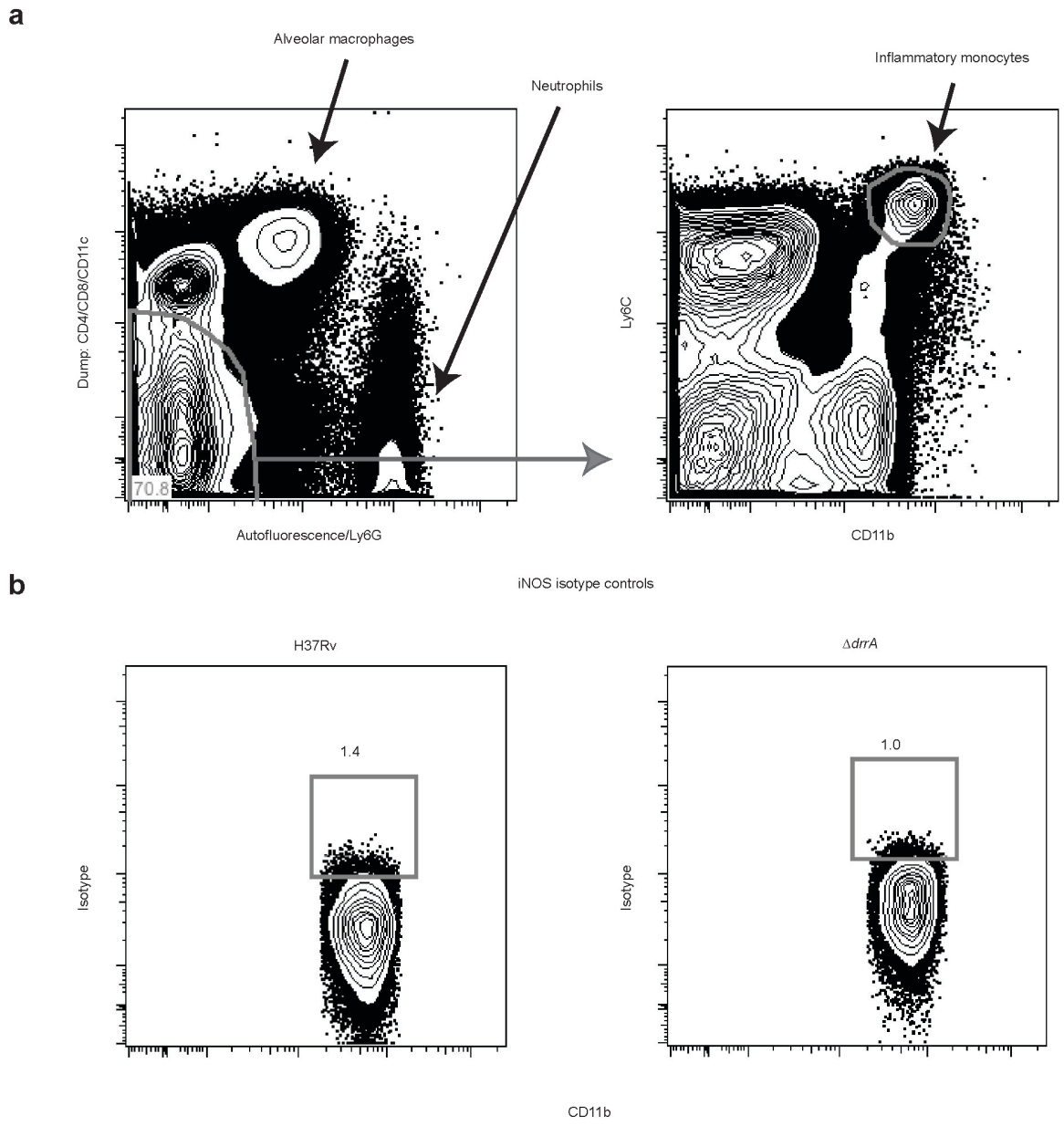

Supplementary Figure 3.7: Gating Strategy and Isotype Controls for iNOS Staining of Mouse Lung. **a,** Representative gating strategy for isolation of inflammatory monocytes. A dump channel containing anti-CD4, CD8, and CD11c was plotted against a channel exhibiting autofluorescence and also containing anti-Ly6G. Using these markers, T cell, dendritic cell, alveolar macrophage, and neutrophil cell populations were excluded from the double negative gate. Inflammatory monocytes were identified within the double negative population by their co-expression of Ly6C and CD11b. These cells were then evaluated for intracellular iNOS expression (Figure 2a,b) or **b**, with isotype control antibodies.

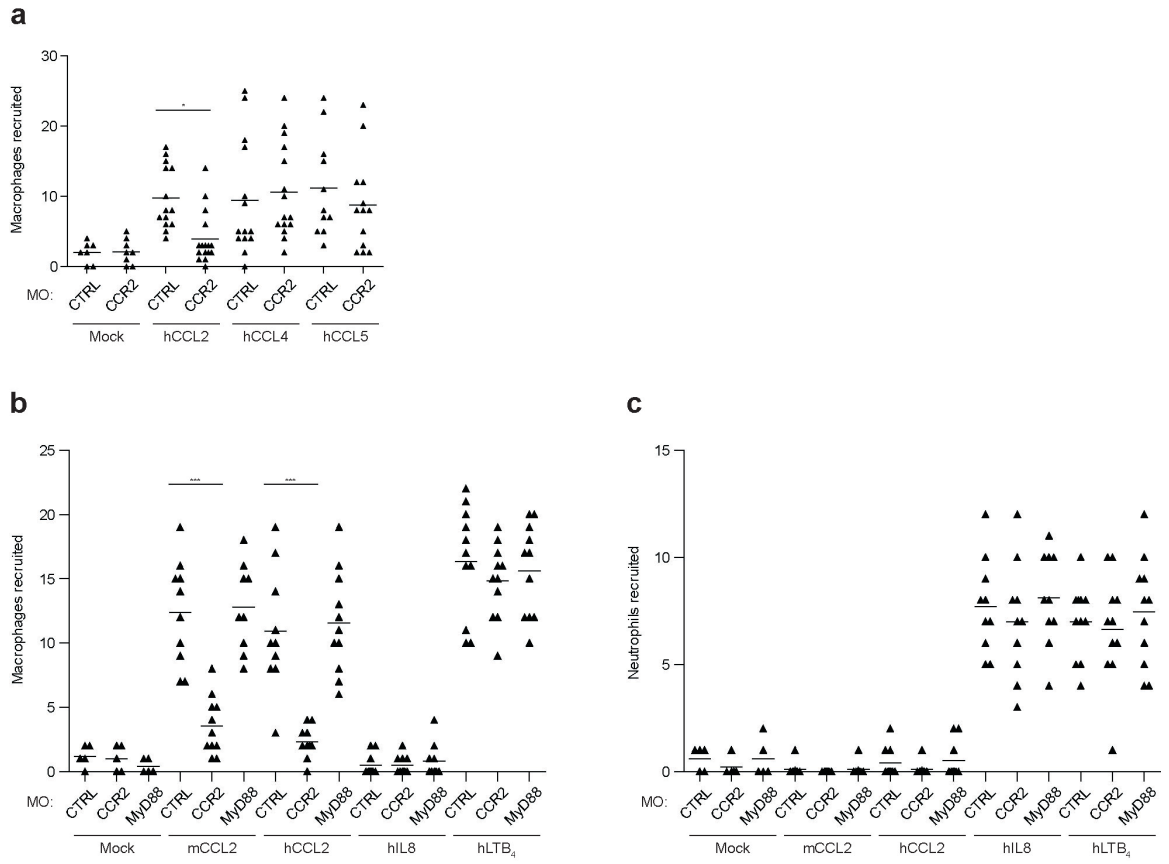

Supplementary Figure 3.8: Specificity of CCL2-mediated macrophage recruitment in wild-type and CCR2 morphant larvae a, Mean macrophage recruitment at 3 HPI into the HBV of control (ctrl), or CCR2 MO (ccr2) larvae following injection of vehicle control ("mock"; 0.1% BSA in PBS), human CCL2 (hCCL2), human CCL4 (hCCL4), or human CCL5 (hCCL5) **b-c,** Mean macrophage (**b**) and neutrophil (**c**) recruitment at 3HPI into the HBV of control (ctrl), CCR2 MO (ccr2), or MyD88 MO (myd88) larvae following injection of vehicle control (mock), murine CCL2 (mCCL2), human CCL2 (hCCL2), human interleukin-8 (hIL-8), or human leukotriene B4 ($hLTB_4$). Representative of three separate experiments. Significance assessed by one-way ANOVA with Bonferroni's post test for the comparisons shown.

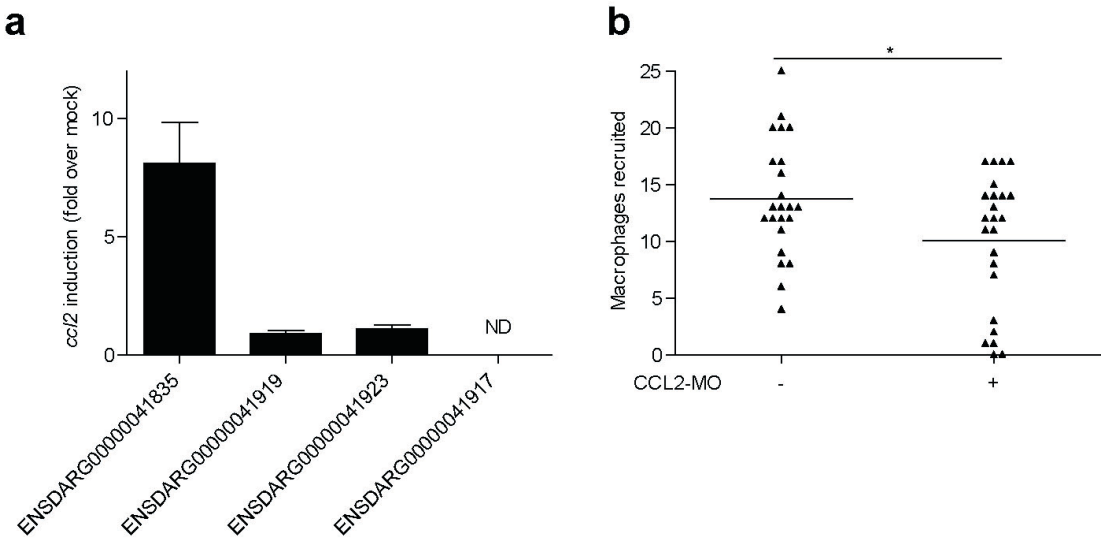

Supplementary Figure 3.9: Identification of zebrafish CCL2 orthologue. **a,** mRNA levels of potential CCL2 orthologues (mean +/- SEM of four individual experiments) induced at 3 hours post caudal vein infection of 2dpf larvae with 250-300 wild-type *M. marinum.* These assays were performed on the same cDNA pools as the data presented in Figure 4b. **b,** Mean macrophage recruitment at 3 HPI into the HBV of wild-type or CCL2 MO fish following infection with 80 *M. marinum*. Representative of two separate experiments.

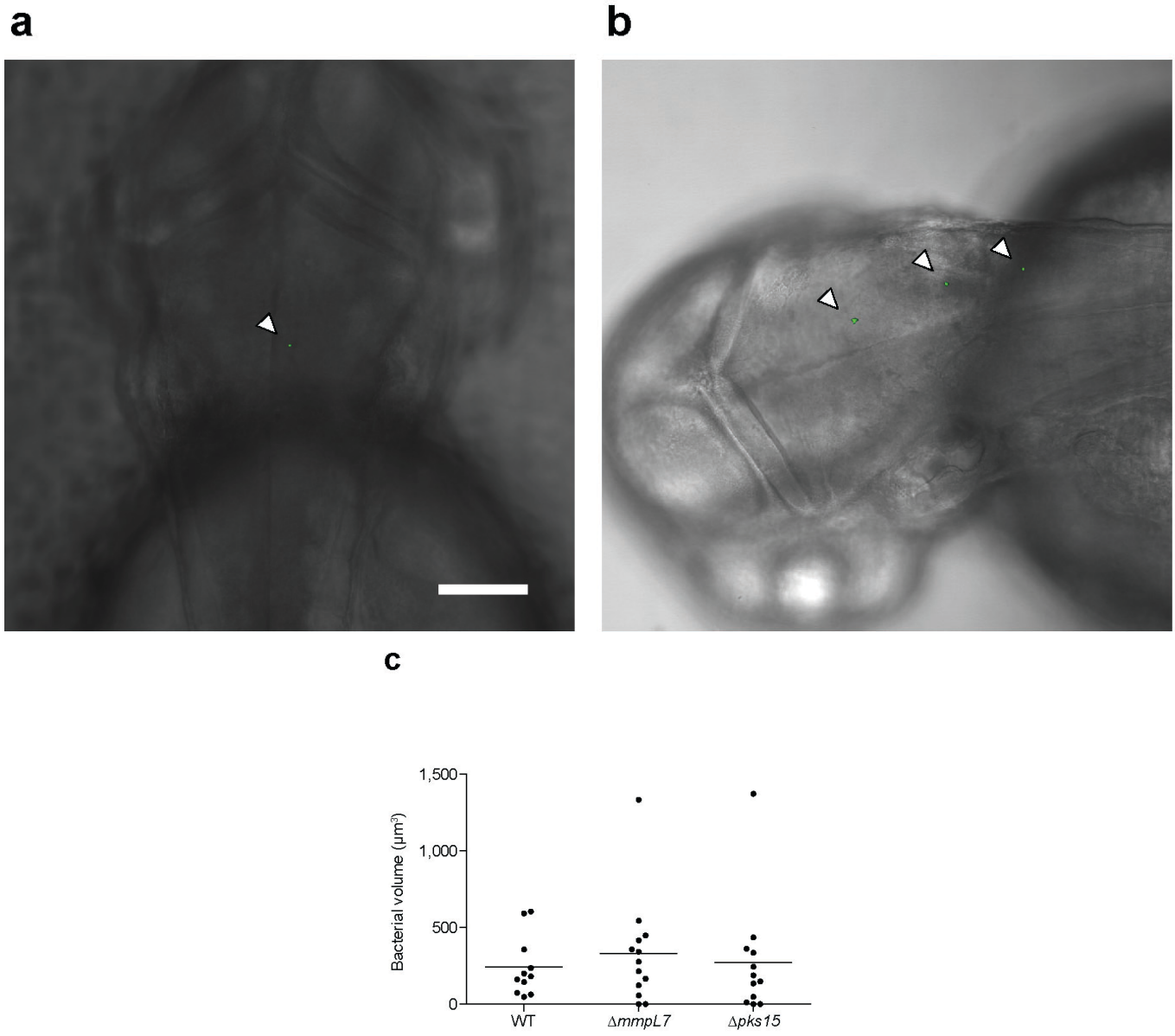

Supplementary Figure 3.10: Infectivity Assay. **a-b**, Representative 5 HPI images from Figure 4d following HBV infection with (**a**) one or (**b**) three *M. marinum*. Scale bar = 100 µm. **c**, Mean bacterial burdens 5 HPI HBV infection with 1-3 wild-type (WT), Δ*mmpL7*, or Δ*pks15 M. marinum*.

Chapter 4: Early Clearance of Pathogenic Mycobacteria by Tissue-Resident Macrophages.

SUMMARY

A Johannes factotum amongst cells, tissue resident macrophages must balance maintaining tissue homeostasis with rapidly responding to infection. *Mycobacterium tuberculosis* is limited to establishing infection via the aerosol route, so it must first encounter tissue resident alveolar macrophages, which we show are the predominant cell type infected following aerosol administration of *M. tuberculosis* in mice. We then demonstrate a conserved and protective first response of tissue resident macrophages towards invading microbes in zebrafish. This protective response is operant against the pathogenic mycobacteria as well. However, the pathogenic mycobacteria have in turn evolved to take advantage of these relatively hostile cells. Their cell surface lipid phthiocerol dimycoceroserate (PDIM) prevents early Toll-like receptor (TLR) detection driven recruitment of iNOS high monocytes, thereby promoting uptake by tissue resident macrophages. The related mycobacterial phenolic glycolipids (PGLs) then induce expression of the macrophage chemokine CCL2 in these resident macrophages to recruit permissive circulating monocytes, to which they can transfer. In the absence of PGL, tissue resident macrophages are 3-4 times more likely to clear infection, whereas direct administration to the bloodstream monocyte compartment restores PGL-deficient mycobacteria's ability to establish infection. These data show how mycobacteria exploit resident macrophages to enter a permissive "transporter" myeloid cell to establish infection within the host.

INTRODUCTION

M. tuberculosis is an incredibly successful pathogen that has made the human lung its exclusive ecological niche. Over an estimated 70,000 years (Comas et al., 2013), *M. tuberculosis* has been under the selective pressures of this niche from which it has developed several mechanisms to evade and manipulate human immune responses. While it has long been thought that *M. tuberculosis* is rarely if ever cleared following infection (Robertson, 1933), recent epidemiological evidence suggests that early clearance does happen following infection (Ewer et al., 2006). This underlying assumption that a protective immune response does not occur has led to a lack of studies focusing on this mechanism. Perhaps the most convincing data that supports the idea of clearance comes from infection in macaques (Lin et al., 2014). Studies found that within the same host, some granulomatous lesions can clear infection, while others are replete with bacteria. These data also demonstrated that most granulomas arise from a single bacterium, suggesting that clearance happens on a case-by-case basis and that heterogeneity exists in the immune response to individual bacteria within the same host (Lin et al., 2014). Furthermore, previous studies have shown that *M. tuberculosis*'s ability to establish infection is limited by the ability of the infectious particle to reach the lower airway. These constraints limit particle size in such a way that particles harboring more than 3 bacteria become lodged in the upper airway where they are readily cleared (Wells et al., 1948). Additionally epidemiological studies have shown that transmission occurs most readily in scenarios where individuals are exposed to infectious particles containing 1-3 bacteria (Bates et al., 1965). When modeling low infectious doses in the zebrafish, we previously showed that wild-type *Mycobacterium marinum* is cleared 10% of the time (Cambier et al., 2014). Therefore we argue that clearance is a potential result of a normal immune response to mycobacterial infection, and that using

physiologically relevant low infectious doses is necessary to study the mechanisms underlying clearance.

In the context of a high infectious dose (100cfu), non-cleared mycobacteria persist and manipulate the immune response on several levels. The most appreciated manipulation of immune responses is the delay in antigen specific T cell responses (Ernst, 2012), which have been demonstrated to be protective in lower vertebrate animal models (Mogues et al., 2001), as well as being associated with disease severity in humans (Shafer et al., 1996). While an appropriate adaptive response is required to prevent infection from overwhelming and eventually killing its host, the 10% clearance we measured following low dose infection in the zebrafish occurred in the absence of an adaptive immune response. Nevertheless, the delay in priming of the adaptive immune response has led to efforts to understand how mycobacteria might manipulate innate immune responses responsible for priming adaptive immunity. These studies have shown that mycobacteria reside in several innate cell populations following infection, including tissue resident alveolar macrophages, monocytes, dendritic cells, and neutrophils (Wolf et al., 2007). Interestingly, the only innate population that is transiently infected with *M. tuberculosis* in the lung is the tissue resident alveolar macrophage population. At day 14 post infection, alveolar macrophages are found to comprise 25% of the total infected cell population. However by day 19 post infection, alveolar macrophages were found to comprise less than 5% of the total infected population. Instead *M. tuberculosis* was found to persist in monocyte populations recruited from the periphery(Wolf et al., 2007). These data suggest that *M. tuberculosis* is actively leaving the intracellular niche of the alveolar macrophage, therefore we hypothesized that tissue resident macrophages are mediating the early clearance events during mycobacterial infection.

Resident macrophage cells can be found in every tissue of the body where their function can be broadly characterized into two areas (Ransohoff and Perry, 2009). To begin with, resident macrophages are often tasked with aiding the development of tissues and their eventual maintenance. These functions often manifest in the form of clearing apoptotic and foreign debris, as well as maintaining anti-inflammatory states to prevent unwarranted tissue damage from infiltrating immune cells (Hussell and Bell, 2014; Ransohoff and Perry, 2009). However, they also respond to infection. They can directly kill invading microbes (Goldstein et al., 1974), can produce inflammatory cytokines to initiate the recruitment of other immune cells (Steinmüller et al., 2000), and are also tasked with promoting healing after bacterial clearance by eliminating pro-inflammatory cells (Cox et al., 1995) and through the production of anti-inflammatory mediators (Laskin et al., 2011). Therefore, functionally speaking, tissue resident macrophages are under higher burdens than their non-tissue resident myeloid counterparts. Besides having distinct functional roles, it is now known that tissue resident macrophages have a distinct ontogeny compared to peripheral myeloid cells (Gomez Perdiguero et al., 2013). Tissue resident macrophages develop from yolk sac derived progenitors and do not depend on hematopoietic stem cells for their maintenance. In contrast, peripheral myeloid cells depend on conventional hematopoietic stem cells derived from the bone marrow for their development and continued maintenance (Gomez Perdiguero et al., 2013). Therefore, it's not surprising that these different macrophage populations behave differently in the context of mycobacterial infection.

Here we demonstrate that tissue resident alveolar macrophages are the predominate cell type harboring *M. tuberculosis* following aerosol infection in the mouse. Taking advantage of the optical transparency of the zebrafish, we show that tissue resident microglia are the first cells to respond to bacterial infection in the hindbrain ventricle (HBV), including in response to *M.*

marinum and the commensal pathogens *Pseudomonas aeruginosa*, and *Staphylococcus aureus*. Using high dose infection (80-100 bacteria) we were able to determine the order in which macrophage populations respond to infecting mycobacteria and the mechanisms underlying this response. We found that pathogenic *M. marinum* prevent detection via TLRs through the expression of PDIM on their surface. This prevented the recruitment of $iNOS^{+}$ monocytes from the periphery and therefore promoted uptake of mycobacteria into tissue resident microglia. However, the occupancy of microglia appeared to be a transient niche if mycobacteria were to establish infection. Using low dose infection (1-3 bacteria) we showed that if mycobacteria did not eventually transfer from microglia into a permissive monocyte then they would be cleared. Mycobacterial PGL was found to induce CCL2 by the infected microglia, which was then responsible for the recruitment of permissive monocytes to the site of infection. Mycobacteria lacking PGL were 3-4 times more likely to be cleared following low dose infection in the HBV. However, if mycobacteria were delivered directly into the blood by caudal vein (CV) injection, then the need for PGL to establish infection was alleviated. These data demonstrate that PGL's role in virulence is to promote the transfer of mycobacteria from the tissue resident macrophage into the immature monocyte compartment, mycobacteria's preferred intracellular niche.

RESULTS

Recruitment of Tissue Resident Macrophages Towards *Mycobacterium marinum*

We previously detailed the mechanisms of macrophage recruitment towards wild-type (WT) *Mm*. We found that the mycobacterial surface glycolipid PGL was required for recruitment of macrophages towards WT *Mm*. PGL was found to be required for the induction of CCL2 following infection, which then drove recruitment of macrophages in a CCR2-

dependent manner (Cambier et al., 2014). However, recruitment of macrophages was not completely abrogated in the absence of PGL. In fact, upon closer examination, recruitment of macrophages towards the PGL deficient Δ*pks15 Mm* strain, while significantly less than macrophage recruitment towards WT *Mm*, was significantly higher than mock injection (Figure 4.1A). Previous studies found that abrogation of mycobacterial lipids led to altered cell wall composition (Gómez-Velasco et al., 2013). Therefore, in order to determine whether or not this minimal recruitment is an artifact of a potential altered cell wall of Δ*pks15 Mm*, we used morpholino knockdown fish to create fish deficient in CCR2, the chemokine receptor previously identified to be required for normal macrophage recruitment towards WT *Mm* (Cambier et al., 2014). Again macrophage recruitment was decreased but still significantly higher than mock injection (Figure 4.1B). In order to determine if this response is unique to PGL stimulated CCL2 signaling we decided to re-examine recruitment towards Δ*mmpl7 Mm*, which lack the MMPL7 transport protein required for PDIM localization on the mycobacterial surface. We previously showed that macrophage recruitment towards this mutant was independent of CCR2 and, instead, was dependent on TLR-MyD88 signaling (Cambier et al., 2014). In the absence of MyD88, recruitment towards Δ*mmpL7 Mm* was decreased but was still significantly above mock injection (Figure 4.1C). Therefore, it appears that while CCR2 and MyD88 are required for normal recruitment towards WT and Δ*mmpL7 Mm* respectively, in their absence macrophage recruitment is not completely abrogated. These data suggest that another signal, independent of CCR2 and MyD88, is operant during infection and is responsible for a portion of the total macrophages being recruited early on. We wondered if this separate signal was operating to recruit a distinct population of macrophages.

Following *M. tuberculosis* infection in the lung, several mononuclear cell populations are found to be infected relatively early during infection, including tissue resident alveolar macrophages and monocyte populations recruited from the periphery (Wolf et al., 2007). Therefore, we wondered if the population of macrophages recruited towards the HBV following infection in the fish is also a mix of tissue resident and peripheral mononuclear cells. The HBV is directly anterior to the brain of the zebrafish which harbor microglia, the tissue resident macrophage population of the brain. While in distinct anatomical compartments, microglia and alveolar macrophages share characteristics unique to tissue dwelling macrophages (Gomez Perdiguero et al., 2013). As is the case for all tissue resident macrophages studied to date, alveolar macrophages and microglia both arise from the *pu.1*-dependent yolk sac progenitors around day 8 of embryonic development (Gomez Perdiguero et al., 2013). Both cells function in maintaining homeostasis at their respective tissue sites, constantly monitoring their environments for apoptotic debris and infectious threats (Hussell and Bell, 2014; Kierdorf and Prinz, 2013). Furthermore, microglia were found to harbor and respond to *M. tuberculosis* infection in a similar manner as alveolar macrophages (Curto et al., 2004). Therefore in order to take advantage of the reliable tractability of responding cellular populations during infections in zebrafish, we decided to study the microglia as a model for tissue resident macrophage responses.

In order to distinguish between microglia and recruited mononuclear cells from the periphery, here after referred to as monocytes, we took advantage of the anatomical localization of microglia to the brain. The nuclear dye Hoechst 33342 is impenetrable to the blood-brain barrier and has previously been used to identify newly arriving macrophages to the nascent granuloma (Davis and Ramakrishnan, 2009). Zebrafish were injected with Hoechst 33342 via

the caudal vein two hours prior to HBV infection. Three hours following infection total macrophages were quantified and identified as either tissue resident microglia (Hoechst 33342 negative) or monocytes (Hoechst 33342 positive). Microglia and monocytes were recruited in equal numbers towards WT *Mm*. Δ*pks15 Mm* recruited equal numbers of microglia as WT and Δ*mmpL7 Mm* but recruited very few monocytes (Figure 4.1E and 4.1D). More importantly, monocyte recruitment towards Δ*pks15 Mm* was not significantly higher than mock injection (Figure 4.1E). Suggesting that Δ*pks15 Mm's* partial defect in total macrophage recruitment (Figure 4.1A) is due to the inability of this mutant to specifically recruit monocytes from the periphery. Consistent with PGL's role in inducing CCL2, we found the CCR2 morphant fish were able to induce recruitment of microglia but not monocytes towards WT *Mm* (Figure 4.1F). Similarly, we found that the partial MyD88-dependent macrophage recruitment towards Δ*mmpL7 Mm* was restricted to the monocyte compartment (Figure 4.1G). Together, these data suggest that mycobacteria recruit microglia independently of CCL2 and TLR-dependent mechanisms.

Alveolar Macrophages are First Responders to *Mycobacterium tuberculosis* Infection in the Lung

Although alveolar macrophages are widely believed to be the first phagocytic cell type to uptake *M. tuberculosis* after aerosol infection, this has not been experimentally shown (Srivastava et al., 2014). Previous studies using GFP expressing reporter strains of *M. tuberculosis* to track infected cells in the murine lung concluded that CD11b+ DCs were the primary infected cell type after day 14 of infection, whereas alveolar macrophages comprised a

minor fraction of the infected cells (Wolf et al., 2007). Assessment of earlier time points was not possible in these studies, perhaps in large part because alveolar macrophages are autofluorescent in the GFP/FITC channel, making it difficult to distinguish infected cells from uninfected alveolar macrophages (Vermaelen and Pauwels, 2004) especially at very early time points when the bacterial burden is quite low. To overcome this problem we infected mice with an *M. tuberculosis* reporter strain expressing mCherry, a fluorescent protein with distinct fluorescent spectra from the autofluorescent signal produced by alveolar macrophages, and left the GFP/FITC channel open to facilitate identification of alveolar macrophages using their autofluorescent properties. Using this strategy we detected *M. tuberculosis* - infected cells with flow cytometry as early as day 8 post-infection (Supplementary Figure 4.1 and 4.2). Between days 8-13, ~40-60% of mCherry+ cells in the lung had an alveolar macrophage phenotype, specifically $CD11c^{HI}$, F4/80+, and autofluorescent (Figure 4.2A and 4.2B). mCherry+ non-alveolar macrophage cells were heterogeneous and difficult to identify phenotypically, most expressed Ly6C, consistent with a monocyte derived population, but low levels of CD11b, which would be inconsistent with the phenotypes of neutrophils or classically defined "inflammatory" monocyte populations, which would both be expected to be $CD11b^{hi}$ (Figure 4.2B and Supplementary Figure 4.3). In contrast to published results after day 14, very few, if any DCs were found within the mCherry+ population prior to day 13 (Figure 4.2B). Overall, these findings provide experimental evidence that alveolar macrophages are a predominant infected cell type at early time points post infection and serve as an important initial reservoir for *M. tuberculosis* in the lung.

Microglia are the First Responders to Infection with *M. marinum* and Commensal Pathogens in the Hindbrain Ventricle of Zebrafish

Considering that alveolar macrophages comprise the predominant infected cell population in the lung relatively early during infection, we wondered if microglia were the first responders during *Mm* infection in the HBV. In order to determine this we again injected Hoechst 33342 into the caudal vein of the fish and then infected the fish 2 hours later. Immediately following infection we quantified macrophage recruitment every 30min for the first 2-3hours. We found that microglia were recruited to half of their maximum recruitment by 30 minutes post infection (Figure 4.3A). Contrary to the 3-hour time point we measured earlier (Figure 4.1F); there was no dependence on CCR2 for microglia recruitment at 30 minutes post infection (Figure 4.3A). Monocyte recruitment did not reach half of its maximum until 60 minutes post infection following WT *Mm* infection and was completely dependent on CCR2 signaling (Figure 4.3A). Microglia were also the first responders to Δ*mmpL7 Mm* infection in a MyD88 independent fashion (Figure 4.3B). Microglia are additionally the first responders to *P. aeruginosa* and *S. aureus* infection (Figure 4.3C and 4.3D). Taken together, our data suggest that tissue resident microglia are the first responders to mycobacterial infection in the HBV, and that this response is conserved among several pathogens.

Microglia Respond to a Secreted Bacterial Signal

Considering that microglia are responding to all of the bacterial challenges we have thus far given suggests that maybe the signal leading to this recruitment is more basic in its origin. A plausible alternative explanation could be that the presence of a foreign body being recognized through mechanosensing at the infection site is driving microglia recruitment (Wang et al.,

2009). To test this hypothesis we used sterile beads to determine if microglia are potentially responding to a non-bacterial specific signal. Neither microglia nor monocytes were recruited towards the sterile beads at levels above mock injection suggesting that a signal that is broadly present in bacteria is required for their recruitment (Figure 4.4A).

Knowing that the signal driving microglia recruitment was bacterial in origin we wanted to know whether the signal is a secreted factor or if the bacteria need to be present to stimulate a response. We decided to screen bacterial supernatants for their ability to induce recruitment. Bacterial cultures were grown to an OD600 of 0.6-0.8, bacteria were pelleted, and supernatants were sterile filtered twice and then immediately injected into the HBV of Hoechst 33342 loaded fish. Microglia were found to be recruited towards WT *Mm* supernatants above mock levels and with similar kinetics as microglia recruited towards in tact mycobacteria (Figure 4.4B). Additionally, Δ*mmpL7 Mm* supernatant also recruited microglia (Figure 4.4C), as well as *P. aeruginosa* and *S. aureus* supernatant (Figure 4.4D and 4.4E). Monocytes were not recruited towards any of the supernatants tested (Figure 4.4A-4.4D). Interestingly, *P. aeruginosa* and *S. aureus* supernatants were able to recruit neutrophils from the periphery. Therefore microglia are responding to a secreted factor, however bacteria need to be present in order to induce recruitment of monocytes to the site of infection.

Heat-killed Mycobacteria and Monocyte Recruitment

Considering that monocytes do not respond to bacterial supernatants, we next wondered if the physical presence alone of mycobacteria would induce monocyte recruitment or if the bacteria need to be living. In order to test this hypothesis we heat-killed mycobacteria at 80C for 20min (Doig et al., 2002), prior to injecting into the HBV of Hoechst 33342 loaded fish. We

found that while heat-killed WT *Mm* did recruit microglia to the site of infection, it did not induce recruitment of monocytes from the periphery (Figure 4.5A). On the other hand, heat-killed Δ*mmpL7 Mm* did recruit monocytes from the periphery with the same kinetics as live Δ*mmpL7 Mm* (Figure 4.5B). Therefore, it appears that not only are the signaling pathways recruiting monocytes towards WT *Mm* and Δ*mmpL7 Mm* distinct, CCR2 and MyD88 respectively, but now the mechanism leading to the activation of these two pathways appears to be different.

Distinct Monocyte Kinetics Between WT and Δ*mmpL7 Mm* Infection

Evaluating the independent kinetics data of WT *Mm* (Figure 4.3A) and Δ*mmpL7 Mm* (Figure 4.3B) suggests that monocyte recruitment is on par between the two strains. However, given the sensitive nature of the experiment to infectious dose and age of fish, we wanted to compare the strains head to head. WT *Mm* displayed their characteristic response: by 30 minutes only microglia were recruited, with monocyte recruitment lagging (Figure 4.5C). Similar to WT, Δ*mmpL7 Mm* have about half of their microglia responding by 30min, but in contrast to WT *Mm*, monocytes are recruited at 30min towards Δ*mmpL7 Mm* (Figure 4.5C). About half of the maximum monocyte recruitment occurs in the first 30min towards Δ*mmpL7 Mm*, similar to the microglia response (Figure 4.5C). This difference in kinetics suggests that the mechanism behind driving monocyte recruitment towards Δ*mmpL7 Mm* is happening sooner than the mechanism responsible for driving monocyte recruitment towards WT *Mm*.

Live WT *Mm* and Macrophages are Required for *ccl2* Induction

The lack of monocyte recruitment towards heat-killed WT *Mm* suggests that PGL as well as another active process are required to induce *ccl2*. In order to determine that the lack of monocyte recruitment was in fact due to a loss of Ccl2 production and not another, as of yet unidentified signal, we measured *ccl2* expression following infection with heat-killed WT *Mm*. *ccl2* was 10 fold induced over mock injection following infection with in tact WT *Mm*, while induction was significantly reduced to roughly 1.5 fold following infection with heat-killed WT *Mm* (Figure 4.5D). Considering that the recruitment kinetics are such that microglia respond 30min prior to monocyte responses, that WT *Mm* need to be alive and expressing PGL to recruit monocytes, and that PGL induced Ccl2 is required for monocyte but not microglia recruitment led us to the hypothesis that microglia are responsible for the *ccl2* expression following infection. To test this hypothesis we depleted macrophages prior to infection with a morpholino against the myeloid specific transcription factor PU.1(Tobin et al., 2010). Without macrophages fish were unable to express *ccl2* following infection with WT *Mm* (Figure 4.5E).

Microglia are Required for Normal Monocyte Recruitment Towards WT *Mm*

While we have shown that macrophages are required for *ccl2* induction following infection, we still have not determined whether or not microglia are required for recruiting monocytes towards WT *Mm*. In order to address this question directly, we decided to use the *panther* zebrafish mutants, which lack a functional macrophage colony stimulating factor receptor (M-CSFR) (Herbomel et al., 2001). *Panther* fish have normal monocyte development but have decreased development of tissue resident macrophages, including microglia. To count macrophages in the brain tissue of fish we used neutral red, which stains lysosomes bright red

and makes distinguishing microglia from neighboring brain tissue possible (Davis and Ramakrishnan, 2009). *Panther* fish on average contained only five microglia compared to the twenty in wild-type fish (Supplementary Figure 4.4). Following infection with both WT and Δ*mmpL7 Mm* we saw a delay in the kinetics of microglia recruitment in the *panther* mutants compared to wild-type fish, which is expected given their deficiency in microglial numbers to begin with (Figure 4.5F and 4.5G). WT *Mm* failed to induce a robust monocyte response following infection in *panther* mutants (Figure 4.5F). However, Δ*mmpL7 Mm* recruited monocytes just as robustly in the *panther* mutants compared to wild-type fish (Figure 4.5G). These data demonstrate that tissue resident microglia are required for the recruitment of monocytes towards WT *Mm*, but are dispensable for the recruitment of monocytes towards Δ*mmpL7 Mm*. Similar to the monocyte response to Δ*mmpL7 Mm*, the neutrophil response to *P. aeruginosa* and *S. aureus* was unaffected in the *panther* mutants (Supplementary Figure 4.5). The difference in kinetics of the monocyte response towards WT and Δ*mmpL7 Mm* and now the differential requirement for microglia to induce this response, suggests that WT *Mm* use PDIM not only to avoid MyD88 dependent detection but to also avoid earlier detection by a non-macrophage cell population.

Microglia are Responsible for Δ*pks15 Mm's* Decrease in Infectivity

Previously we found that CCR2-dependent recruitment in response to PGL was required for mycobacteria to establish infection following low infectious doses, highlighting its role in increasing bacterial fitness through increasing transmission (Cambier et al., 2014). By infecting fish with 1-3 bacteria, the predicted infectious dose during transmission of *M. tuberculosis* amongst humans (Bates et al., 1965), and then screening for the presence of bacteria at 5 days

post infection, we can model infectivity, an important step in transmission. Δ*pks15 Mm* were previous shown to be attenuated during infectivity, only being able to establish infection in ~20% of injected fish, compared to the ~89% of fish that remained infected following injection of 1-3 WT *Mm*. Now that we know the only macrophages responding to Δ*pks15 Mm* during infection in the HBV are microglia, we wondered if this population was responsible for Δ*pks15 Mm's* decreased infectivity. Again using the PU.1 morpholino to deplete macrophages, we found that Δ*pks15 Mm's* defect in infectivity was rescued in the absence of microglia (Figure 4.6A). Thus suggesting that microglia are responsible for the decrease in Δ*pks15 Mm's* infectivity.

Microglia are the First Infected Cell Population Following High and Low Dose Infections

While high dose infection (80-100 bacteria) has allowed us to better understand the mononuclear cell response towards mycobacteria, we wanted to know how these responses compared to low dose infections. Since PGL's role in virulence is only uncovered during low dose infection, evaluation of the cellular response in this context is warranted. Based on the results of our high dose kinetics assays, we believe the cellular mechanism driving the infectivity attenuation of Δ*pks15 Mm* is its inability to recruit and eventually infect the monocyte population. Instead, Δ*pks15 Mm* remain within microglia, which we believe is driving its attenuation. In order to evaluate the cellular response to low dose infections, we decided to take a more rigorous approach and monitored infection in Tg(*mpeg1*:YFP) zebrafish, transgenic fish previously shown to specifically label macrophages through the production of YFP downstream of the promoter for the macrophage specific gene *mpeg1* {Cambier, 2014, Mycobacteria manipulate macrophage recruitment through coordinated use of membrane lipids}. Injecting

these fish with Hoechst 33342 allowed us to distinguish microglia from monocytes by confocal microscopy every 10 min from 1-13 hours post infection. Very few microglia were recruited at any given time point post infection, and even fewer monocytes were recruited within the first 16 hours (Figure 4.6B). Next we noticed that on average the bacteria remained extracellular in the HBV until 7 hours post infection (Figure 4.6C), and of all the 28 fish imaged during these experiments, every extracellular bacterium was phagocytosed by a tissue resident microglia. This is both similar to and different from what we see following high dose infection. It differs because following high dose infection we see that bacteria are already phagocytosed by thirty minutes, but it is similar because in both cases, microglia are the first cells to respond and to become infected.

WT *Mm* Remain in the Initial Infected Microglia for the First 54-66 Hours Following Low Dose Infection

In order to determine if and when monocytes serve as intracellular reservoirs for mycobacteria following a low dose infection, we imaged cohorts of 7-8 Tg(*mpeg1*:YFP) fish infected with TdTomato expressing WT *Mm* over time periods comprising 1-108 hours (4.5 days) post infection. For the first 48 hours we were able to image fish for 12-hour periods with no photobleaching evident, and from 48-108 hours, we were able to image the fish for 6-hour periods. Separate fish were imaged for each time period, as sequential imaging of the same fish for these durations influenced cellular behavior (data not shown). We found that WT *Mm* remained in the first microglia cell they infected for up to 54 hours post infection (Figure 4.6D). From 54 to 90 hours post infection infected cells were found to be overtaken by uninfected cells, a process we termed a transfer event, with the majority of events occurring from 66 to 72 hours

post infection (Figure 4.6D, 4.6F, and 4.6G). This data argues that a majority of WT *Mm* remains in the first infected microglia for the first 66 hours (2.75 days) post infection.

Microglia are More Restrictive to WT *Mm* Growth than Monocytes

Calculating the bacterial volume over the first 24 hours post infection in the HBV revealed a significant decrease in bacterial volume from between the 2 hour and 22 hour time point, suggesting that microglia are not only restricting bacterial growth but are also killing bacteria (Figure 4.6E). These data, along with our previous findings that in the absence of a strong monocyte response mycobacteria are less efficient at establishing infection led us to hypothesize that microglia are more restrictive to intracellular mycobacterial growth than monocytes. Our observations that WT *Mm* are restricted to the microglia niche following low dose HBV infection for 2.75 days allowed us to formally address this hypothesis. 2dpf fish were injected with an infectious dose of 0.5 bacteria per fish into the HBV or the CV. Fish were then screened for those receiving a single bacterium. Bacterial volume was then determined using confocal microscopy at 1 and 4dpi. While after 24 hours bacterial volume was indistinguishable between HBV and CV, by 4dpi the bacterial volume was significantly higher in the CV compared to the HBV (Figure 4.7A). Even despite being extracellular for an additional 7 hours in the HBV compared to the CV (Figure 4.6C), mycobacteria were still able to grow better in the monocyte compartment. These data suggest that monocytes represent a more favorable niche for mycobacteria to thrive in.

Mycobacteria's Dependence on PGL Induced CCL2 Expression to Establish Infection is Relieved During Caudal Vein Injections

Taken together our data suggest that the reason why PGL deficient mycobacteria, as well as WT *Mm* in the context of a CCR2 deficient host, have a defect in establishing infection is due to the fact that they are restricted to the microglial niche following HBV infection. If this restrictive cellular compartment is the reason PGL deficient mycobacteria cannot establish infection, then bypassing this compartment by directly testing infectivity in the CV should rescue PGL deficient mycobacteria's infectivity defect. Following infection of 1-3 bacteria, Δ*pks15 Mm* were significantly decreased in their infectivity rates compared to WT *Mm* in the HBV. However, their infectivity rates were on par with WT *Mm* following infection in the CV (Figure 4.7B). Additionally, CCR2 no longer appeared to be a susceptibility factor in the context of establishing infection when challenged via the CV route. CCR2 morphants were resistant to WT *Mm* establishing infection during the HBV infectivity assay but not the CV infectivity assay (Figure 4.7C). Therefore, mycobacteria actively induce *ccl2* expression through the production of PGL in order to reach the monocyte niche, which is more permissive to mycobacterial growth. Additionally, considering that Δ*mmpL7 Mm* recruit iNOS high monocytes independently of microglia, suggests that they are being recognized independently of tissue resident macrophages. Therefore we hypothesized that their defect in infectivity should not be rescued during CV challenge, which was the case (Figure 4.7D).

DISCUSSION

Our data suggest that, in the context of physiologically relevant infectious doses of mycobacteria, responding tissue resident macrophages are capable of clearing a portion of the

infection. These data help to explain the epidemiological findings that contacts of sputum-smear positive individuals convert to a positive tuberculin skin test only 30-50% more often than age-matched community controls(Sepkowitz, 1996). A number that is shockingly low considering the reliably high bacterial burdens following aerosol dose infection of mice with only 100 bacteria (Shafiani et al., 2010). This host clearance mechanism is clearly not absolute and, considering that *M. tuberculosis* is still a thriving global pathogen, demonstrates that it has evolved ways to overcome this response.

The cellular immune response to *M. tuberculosis* is an important mediator of its pathogenesis given that it ultimately results in the formation of the hallmark structures of tuberculosis, the granuloma. While classically believed to be a host protective structure that functions to wall off the invading pathogen, granulomas have also been shown to facilitate expansion of mycobacteria's preferred intracellular niche (Ramakrishnan, 2012). Additionally, the finding that granulomas form in the absence of adaptive immunity (Davis et al., 2002), further promotes the idea that granulomas are beneficial to bacterial growth, which is often unchecked in the absence of adaptive immune responses (Ernst, 2012). We rationalized that understanding how mycobacteria manipulate this early cell response to arrive at its preferred intracellular niche within the granuloma, would allow us to understand which cells mycobacteria prefer to call home.

We found that tissue resident macrophages were the first responders to a number of bacterial challenges in the zebrafish, suggesting that this response is a conserved host response to invading pathogens. Interestingly, mycobacteria did not remain in these tissue resident populations and, if not cleared by tissue resident macrophages, eventually took up residence within a recruited peripheral monocyte population. We showed that to reach this population two

bacterial factors were required. First mycobacteria needed to express the surface associated lipid, PDIM. PDIM prevented MyD88-dependent detection of mycobacteria by a yet unknown cell type. This detection occurred independently of tissue resident macrophages and resulted in the recruitment of $iNOS^+$ monocytes to the infection site that were detrimental to the bacteria establishing infection. In the presence of PDIM, mycobacteria only recruited tissue resident macrophages early in infection, and these cell types were the first to be infected. Once inside the tissue resident macrophage population, we found that the surface lipid PGL was required to induce CCL2 by these tissue resident macrophages to drive recruitment of $iNOS^-$ monocytes from the periphery. If mycobacteria lacked PGL they were 3-4 times less likely to establish infection at tissue sites. However, if PGL deficient bacteria were delivered directly into the blood stream, bypassing any tissue resident macrophages, they were able to establish infection at the same rate as WT mycobacteria. Furthermore, comparison of bacterial burdens following infection with a single bacterium showed that WT mycobacteria grew faster in monocytes than in microglia. Therefore we propose that CCL2 elicited monocytes represent mycobacteria's preferred intracellular niche, a claim that is not only supported by our data. CCL2 recruited monocytes have been previously shown to be more permissive to *M. tuberculosis* growth in the lungs of mice (Antonelli et al., 2010), and mice overexpressing CCL2 were found to be more susceptible to challenge with *M. tuberculosis* (Rutledge et al., 1995).

The development of an effective vaccine against *M. tuberculosis* is truly the ultimate goal for the mycobacterial research community. Therefore, understanding the immune responses that result in clearance of the pathogen is key to developing strategies to amplify these responses. Given that recent epidemiological studies saw clearance of *M. tuberculosis* infections in the absence of immunological memory (Ewer et al., 2006), suggest a clearance mechanism that is

present during the early stages of the innate immune response. However, granuloma sterilization in a model of Mycobacterium tuberculosis infection suggests that clearance might also be partially mediated by an intact adaptive immune response (Lin et al., 2014), although formal testing of this is still needed. Nevertheless, our data demonstrates that clearance does happen in an unimmunized host. Determining the molecular mechanisms underlying the ability of tissue resident macrophages to clear infection and whether or not these can be artificially amplified will prove valuable to the development of an effect vaccine against *M. tuberculosis*.

METHODS

Bacterial Strains and Methods. *M. marinum* strain M (ATCC BAA-535) Δ*mmpL7,* and Δ*pks15* mutants have previously been described(Cambier et al., 2014). To prepare heat-killed *M. marinum,* bacteria were incubated at 80°C for 20 minutes. The *P. aeruginosa* PAO1 fluorescent strain has been described(Brannon et al., 2009). The *S. aureus* Newman strain expressing pOS1-SdrC-mCherry #391 was a gift from Dr. Juliane Bubeck Wardenburg.

Zebrafish Husbandry and Infections. Wild-type AB zebrafish were maintained as described(Takaki et al., 2013). Larvae (of undetermined sex given the early developmental stages used) were infected at 36–48 hours post-fertilization (hpf) via caudal vein or hindbrain ventricle injection using thawed single-cell suspensions of known titer(Takaki et al., 2012; Takaki et al., 2013). Number of animals to be used for each experiment was guided by past results with other bacterial mutants and/or zebrafish morphants. Larvae were randomly allotted to the different experimental conditions. Zebrafish husbandry and all experiments performed on them were in compliance with Institutional Animal Care and Use Committee approved protocols.

Microscopy and Image-Based Quantification of Infection Level. Larvae were imbedded in 1.5% agarose (low melting point)(Davis and Ramakrishnan, 2009). A series of z-stack images with a 2 μm step size was generated through the infected HBV, using the galvo scanner (laser scanner) of the Nikon A1 confocal microscope with a 20x Plan Apo 0.75 NA objective. Bacterial burdens were determined by using the 3D surface-rendering feature of Imaris (Bitplane Scientific Software)(Yang et al., 2012).

Hindbrain Assays. Macrophage recruitment assays were performed as previously described(Takaki et al., 2013). For determination of hindbrain ventricle infection burdens, 1 and 3 DPI larvae were mounted in 1.5% agarose and confocal z-stacks of 2 μm were obtained.

Hoechst Dye. Embryos were injected with 200 mg/ml Hoechst 33342 (Invitrogen) via caudal vein as previously described(Davis and Ramakrishnan, 2009).

Morpholinos. CCR2 and MyD88 morpholinos previously described(Cambier et al., 2014) were injected into the 1-4 cell stage of the developing embryo(Tobin et al., 2010).

Quantitative Real-time PCR (qRT-PCR). cDNA was synthesized from pools of 20-40 larvae as previously described(Clay et al., 2007). Quantification of ccl2 RNA levels were determined using SYBR green and the following primer pair; 5'GTCTGGTGCTCTTCGCTTTC3' and 5'TGCAGAGAAGATGCGTCGTA3'.

Infectivity Assay. 2 DPF larvae were infected via the HBV with an average of 0.8 bacteria per injection. Fish harboring 1-3 bacteria were then identified at 5 HPI by confocal microscopy. These infected fish were then evaluated at 5 DPI and were scored as infected or uninfected, based on the presence or absence of fluorescent bacteria.

Statistics. Statistical analyses were performed using Prism 5.01 (GraphPad). Post-test *P* values are as follows: **P* < 0.05; ***P* < 0.01; ****P* < 0.001.

Chapter 4 Figures

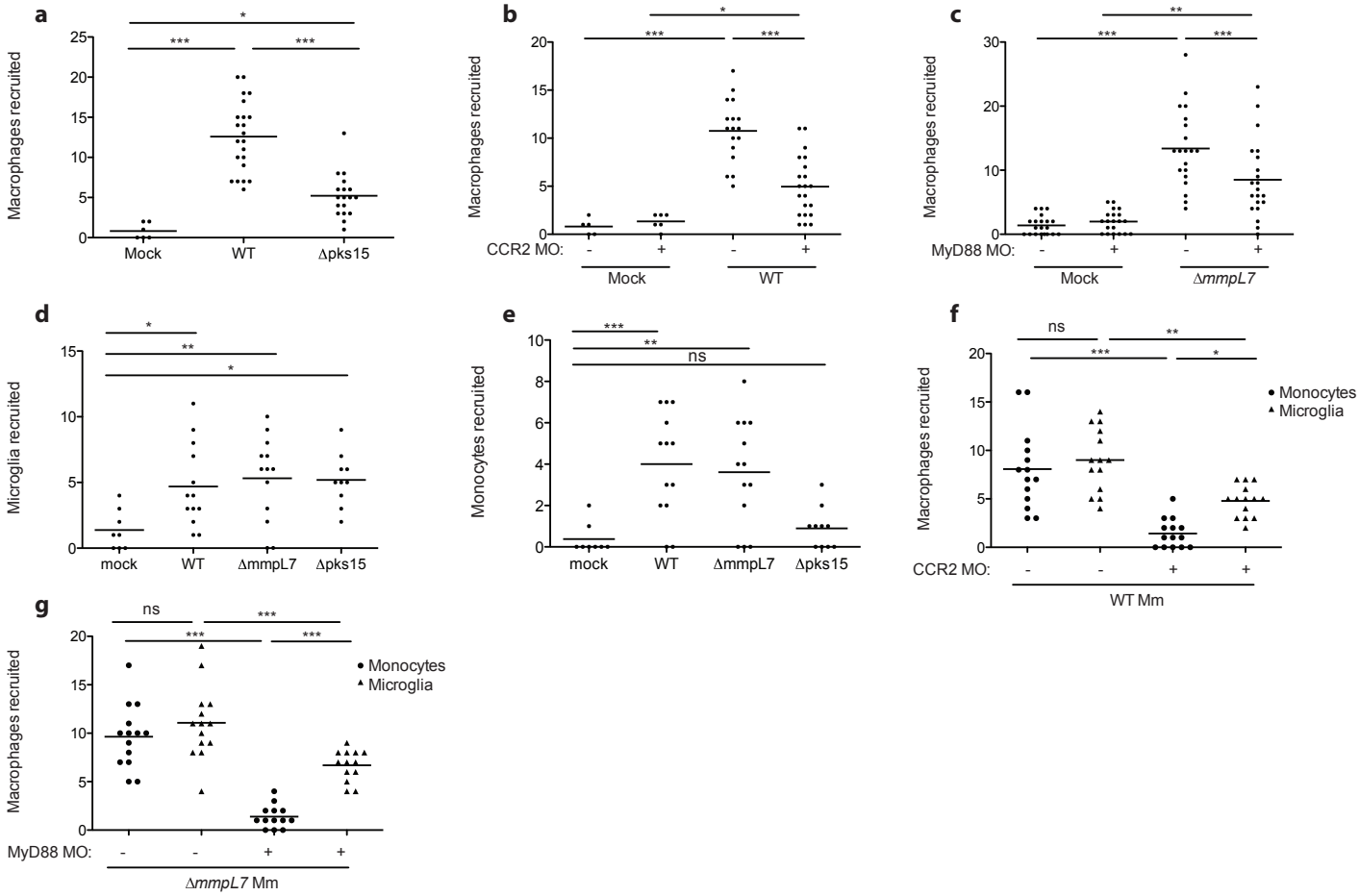

Figure 4.1: Recruitment of Tissue Resident Microglia Towards *Mycobacterium marinum.* (A) Mean macrophage recruitment at 3 h post-infection (hpi) into the HBV after infection with 80 WT or Δpks15 Mm. (B) Mean macrophage recruitment at 3hpi into the HBV of wild-type or CCR2-morphant fish after infection with 80 WT Mm. (C) Mean macrophage recruitment at 3hpi into the HBV of wild-type or MyD88-morphant fish after infection with 80 ΔmmpL7 Mm. (D-E) Mean microglia (D) or monocyte (E) recruitment at 3hpi into the HBV of wild-type fish after infection with 80 WT, ΔmmpL7, or Δpks15 Mm. (F) Mean monocyte and microglia recruitment at 3hpi into the HBV of wild-type or CCR2-morphant fish after infection with 80 WT Mm. (G) Mean monocyte and microglia recruitment at 3hpi into the HBV of wild-type or MyD88-morphant fish after infection with 80 ΔmmpL7 Mm. Results in (A)-(E) representative of at least 3 separate experiments. Significance testing done using one-way ANOVA, with Bonferroni's post-test for comparisons shown. *$P < 0.05$, **$P < 0.01$, ***$P < 0.001$.

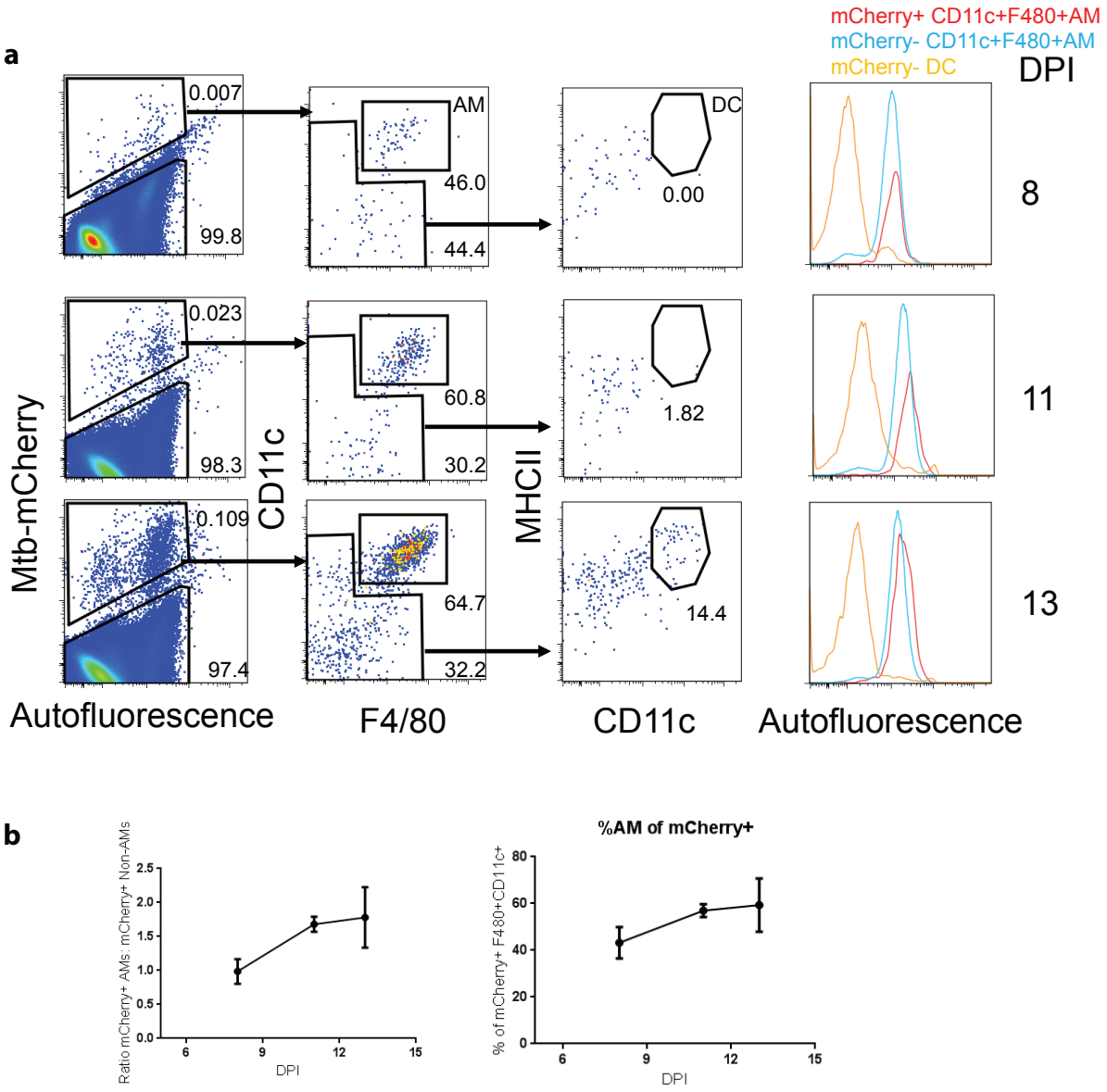

Figure 4.2: Alveolar Macrophages are the Predominant Infected Cell Type in the Lung Prior to Day 14 Post Infection with H37Rv. B6 mice were infected via the aerosol route with ~200 colony forming units of H37Rv expressing mCherry, sacrificed on days 8, 11, and 13 post infection and lungs analyzed for infected myeloid cell subsets. (A) Identification of infected mCherry+ and uninfected mCherry- myeloid cells in the lungs on days 8, 11 and 13 post infection. Alveolar macrophages are identified by F480 and CD11c expression whereas DCs are CD11c+F480-. Autofluorescence can be used to further identify alveolar macrophages. The far right column demonstrates the autofluorescent nature of mCherry- and mCherry+ CD11c+F480+ macrophages compared to mCherry- CD11c+MHCII+ DCs within the same lung. (B) Alveolar macrophages are the predominant mCherry+ infected cell type in the lung as shown by the ratio of mCherry+ CD11c+F480+ alveolar macrophages to mCherry+ non-alveolar macrophages and percent of mCherry+ cells with an alveolar macrophage phenotype. Representative of two separate experiments.

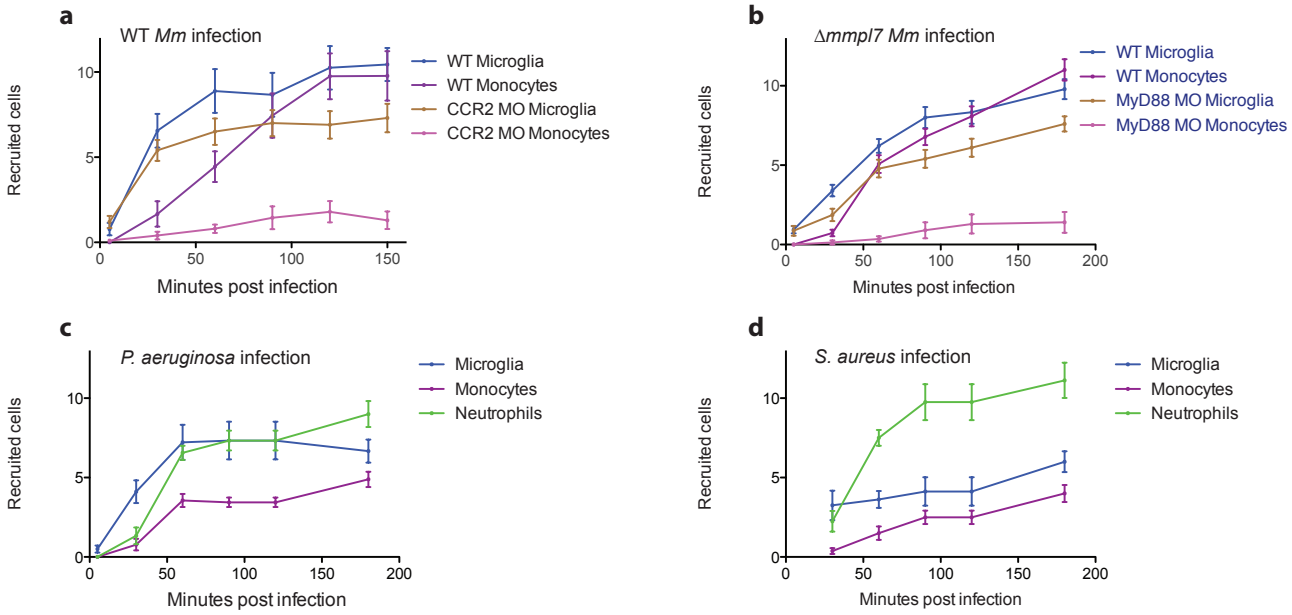

Figure 4.3: Microglia are the First Myeloid Cell Population to Respond to *Mycobacterium marinum* Infection in the HBV. (A) Mean microglia and monocyte recruitment from 5 to 150 minutes post infection (mpi) in the HBV of wild-type or CCR2-morphant fish after infection with 80 WT Mm. (B) Mean microglia and monocyte recruitment from 5 to 180mpi in the HBV of wild-type or MyD88-morphant fish after infection with 80 ΔmmpL7 Mm. (C-D) Mean microglia, monocyte, and neutrophil recruitment from 5 to 180mpi in the HBV of wild-type fish following infection with 156 P. aeruginosa (C) or 138 S. aureus (D). Results in (A) – (D) representative of two separate experiments.

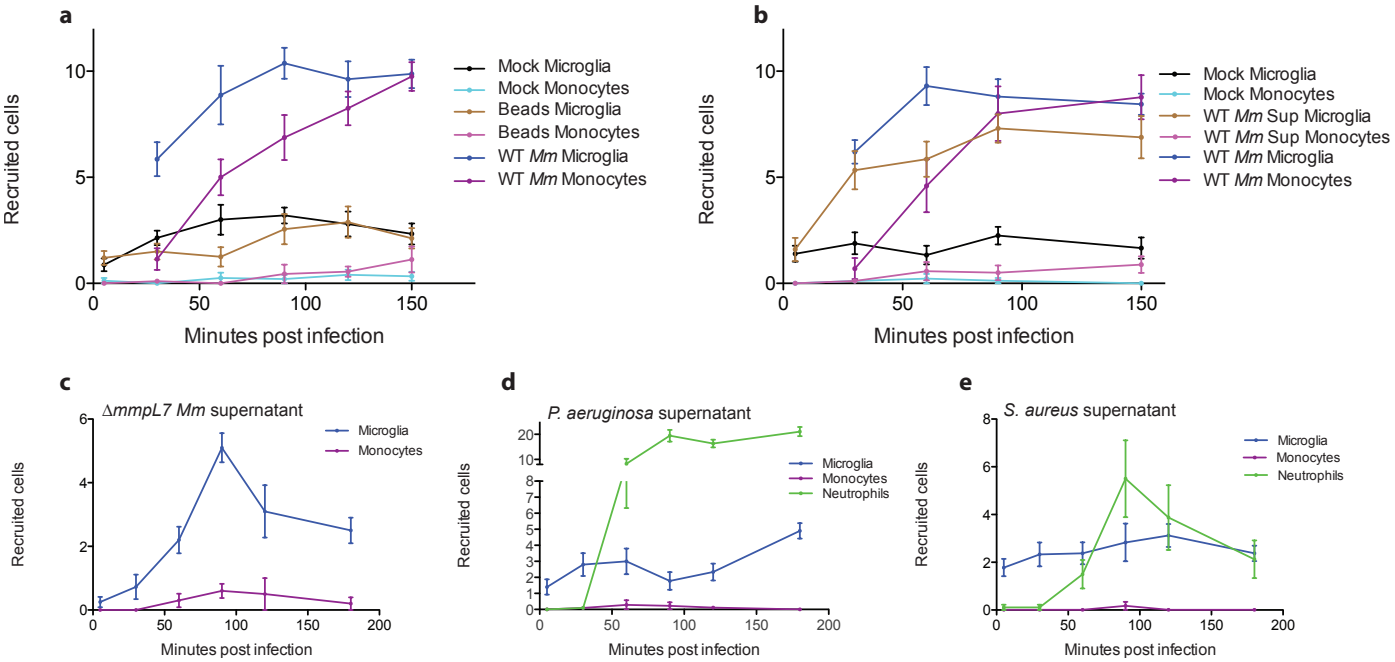

Figure 4.4: Microglia Respond to a Secreted Bacterial Factor. (A) Mean microglia and monocyte recruitment from 5 to 150mpi in the HBV of wild-type fish after injection with 300 Beads or infection with 80 WT Mm. (B) Mean microglia and monocyte recruitment from 5 to 150mpi in the HBV of wild-type fish after injection with WT Mm supernatant (Sup) or infection with 80 WT Mm. (C) Mean microglia and monocyte recruitment from 5 to 150mpi in the HBV of wild-type fish after injection with ΔmmpL7 Mm supernatant. (D-E) Mean microglia and monocyte recruitment from 5 to 150mpi in the HBV of wild-type fish after injection with P. aeruginosa supernatant (D) or S. aureus supernatant (E). Results in (A) – (E) representative of two separate experiments.

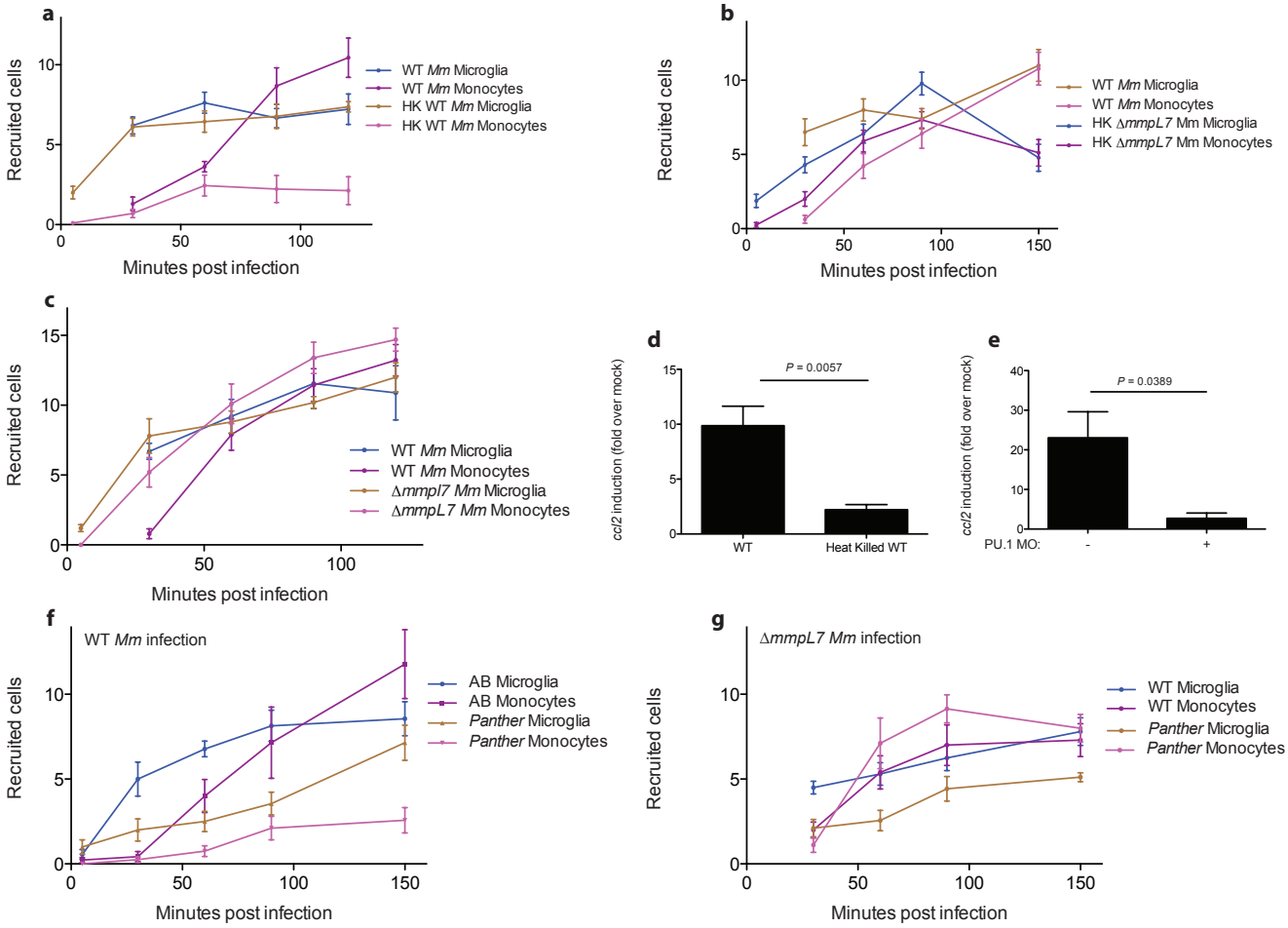

Figure 4.5: Microglia are Required for Monocyte Recruitment Towards WT but not Δ*mmpL7 Mycobacterium marinum*. (A-B) Mean microglia and monocyte recruitment from 5 to 150mpi in the HBV of wild-type fish after infection with 80 WT Mm and 80 heat-killed (HK) WT Mm (A) or 80 HK ΔmmpL7 Mm (B). (C) Mean microglia and monocyte recruitment from 5 to 150mpi in the HBV of wild-type fish after infection with 80 WT or ΔmmpL7 Mm. (D) *ccl2* messenger RNA levels (mean +/- standard error of the mean (s.e.m.) of four biological replicates) induced at 3 h after caudal vein infection of 2 dpf fish with 250–300 WT or 250-300 HK WT Mm. (E) *ccl2* messenger RNA levels (mean +/- s.e.m. of three biological replicates) induced at 3 h after caudal vein infection of 2 dpf wild-type or PU.1 morphant fish with 250–300 WT Mm. (F-G) Mean microglia and monocyte recruitment from 5 to 150mpi in the HBV of wild-type or *panther* mutant fish after infection with 80 WT Mm (F) or 80 ΔmmpL7 Mm (G). (A) – (G) Representative of at least three separate experiments. Student's unpaired *t*-test.

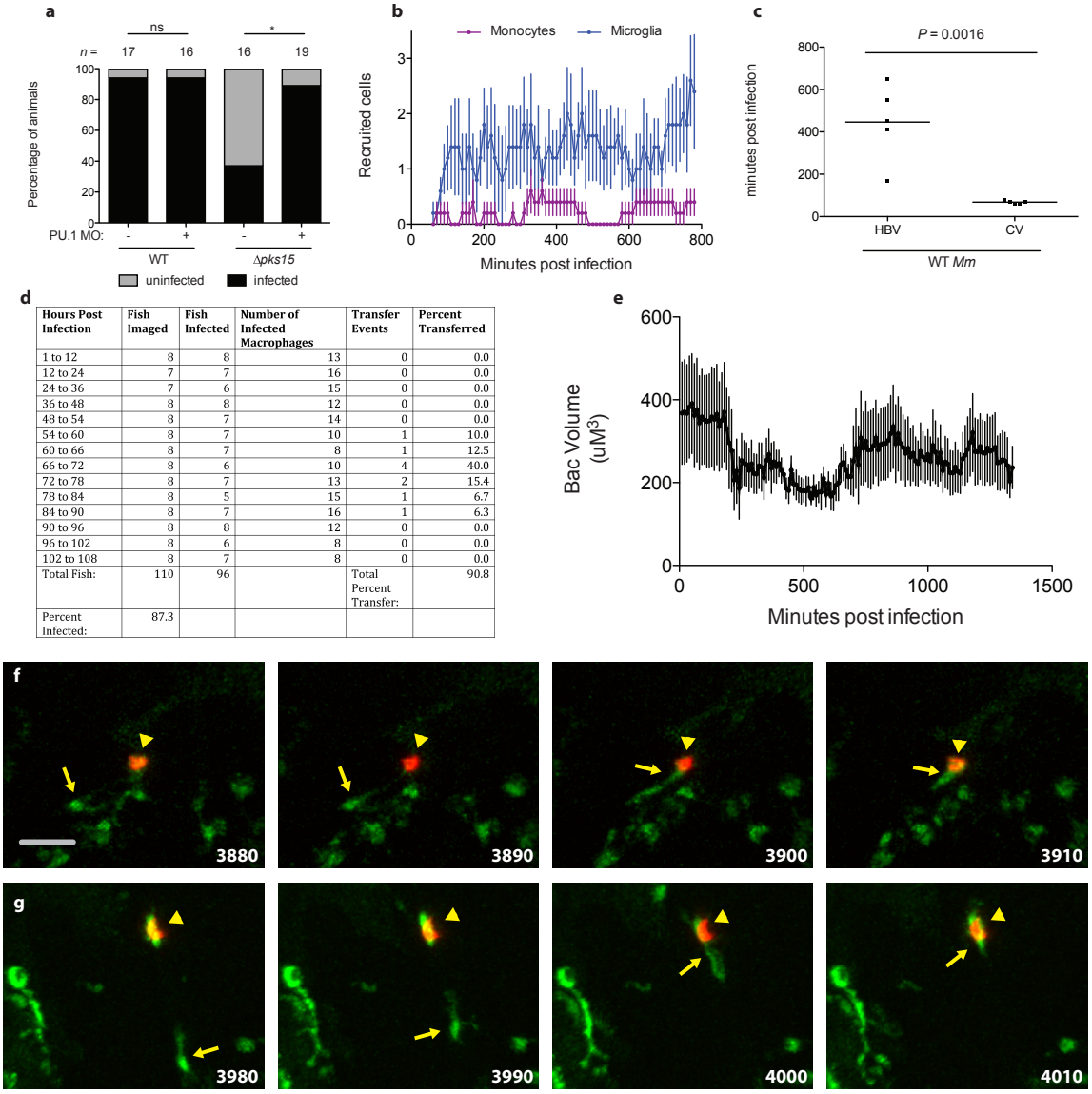

Hours Post Infection	Fish Imaged	Fish Infected	Number of Infected Macrophages	Transfer Events	Percent Transferred
1 to 12	8	8	13	0	0.0
12 to 24	7	7	16	0	0.0
24 to 36	7	6	15	0	0.0
36 to 48	8	8	12	0	0.0
48 to 54	8	7	14	0	0.0
54 to 60	8	7	10	1	10.0
60 to 66	8	7	8	1	12.5
66 to 72	8	6	10	4	40.0
72 to 78	8	7	13	2	15.4
78 to 84	8	5	15	1	6.7
84 to 90	8	7	16	1	6.3
90 to 96	8	8	12	0	0.0
96 to 102	8	6	8	0	0.0
102 to 108	8	7	8	0	0.0
Total Fish:	110	96		Total Percent Transfer:	90.8
Percent Infected:	87.3				

Figure 4.6: Microglia are the Exclusive Intracellular Niche for the First 2.75 Days Following Low Dose Infection of WT Mm and Mediate Clearance of Δpks15 Mm. (A) Wild-type and PU.1-morphant fish were infected in the HBV with 1–3 WT or Δpks15 Mm. Graph shows the percentage of fish that were infected (black) or uninfected (grey) after 5 days. *n* = number of larvae per group. Significance testing done using one-way ANOVA, with Bonferroni's post-test for comparisons shown. **P* < 0.05. (B) Mean (+/- s.e.m. of 5 biological replicates) microglia and monocyte recruitment quantified every 10 min from 1 to 13hpi in the HBV of Tg(*mpeg1*:YFP) fish after infection with 1-3 WT Mm. (C) Mean time to phagocytosis (Minutes post infection) of WT Mm following infection of 1-3 bacteria into the HBV or CV of Tg(*mpeg1*:YFP) fish. Student's unpaired *t*-test. (D) Summary of infection dynamics following HBV infection of 1-3 WT Mm into Tg(*mpeg1*:YFP) fish. Groups of 7 or 8 fish were imaged for 12 or 6 hour periods spanning the first 108 hours (4.5 days) of infection. (E) Mean (+/- s.e.m. of 7 or 8 biological replicates) bacterial burden corresponding to the first 24 hours of infection observed in (D). (F-G) Representative images of two separate fish whose infected microglia are undergoing a transfer event following HBV infection of 1-3 WT Mm as summarized in (D). Mpeg1 expressing (Green) macrophages (yellow arrows) are seen phagocytosing mpeg1 expressing cells infected with TdTomato expressing (red) WT Mm (arrowheads). Scale bar, 50μm. Time stamp, minutes post infection. (A) – (G) Representative of two separate experiments.

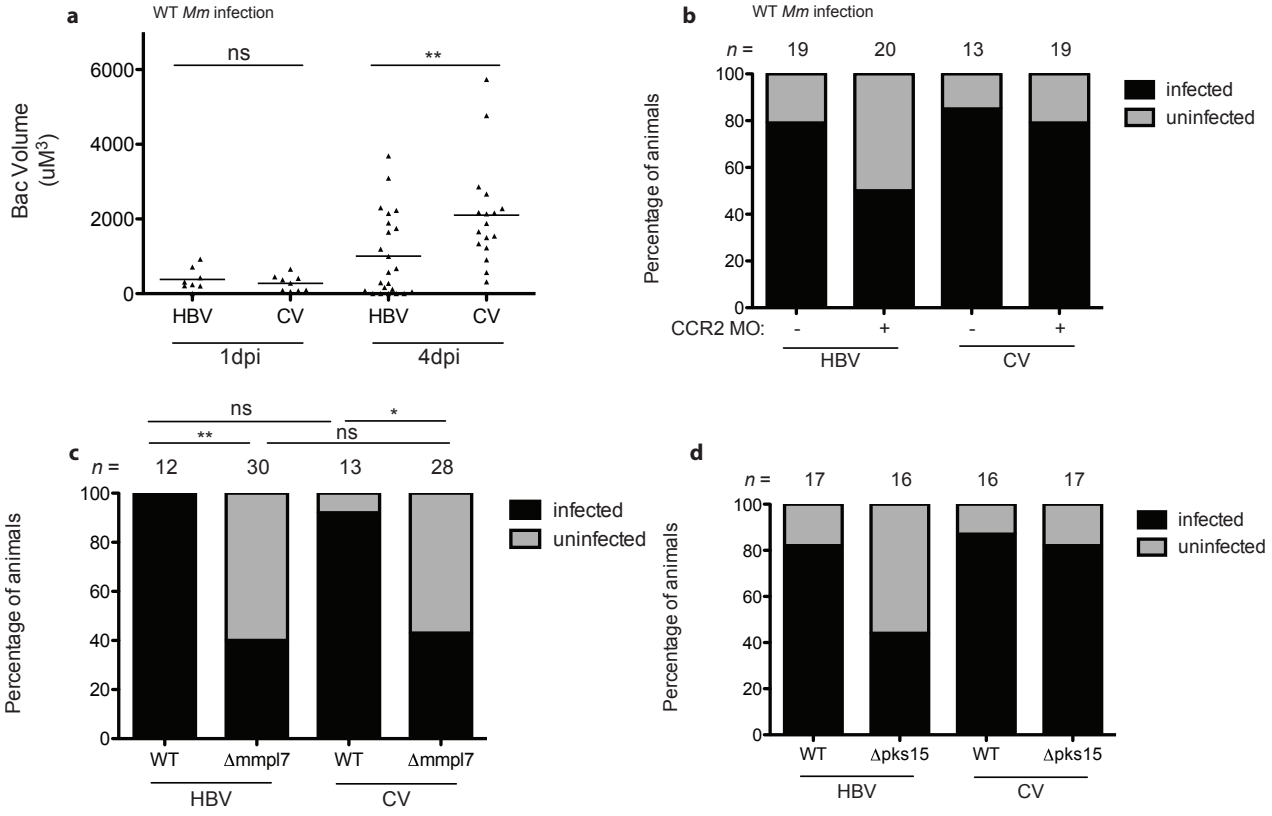

Figure 4.7: Microglia are more Restrictive to Intracellular Growth and Establishing Infection than Monocytes. (A) Mean bacterial burdens of wild-type fish at 1 and 4dpi following infection of 1 WT Mm into the HBV or CV. (B) Wild-type and CCR2-morphant fish were infected in the HBV or CV with 1–3 WT Mm. Graph shows the percentage of fish that were infected (black) or uninfected (grey) after 5 days. *n* = number of larvae per group. (C) Wild-type fish were infected in the HBV or CV with 1–3 WT or ΔmmpL7 Mm. Graph shows the percentage of fish that were infected (black) or uninfected (grey) after 5 days. *n* = number of larvae per group. (D) Wild-type fish were infected in the HBV or CV with 1–3 WT or Δpks15 Mm. Graph shows the percentage of fish that were infected (black) or uninfected (grey) after 5 days. *n* = number of larvae per group. (A) – (D) Representative of two separate experiments. Significance testing done using one-way ANOVA, with Bonferroni's post-test for comparisons shown. $*P < 0.05$, $**P < 0.01$.

Chapter 4 Supplementary Figures

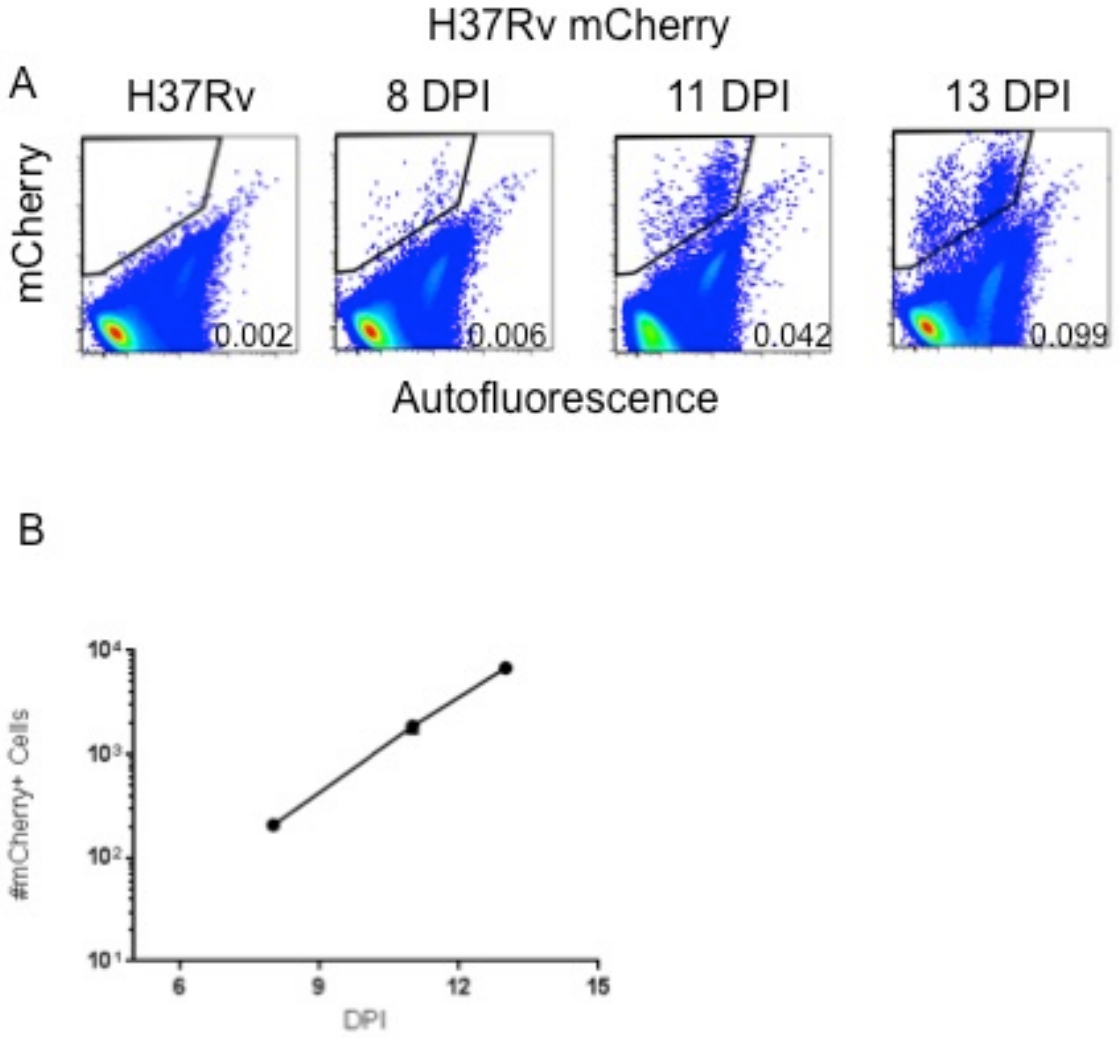

Supplementary Figure 4.1: Identification of Mtb-infected cells after low dose aerosol infection using H37Rv expressing mCherry. B6 mice were infected with a low dose (50-100 CFU) aerosol of H37Rv expressing mCherry and euthanized on days 8, 11, and 13 post infection. (A) mCherry+ Mtb-infected cells are readily identified as early as day 8 post infection by flow cytometry. (B) The absolute number of mCherry+ cells increases as the infection progresses from days 8 to 13.

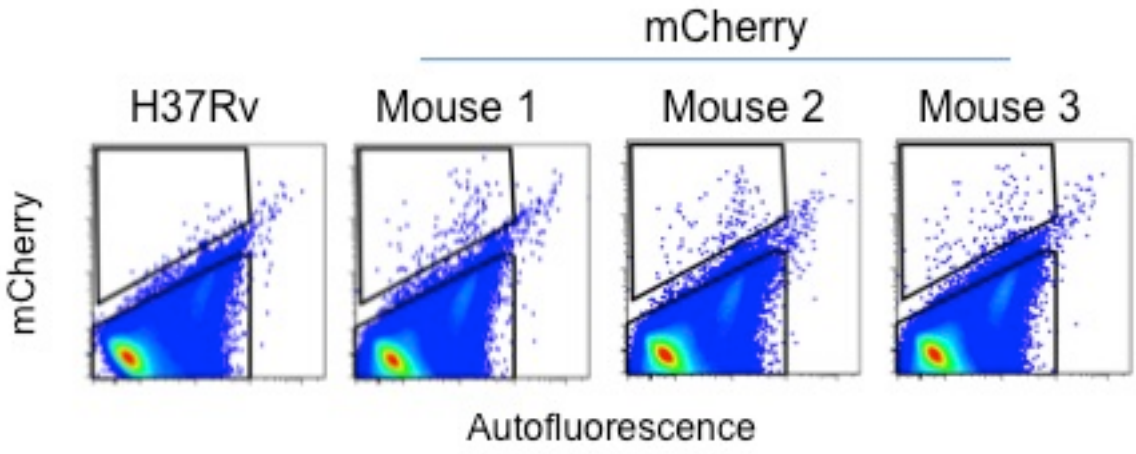

Supplementary Figure 4.2: Identification of Mtb-infected cells after low dose aerosol infection with H37Rv expressing mCherry on day 8 post infection. Consistent identification of mCherry+ cells on day 8 post aerosol infection with H37Rv expressing mCherry in multiple mice.

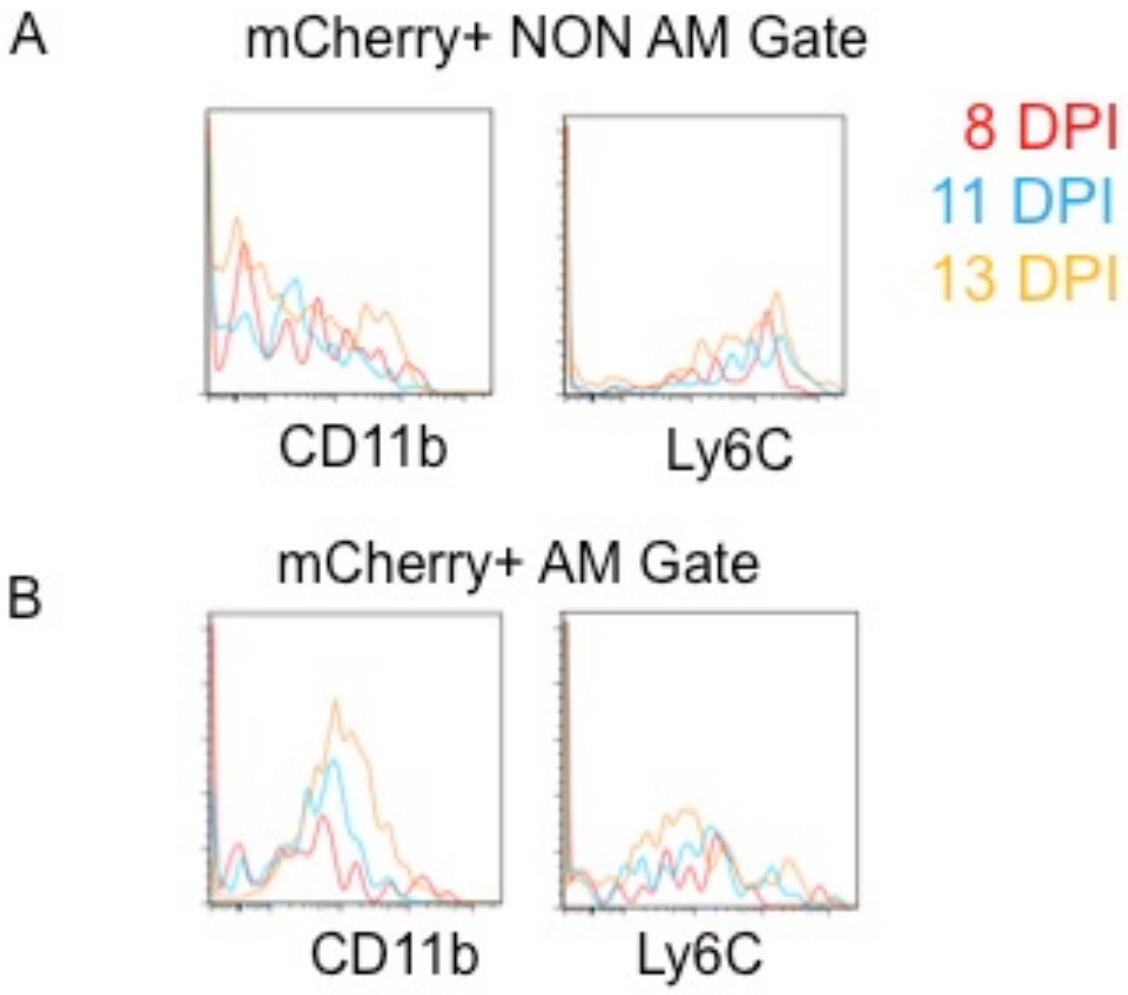

Supplementary Figure 4.3: CD11b and Ly6C expression by mCherry+ non alveolar macrophages and alveolar macrophages. To further characterize the mCherry+ cells at each timepoint we measured the expression of Ly6C and CD11b on both non-alveolar macrophages and alveolar macrophages. (A) Around 30-50% of mCherry+ cells on days 8, 11, and 13-post infection do not fit into the alveolar macrophage phenotype based on CD11c and F480 co-expression. These cells are predominantly $CD11b^{low/neg}$ with a subpopulation expressing Ly6C. (B) mCherry+ alveolar macrophages, identified based on their expression of CD11c and F480 as well as their autofluorescence are primarily $CD11b^{low/neg}$ and $Ly6C^{low/neg}$.

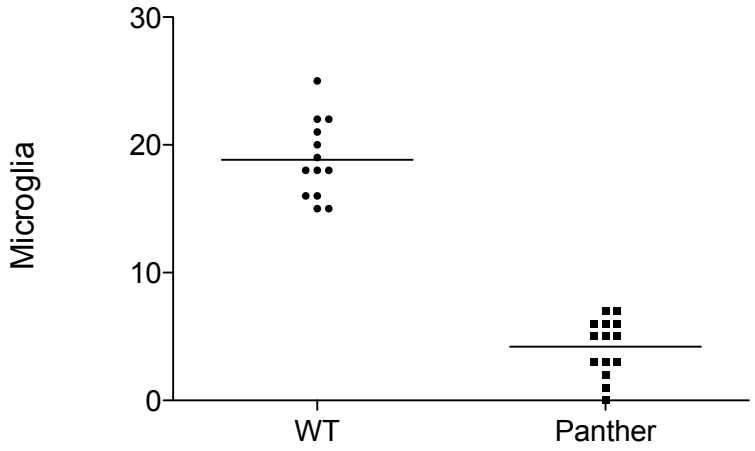

Supplementary Figure 4.4: *Panther* mutants have fewer microglia than wild-type fish under homeostatic conditions. Mean microglial numbers in the brain tissue of 2dpf larvae of wild-type (WT) and *panther* mutant zebrafish.

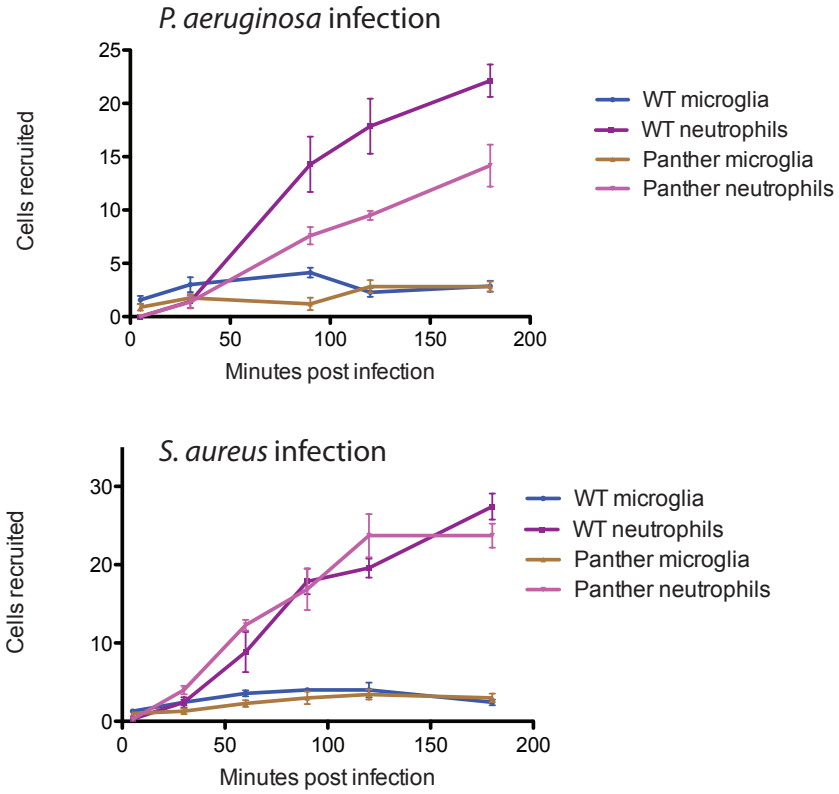

Supplementary Figure 4.5: Normal Recruitment of Neutrophils Towards Commensals in *Panther* Fish. Mean microglia and monocyte recruitment from 5 to 180mpi in the HBV of wild-type or *panther* mutant fish after infection with 164 P. aeruginosa or 146 S. aureus.

CONCLUDING REMARKS

Mycobacterium tuberculosis is unique in its pathogenicity of humans. Often pathogens are a zoonosis, such as plague, or reside as commensals that occasionally invade tissue barriers to cause disease, such as pneumococcus. Disease in humans caused by these pathogens has little impact on their evolutionary survival. In contrast, *M. tuberculosis* has made the lung its exclusive environmental niche for the past 70,000 years (Comas et al., 2013), opting not to partake in any alternative lifestyles such as another animal reservoir or taking up residence among our diverse microbiota. This restraint makes human disease a necessity for the transmission and ultimate survival of *M. tuberculosis*. Because of this, natural selection has finely tuned mycobacteria's pathogenicity in unique ways. The cellular immune response to *M. tuberculosis* is a hallmark example of how evolution has shaped immune responses towards this pathogen. The culmination of this response is the eventual formation of granulomas, complex organized aggregates of innate and adaptive immune cells that are the eventual drivers of disease symptoms (Ramakrishnan, 2012). Given that disease is required for transmission, its no surprise that pathogenic mycobacteria actively drive the formation of granulomas (Davis et al., 2002). Another example of *M. tuberculosis's* unique pathogenesis is its ability to delay adaptive immune responses, in particular the arrival of antigen specific CD4 T cells, a cell type that is well known to play a protective role during infection (Ernst, 2012). Given the dependence of adaptive immune responses on innate immunity we set out to better understand how pathogenic mycobacteria manipulate the very first cellular innate immune responses.

Taking advantage of the optical transparency of the zebrafish, infection with pathogenic *Mycobacterium marinum* has shed light on the early interactions of innate immune cells with mycobacteria. My thesis work has detailed the first interactions of mycobacteria with the host

and, by comparing responses with commensals, we have been able to uncover the unique aspects of mycobacterial pathogenesis that have been shaped by natural selection. A unifying theme that has emerged throughout my work is that instead of using classical virulence factors to establish infection, such as a toxin, pili, or flagella, mycobacteria instead prefer to evade detrimental immune responses.

My work has shown that extracellular mycobacteria actively avoid the recruitment of neutrophils and iNOS-positive monocytes from the periphery. Manipulation allowing these cells to harbor mycobacteria resulted in decreased fitness of the pathogen. While the mechanism behind how mycobacteria avoid neutrophils is not completely understood, the surface lipid PDIM is required to mask pathogen associated molecular patterns (PAMPs) on the surface of the bacteria to prevent Toll-like receptor (TLR)-dependent recruitment of iNOS-positive monocytes. In the absence of PDIM, mycobacteria were readily killed by iNOS-positive monocytes; furthermore PDIM-sufficient mycobacteria were found to be attenuated when co-infected with PDIM-deficient mycobacteria. These data demonstrate that iNOS-positive monocytes, if recruited to the site of infection, can even kill WT *M. marinum*, thus highlighting the importance of PDIM mediating evasion of TLR-signaling. Furthermore, commensal pathogens were found to recruit iNOS-positive monocytes in a TLR-dependent fashion, and these pathogens also transferred attenuation to WT *M. marinum*. These results provide an explanation as to why *M. tuberculosis* is known to initiate infection in the relatively sterile environment of the lower lung instead of the upper respiratory tract that is replete with commensal competition. Directly addressing whether commensals provide protection against M. tuberculosis infection in the context of the lung still needs to be done.

Additionally, this work brings to light a new obstacle to the development of a protective vaccine against *M. tuberculosis*. The most recent vaccine regime to advance to clinical trials, MVA85A, failed to provide additional protection above the current vaccine standard BCG (Tameris et al., 2013), despite displaying induction of known protective immune responses in mice and humans, including antigen specific CD4 and CD8 T cell responses (McShane et al., 2005). Advances in understanding how memory cells respond to subsequent challenges has revealed a role for innate detection at the site of infection in order to elicit recruitment of memory cells to the infection site. These responses, which included those mediated by TLR signaling, were found to be required for the memory cells to exhibit protection (Nolz and Harty, 2014). In this light, our data that mycobacteria avoid TLR-mediated innate immune detection, suggests that a robust adaptive memory compartment won't provide additional protection from infection in the absence of innate immune recognition.

Not only do mycobacteria avoid detection by the immune system but they also drive detection in such a way to recruit permissive cells to the site of infection. Mycobacterial PGL was found to induce CCL2 to recruit permissive monocytes to the site of infection, which was required to establish infection at tissue sites. These data help to explain results in mice showing that CCL2 elicited mononuclear cells are more permissive to mycobacterial growth (Antonelli et al., 2010; Rutledge et al., 1995). Additionally these data may help to explain controversies among human studies regarding the role of CCL2 during mycobacterial infection. Persons with promoter polymorphisms leading to higher CCL2 expression in response to infection were found to have a higher association with developing active tuberculosis (Flores-Villanueva et al., 2005). However, these associations were found to be strongest in East Asian populations, which are enriched for being infected with PGL expressing W-Beijing strains of M. tuberculosis (Feng et

al., 2012). Therefore, our data would predict that persons with polymorphisms predisposing them to higher CCL2 production following infection will only be at higher risk of developing active tuberculosis if they are infected with PGL expressing mycobacteria.

Besides discovering cellular responses that are unique to mycobacterial infection we found that tissue resident macrophage populations are the first to respond to an array of bacterial infections, including mycobacteria. Interestingly, these macrophages were able to clear physiologically relevant doses of 1-3 mycobacteria roughly 10% of the time. In fact, it's these macrophages that mycobacteria manipulate to induce CCL2, which was required to recruit permissive monocytes in which the mycobacteria needed to transfer into from the tissue resident macrophage if infection were to be established. PGL-deficient mycobacteria's defect in establishing infection was driven by its prolonged occupation of tissue resident macrophages which cleared PGL-deficient mycobacteria ~60-80% of the time. While the precise mechanism for how these tissue resident macrophages mediate clearance is still unknown, the fact that we have identified a population of immune cells that offer protective immunity has therapeutic potential. Considering that a significant proportion of M. tuberculosis isolates lack PGL, the mechanism behind the increased clearance of PGL deficient *M. marinum* in our model cannot be expected to provide protection against these strains. However, understanding how the 20-40% of PGL deficient bacteria establish infection in our model should provide avenues to pursue in order to further decrease mycobacterial fitness.

In summary, this work details the first cellular responses to mycobacterial infection, highlighting both immune evasion and manipulation strategies employed by the infecting pathogen. This work also highlights a cellular response that can function to clear the pathogen. Further characterization of these responses should prove valuable for the development of

therapeutics as well as an eventual vaccine against the “Captain of all those men of death,” that is *M. tuberculosis*.

REFERENCES

Abadie, V., Badell, E., Douillard, P., Ensergueix, D., Leenen, P.J., Tanguy, M., Fiette, L., Saeland, S., Gicquel, B., and Winter, N. (2005). Neutrophils rapidly migrate via lymphatics after Mycobacterium bovis BCG intradermal vaccination and shuttle live bacilli to the draining lymph nodes. Blood *106*, 1843-1850.

Adams, D.O. (1976). The granulomatous inflammatory response. A review. Am J Pathol *84*, 164-192.

Adams, K.N., Szumowski, J.D., and Ramakrishnan, L. (2014). Verapamil, and its metabolite norverapamil, inhibit macrophage-induced, bacterial efflux pump-mediated tolerance to multiple anti-tubercular drugs. J Infect Dis *210*, 456-466.

Adams, K.N., Takaki, K., Connolly, L.E., Wiedenhoft, H., Winglee, K., Humbert, O., Edelstein, P.H., Cosma, C.L., and Ramakrishnan, L. (2011). Drug tolerance in replicating mycobacteria mediated by a macrophage-induced efflux mechanism. Cell *145*, 39-53.

Alibaud, L., Rombouts, Y., Trivelli, X., Burguière, A., Cirillo, S.L., Cirillo, J.D., Dubremetz, J.F., Guérardel, Y., Lutfalla, G., and Kremer, L. (2011). A Mycobacterium marinum TesA mutant defective for major cell wall-associated lipids is highly attenuated in Dictyostelium discoideum and zebrafish embryos. Mol Microbiol *80*, 919-934.

Alix, E., Mukherjee, S., and Roy, C.R. (2011). Subversion of membrane transport pathways by vacuolar pathogens. J Cell Biol *195*, 943-952.

Amulic, B., Cazalet, C., Hayes, G.L., Metzler, K.D., and Zychlinsky, A. (2012). Neutrophil function: from mechanisms to disease. Annu Rev Immunol *30*, 459-489.

Andersen, K.G., Nissen, J.K., and Betz, A.G. (2012). Comparative Genomics Reveals Key Gain-of-Function Events in Foxp3 during Regulatory T Cell Evolution. Front Immunol *3*, 113.

Antonelli, L.R.V., Gigliotti Rothfuchs, A., Gonçalves, R., Roffê, E., Cheever, A.W., Bafica, A., Salazar, A.M., Feng, C.G., and Sher, A. (2010). Intranasal Poly-IC treatment exacerbates tuberculosis in mice through the pulmonary recruitment of a pathogen-permissive monocyte/macrophage population. Journal of Clinical Investigation *120*, 1674-1682.

Banaiee, N., Kincaid, E.Z., Buchwald, U., Jacobs, W.R., and Ernst, J.D. (2006). Potent inhibition of macrophage responses to IFN-gamma by live virulent Mycobacterium tuberculosis is independent of mature mycobacterial lipoproteins but dependent on TLR2. J Immunol *176*, 3019-3027.

Bates, J.H., Potts, W.E., and Lewis, M. (1965). EPIDEMIOLOGY OF PRIMARY TUBERCULOSIS IN AN INDUSTRIAL SCHOOL. The New England journal of medicine *272*, 714-717.

Bekker, L.G., and Wood, R. (2010). The changing natural history of tuberculosis and HIV coinfection in an urban area of hyperendemicity. Clin Infect Dis *50 Suppl 3*, S208-214.

Belkaid, Y., and Hand, T.W. (2014). Role of the microbiota in immunity and inflammation. Cell *157*, 121-141.

Bernut, A., Herrmann, J.L., Kissa, K., Dubremetz, J.F., Gaillard, J.L., Lutfalla, G., and Kremer, L. (2014). Mycobacterium abscessus cording prevents phagocytosis and promotes abscess formation. Proc Natl Acad Sci U S A *111*, E943-952.

Berry, M.P.R., Graham, C.M., McNab, F.W., Xu, Z., Bloch, S.A.A., Oni, T., Wilkinson, K.A., Banchereau, R., Skinner, J., Wilkinson, R.J.*, et al.* (2010). An interferon-inducible neutrophil-driven blood transcriptional signature in human tuberculosis. Nature *466*, 973-977.

Boritsch, E.C., Supply, P., Honoré, N., Seeman, T., Stinear, T.P., and Brosch, R. (2014). A glimpse into the past and predictions for the future: the molecular evolution of the tuberculosis agent. Mol Microbiol *93*, 835-852.

Bos, K.I., Harkins, K.M., Herbig, A., Coscolla, M., Weber, N., Comas, I., Forrest, S.A., Bryant, J.M., Harris, S.R., Schuenemann, V.J.*, et al.* (2014). Pre-Columbian mycobacterial genomes reveal seals as a source of New World human tuberculosis. Nature *514*, 494-497.

Bouley, D.M., Ghori, N., Mercer, K.L., Falkow, S., and Ramakrishnan, L. (2001). Dynamic nature of host-pathogen interactions in Mycobacterium marinum granulomas. Infect Immun *69*, 7820-7831.

Brannon, M.K., Davis, J.M., Mathias, J.R., Hall, C.J., Emerson, J.C., Crosier, P.S., Huttenlocher, A., Ramakrishnan, L., and Moskowitz, S.M. (2009). Pseudomonas aeruginosaType III secretion system interacts with phagocytes to modulate systemic infection of zebrafish embryos. Cellular Microbiology *11*, 755-768.

Brennan, P.J. (2003). Structure, function, and biogenesis of the cell wall of Mycobacterium tuberculosis. Tuberculosis (Edinb) *83*, 91-97.

Brown, A.E., Holzer, T.J., and Andersen, B.R. (1987). Capacity of human neutrophils to kill Mycobacterium tuberculosis. J Infect Dis *156*, 985-989.

Cambier, C.J., Takaki, K.K., Larson, R.P., Hernandez, R.E., Tobin, D.M., Urdahl, K.B., Cosma, C.L., and Ramakrishnan, L. (2014). Mycobacteria manipulate macrophage recruitment through coordinated use of membrane lipids. Nature *505*, 218-222.

Canetti, G. (1955). The Tubercle Bacillus in the Pulmonary Lesion of Man; Histobacteriology and Its Bearing on the Therapy of Pulmonary Tuberculosis (New York: Springer).

Chan, J., Xing, Y., Magliozzo, R.S., and Bloom, B.R. (1992). Killing of virulent Mycobacterium tuberculosis by reactive nitrogen intermediates produced by activated murine macrophages. The Journal of experimental medicine *175*, 1111-1122.

Chao, M.C., and Rubin, E.J. (2010). Letting sleeping dos lie: does dormancy play a role in tuberculosis? Annu Rev Microbiol *64*, 293-311.

Charlson, E.S., Bittinger, K., Haas, A.R., Fitzgerald, A.S., Frank, I., Yadav, A., Bushman, F.D., and Collman, R.G. (2011). Topographical Continuity of Bacterial Populations in the Healthy Human Respiratory Tract. American Journal of Respiratory and Critical Care Medicine *184*, 957-963.

Cheung, D.O., Halsey, K., and Speert, D.P. (2000). Role of pulmonary alveolar macrophages in defense of the lung against Pseudomonas aeruginosa. Infect Immun *68*, 4585-4592.

Choi, H.H., Shin, D.M., Kang, G., Kim, K.H., Park, J.B., Hur, G.M., Lee, H.M., Lim, Y.J., Park, J.K., Jo, E.K.*, et al.* (2010). Endoplasmic reticulum stress response is involved in Mycobacterium tuberculosis protein ESAT-6-mediated apoptosis. FEBS Lett *584*, 2445-2454.

Cirillo, J.D., Falkow, S., Tompkins, L.S., and Bermudez, L.E. (1997). Interaction of Mycobacterium avium with environmental amoebae enhances virulence. Infect Immun *65*, 3759-3767.

Clay, H., Davis, J.M., Beery, D., Huttenlocher, A., Lyons, S.E., and Ramakrishnan, L. (2007). Dichotomous Role of the Macrophage in Early Mycobacterium marinum Infection of the Zebrafish. Cell Host & Microbe *2*, 29-39.

Clay, H., and Ramakrishnan, L. (2005). Multiplex fluorescent in situ hybridization in zebrafish embryos using tyramide signal amplification. Zebrafish *2*, 105-111.

Clay, H., Volkman, H.E., and Ramakrishnan, L. (2008). Tumor necrosis factor signaling mediates resistance to mycobacteria by inhibiting bacterial growth and macrophage death. Immunity *29*, 283-294.

Cole, S.T., Brosch, R., Parkhill, J., Garnier, T., Churcher, C., Harris, D., Gordon, S.V., Eiglmeier, K., Gas, S., Barry, C.E.*, et al.* (1998). Deciphering the biology of Mycobacterium tuberculosis from the complete genome sequence. Nature *393*, 537-544.

Cole, S.T., Eiglmeier, K., Parkhill, J., James, K.D., Thomson, N.R., Wheeler, P.R., Honoré, N., Garnier, T., Churcher, C., Harris, D.*, et al.* (2001). Massive gene decay in the leprosy bacillus. Nature *409*, 1007-1011.

Comas, I., Chakravartti, J., Small, P.M., Galagan, J., Niemann, S., Kremer, K., Ernst, J.D., and Gagneux, S. (2010). Human T cell epitopes of Mycobacterium tuberculosis are evolutionarily hyperconserved. nature genetics *42*, 498-503.

Comas, I., Coscolla, M., Luo, T., Borrell, S., Holt, K.E., Kato-Maeda, M., Parkhill, J., Malla, B., Berg, S., Thwaites, G.*, et al.* (2013). Out-of-Africa migration and Neolithic coexpansion of Mycobacterium tuberculosis with modern humans. Nat Genet *45*, 1176-1182.

Connolly, L.E., Edelstein, P.H., and Ramakrishnan, L. (2007). Why is long-term therapy required to cure tuberculosis? PLoS Med *4*, e120.

Converse, S.E., and Cox, J.S. (2005). A protein secretion pathway critical for Mycobacterium tuberculosis virulence is conserved and functional in Mycobacterium smegmatis. J Bacteriol *187*, 1238-1245.

Corleis, B., Korbel, D., Wilson, R., Bylund, J., Chee, R., and Schaible, U.E. (2012). Escape of Mycobacterium tuberculosis from oxidative killing by neutrophils. Cell Microbiol *14*, 1109-1121.

Coros, A., Callahan, B., Battaglioli, E., and Derbyshire, K.M. (2008). The specialized secretory apparatus ESX-1 is essential for DNA transfer in Mycobacterium smegmatis. Mol Microbiol *69*, 794-808.

Cosma, C.L., Humbert, O., and Ramakrishnan, L. (2004). Superinfecting mycobacteria home to established tuberculous granulomas. Nat Immunol *5*, 828-835.

Cosma, C.L., Humbert, O., Sherman, D.R., and Ramakrishnan, L. (2008). Trafficking of superinfecting Mycobacterium organisms into established granulomas occurs in mammals and is independent of the Erp and ESX-1 mycobacterial virulence loci. J Infect Dis *198*, 1851-1855.

Cosma, C.L., Klein, K., Kim, R., Beery, D., and Ramakrishnan, L. (2006). Mycobacterium marinum Erp Is a Virulence Determinant Required for Cell Wall Integrity and Intracellular Survival. Infection and Immunity *74*, 3125-3133.

Cosma, C.L., Sherman, D.R., and Ramakrishnan, L. (2003). The secret lives of the pathogenic mycobacteria. Annu Rev Microbiol *57*, 641-676.

Cox, G., Crossley, J., and Xing, Z. (1995). Macrophage engulfment of apoptotic neutrophils contributes to the resolution of acute pulmonary inflammation in vivo. Am J Respir Cell Mol Biol *12*, 232-237.

Crooks, S.W., and Stockley, R.A. (1998). Leukotriene B4. Int J Biochem Cell Biol *30*, 173-178.

Curto, M., Reali, C., Palmieri, G., Scintu, F., Schivo, M.L., Sogos, V., Marcialis, M.A., Ennas, M.G., Schwarz, H., Pozzi, G.*, et al.* (2004). Inhibition of cytokines expression in human microglia infected by virulent and non-virulent mycobacteria. Neurochem Int *44*, 381-392.

Dannenberg, A.M., Jr. (1993). Immunopathogenesis of pulmonary tubercu- losis. Hosp. Pract. (Off. Ed.) 28, 51–58.

Davis, J.M., Clay, H., Lewis, J.L., Ghori, N., Herbomel, P., and Ramakrishnan, L. (2002). Real-time visualization of mycobacterium-macrophage interactions leading to initiation of granuloma formation in zebrafish embryos. Immunity *17*, 693-702.

Davis, J.M., and Ramakrishnan, L. (2009). The Role of the Granuloma in Expansion and Dissemination of Early Tuberculous Infection. Cell *136*, 37-49.

De Leon, J., Jiang, G., Ma, Y., Rubin, E., Fortune, S., and Sun, J. (2012). Mycobacterium tuberculosis ESAT-6 exhibits a unique membrane-interacting activity that is not found in its ortholog from non-pathogenic Mycobacterium smegmatis. J Biol Chem *287*, 44184-44191.

de Mendonça-Lima, L., Bordat, Y., Pivert, E., Recchi, C., Neyrolles, O., Maitournam, A., Gicquel, B., and Reyrat, J.-M. (2003). The allele encoding the mycobacterial Erp protein affects lung disease in mice. Cellular Microbiology *5*, 65-73.

Derrick, S.C., and Morris, S.L. (2007). The ESAT6 protein of Mycobacterium tuberculosis induces apoptosis of macrophages by activating caspase expression. Cell Microbiol *9*, 1547-1555.

Desvignes, L., and Ernst, J.D. (2009). Interferon-gamma-responsive nonhematopoietic cells regulate the immune response to Mycobacterium tuberculosis. Immunity *31*, 974-985.

Dhama, K., Mahendran, M., Tiwari, R., Dayal Singh, S., Kumar, D., Singh, S., and Sawant, P.M. (2011). Tuberculosis in Birds: Insights into the Mycobacterium avium Infections. Vet Med Int *2011*, 712369.

Doig, C., Seagar, A.L., Watt, B., and Forbes, K.J. (2002). The efficacy of the heat killing of Mycobacterium tuberculosis. J Clin Pathol *55*, 778-779.

Doğru, D., Kiper, N., Ozçelik, U., Yalçin, E., and Tezcan, I. (2010). Tuberculosis in children with congenital immunodeficiency syndromes. Tuberk Toraks *58*, 59-63.

Dumarey, C.H., Labrousse, V., Rastogi, N., Vargaftig, B.B., and Bachelet, M. (1994). Selective Mycobacterium avium-induced production of nitric oxide by human monocyte-derived macrophages. J Leukoc Biol *56*, 36-40.

Eddens, T., and Kolls, J.K. (2012). Host defenses against bacterial lower respiratory tract infection. Current Opinion in Immunology *24*, 424-430.

Elkington, P.T., Green, J.A., Emerson, J.E., Lopez-Pascua, L.D., Boyle, J.J., O'Kane, C.M., and Friedland, J.S. (2007). Synergistic up-regulation of epithelial cell matrix metalloproteinase-9 secretion in tuberculosis. Am J Respir Cell Mol Biol *37*, 431-437.

Ernst, J.D. (1998). Macrophage receptors for Mycobacterium tuberculosis. Infect Immun *66*, 1277-1281.

Ernst, J.D. (2012). The immunological life cycle of tuberculosis. Nat Rev Immunol *12*, 581-591.

Eruslanov, E.B., Lyadova, I.V., Kondratieva, T.K., Majorov, K.B., Scheglov, I.V., Orlova, M.O., and Apt, A.S. (2005). Neutrophil responses to Mycobacterium tuberculosis infection in genetically susceptible and resistant mice. Infect Immun *73*, 1744-1753.

Eum, S.Y., Kong, J.H., Hong, M.S., Lee, Y.J., Kim, J.H., Hwang, S.H., Cho, S.N., Via, L.E., and Barry, C.E. (2010). Neutrophils are the predominant infected phagocytic cells in the airways of patients with active pulmonary TB. Chest *137*, 122-128.

Ewer, K., Millington, K.A., Deeks, J.J., Alvarez, L., Bryant, G., and Lalvani, A. (2006). Dynamic antigen-specific T-cell responses after point-source exposure to Mycobacterium tuberculosis. Am J Respir Crit Care Med *174*, 831-839.

Falkow, S. (2006). Is Persistent Bacterial Infection Good for Your Health? Cell *124*, 699-702.

Falkow, S. (2008). I never met a microbe I didn't like. Nat Med *14*, 1053-1057.

Fang, F.C. (2004). Antimicrobial reactive oxygen and nitrogen species: concepts and controversies. Nat Rev Microbiol *2*, 820-832.

Feldman, W.H., and Baggenstoss, A.H. (1938). The residual infectivity of the primary complex of tuberculosis. Am J Pathol *14*, 473-490.473.

Feng, W.X., Flores-Villanueva, P.O., Mokrousov, I., Wu, X.R., Xiao, J., Jiao, W.W., Sun, L., Miao, Q., Shen, C., Shen, D.*, et al.* (2012). CCL2−2518 (A/G) polymorphisms and tuberculosis susceptibility: a meta-analysis. The international journal of tuberculosis and lung disease : the official journal of the International Union against Tuberculosis and Lung Disease *16*, 150-156.

Fields, B.S., Benson, R.F., and Besser, R.E. (2002). Legionella and Legionnaires' disease: 25 years of investigation. Clin Microbiol Rev *15*, 506-526.

Flint, J.L., Kowalski, J.C., Karnati, P.K., and Derbyshire, K.M. (2004). The RD1 virulence locus of Mycobacterium tuberculosis regulates DNA transfer in Mycobacterium smegmatis. Proc Natl Acad Sci U S A *101*, 12598-12603.

Flores-Villanueva, P.O., Ruiz-Morales, J.A., Song, C.-H., Flores, L.M., Jo, E.-K., Montaño, M., Barnes, P.F., Selman, M., and Granados, J. (2005). A functional promoter polymorphism in monocyte chemoattractant protein-1 is associated with increased susceptibility to pulmonary tuberculosis. The Journal of experimental medicine *202*, 1649-1658.

Forrellad, M.A., Klepp, L.I., Gioffré, A., Sabio y García, J., Morbidoni, H.R., de la Paz Santangelo, M., Cataldi, A.A., and Bigi, F. (2013). Virulence factors of the Mycobacterium tuberculosis complex. Virulence *4*, 3-66.

Gagneux, S. (2006). Variable host-pathogen compatibility in Mycobacterium tuberculosis. Proceedings of the National Academy of Sciences *103*, 2869-2873.

Gewirtz, A.T., Yu, Y., Krishna, U.S., Israel, D.A., Lyons, S.L., and Peek, R.M. (2004). Helicobacter pylori flagellin evades toll-like receptor 5-mediated innate immunity. J Infect Dis *189*, 1914-1920.

Glickman, M.S., and Jacobs, W.R. (2001). Microbial pathogenesis of Mycobacterium tuberculosis: dawn of a discipline. Cell *104*, 477-485.

Goldstein, E., Lippert, W., and Warshauer, D. (1974). Pulmonary alveolar macrophage. Defender against bacterial infection of the lung. J Clin Invest *54*, 519-528.

Gomes, M.S., Flórido, M., Pais, T.F., and Appelberg, R. (1999). Improved clearance of Mycobacterium avium upon disruption of the inducible nitric oxide synthase gene. J Immunol *162*, 6734-6739.

Gomez Perdiguero, E., Schulz, C., and Geissmann, F. (2013). Development and homeostasis of "resident" myeloid cells: the case of the microglia. Glia *61*, 112-120.

Gupta, S., Tyagi, S., Almeida, D.V., Maiga, M.C., Ammerman, N.C., and Bishai, W.R. (2013). Acceleration of tuberculosis treatment by adjunctive therapy with verapamil as an efflux inhibitor. Am J Respir Crit Care Med *188*, 600-607.

Gómez-Velasco, A., Bach, H., Rana, A.K., Cox, L.R., Bhatt, A., Besra, G.S., and Av-Gay, Y. (2013). Disruption of the serine/threonine protein kinase H affects phthiocerol dimycocerosates synthesis in Mycobacterium tuberculosis. Microbiology *159*, 726-736.

Hagedorn, M., Rohde, K.H., Russell, D.G., and Soldati, T. (2009). Infection by tubercular mycobacteria is spread by nonlytic ejection from their amoeba hosts. Science *323*, 1729-1733.

Hagedorn, M., and Soldati, T. (2007). Flotillin and RacH modulate the intracellular immunity of Dictyostelium to Mycobacterium marinum infection. Cell Microbiol *9*, 2716-2733.

Hall, C., Flores, M.V., Storm, T., Crosier, K., and Crosier, P. (2007). The zebrafish lysozyme C promoter drives myeloid-specific expression in transgenic fish. BMC Dev Biol *7*, 42.

Henard, C.A., and Vázquez-Torres, A. (2011). Nitric oxide and salmonella pathogenesis. Front Microbiol *2*, 84.

Herbomel, P., Thisse, B., and Thisse, C. (1999). Ontogeny and behaviour of early macrophages in the zebrafish embryo. Development *126*, 3735-3745.

Herbomel, P., Thisse, B., and Thisse, C. (2001). Zebrafish early macrophages colonize cephalic mesenchyme and developing brain, retina, and epidermis through a M-CSF receptor-dependent invasive process. Dev Biol *238*, 274-288.

Houben, E.N., Walburger, A., Ferrari, G., Nguyen, L., Thompson, C.J., Miess, C., Vogel, G., Mueller, B., and Pieters, J. (2009). Differential expression of a virulence factor in pathogenic and non-pathogenic mycobacteria. Mol Microbiol *72*, 41-52.

Houk, V.N. (1980). Spread of tuberculosis via recirculated air in a naval vessel: the Byrd study. Ann N Y Acad Sci *353*, 10-24.

Hsu, T., Hingley-Wilson, S.M., Chen, B., Chen, M., Dai, A.Z., Morin, P.M., Marks, C.B., Padiyar, J., Goulding, C., Gingery, M.*, et al.* (2003). The primary mechanism of attenuation of bacillus Calmette-Guerin is a loss of secreted lytic function required for invasion of lung interstitial tissue. Proc Natl Acad Sci U S A *100*, 12420-12425.

Huang, C.C., Tchetgen, E.T., Becerra, M.C., Cohen, T., Hughes, K.C., Zhang, Z., Calderon, R., Yataco, R., Contreras, C., Galea, J.*, et al.* (2014). The Effect of HIV-Related Immunosuppression on the Risk of Tuberculosis Transmission to Household Contacts. Clinical Infectious Diseases *58*, 765-774.

Hussell, T., and Bell, T.J. (2014). Alveolar macrophages: plasticity in a tissue-specific context. Nat Rev Immunol *14*, 81-93.

Jones, B.D., Ghori, N., and Falkow, S. (1994). Salmonella typhimurium initiates murine infection by penetrating and destroying the specialized epithelial M cells of the Peyer's patches. J Exp Med *180*, 15-23.

Jones, G.S., Amirault, H.J., and Andersen, B.R. (1990). Killing of Mycobacterium tuberculosis by neutrophils: a nonoxidative process. J Infect Dis *162*, 700-704.

Keane, J., Balcewicz-Sablinska, M.K., Remold, H.G., Chupp, G.L., Meek, B.B., Fenton, M.J., and Kornfeld, H. (1997). Infection by Mycobacterium tuberculosis promotes human alveolar macrophage apoptosis. Infect Immun *65*, 298-304.

Kierdorf, K., and Prinz, M. (2013). Factors regulating microglia activation. Front Cell Neurosci *7*, 44.

Kirksey, M.A., Tischler, A.D., Siméone, R., Hisert, K.B., Uplekar, S., Guilhot, C., and McKinney, J.D. (2011). Spontaneous Phthiocerol Dimycocerosate-Deficient Variants of Mycobacterium tuberculosis Are Susceptible to Gamma Interferon-Mediated Immunity. Infection and Immunity *79*, 2829-2838.

Kisich, K.O., Higgins, M., Diamond, G., and Heifets, L. (2002). Tumor necrosis factor alpha stimulates killing of Mycobacterium tuberculosis by human neutrophils. Infect Immun *70*, 4591-4599.

Kröncke, K.D., Fehsel, K., and Kolb-Bachofen, V. (1998). Inducible nitric oxide synthase in human diseases. Clinical and experimental immunology *113*, 147-156.

Laskin, D.L., Sunil, V.R., Gardner, C.R., and Laskin, J.D. (2011). Macrophages and tissue injury: agents of defense or destruction? Annu Rev Pharmacol Toxicol *51*, 267-288.

Lawn, S.D., and Zumla, A.I. (2011). Tuberculosis. Lancet *378*, 57-72.

Le Guyader, D., Redd, M.J., Colucci-Guyon, E., Murayama, E., Kissa, K., Briolat, V., Mordelet, E., Zapata, A., Shinomiya, H., and Herbomel, P. (2008). Origins and unconventional behavior of neutrophils in developing zebrafish. Blood *111*, 132-141.

Lee, P.P., Chan, K.W., Jiang, L., Chen, T., Li, C., Lee, T.L., Mak, P.H., Fok, S.F., Yang, X., and Lau, Y.L. (2008). Susceptibility to mycobacterial infections in children with X-linked chronic granulomatous disease: a review of 17 patients living in a region endemic for tuberculosis. Pediatr Infect Dis J *27*, 224-230.

Lepiller, S., Laurens, V., Bouchot, A., Herbomel, P., Solary, E., and Chluba, J. (2007). Imaging of nitric oxide in a living vertebrate using a diaminofluorescein probe. Free Radical Biology and Medicine *43*, 619-627.

Letek, M., González, P., Macarthur, I., Rodríguez, H., Freeman, T.C., Valero-Rello, A., Blanco, M., Buckley, T., Cherevach, I., Fahey, R.*, et al.* (2010). The genome of a pathogenic rhodococcus: cooptive virulence underpinned by key gene acquisitions. PLoS Genet *6*, e1001145.

Lin, P.L., Ford, C.B., Coleman, M.T., Myers, A.J., Gawande, R., Ioerger, T., Sacchettini, J., Fortune, S.M., and Flynn, J.L. (2014). Sterilization of granulomas is common in active and latent tuberculosis despite within-host variability in bacterial killing. Nature Medicine *20*, 75-79.

Liu, F., and Wen, Z. (2002). Cloning and expression pattern of the lysozyme C gene in zebrafish. Mech Dev *113*, 69-72.

Liu, P.T., Stenger, S., Li, H., Wenzel, L., Tan, B.H., Krutzik, S.R., Ochoa, M.T., Schauber, J., Wu, K., Meinken, C.*, et al.* (2006). Toll-like receptor triggering of a vitamin D-mediated human antimicrobial response. Science *311*, 1770-1773.

Lowe, D.M., Redford, P.S., Wilkinson, R.J., O'Garra, A., and Martineau, A.R. (2012). Neutrophils in tuberculosis: friend or foe? Trends Immunol *33*, 14-25.

Lyczak, J.B., Cannon, C.L., and Pier, G.B. (2000). Establishment of Pseudomonas aeruginosa infection: lessons from a versatile opportunist. Microbes Infect *2*, 1051-1060.

MacCarthy, E.M., Burns, I., Irnazarow, I., Polwart, A., Greenhough, T.J., Shrive, A.K., and Hoole, D. (2008). Serum CRP-like protein profile in common carp Cyprinus carpio challenged with Aeromonas hydrophila and Escherichia coli lipopolysaccharide. Dev Comp Immunol *32*, 1281-1289.

Majeed, M., Perskvist, N., Ernst, J.D., Orselius, K., and Stendahl, O. (1998). Roles of calcium and annexins in phagocytosis and elimination of an attenuated strain of Mycobacterium tuberculosis in human neutrophils. Microb Pathog *24*, 309-320.

Manzanillo, P.S., Shiloh, M.U., Portnoy, D.A., and Cox, J.S. (2012). Mycobacterium Tuberculosis Activates the DNA-Dependent Cytosolic Surveillance Pathway within Macrophages. Cell Host & Microbe *11*, 469-480.

Martineau, A.R., Newton, S.M., Wilkinson, K.A., Kampmann, B., Hall, B.M., Nawroly, N., Packe, G.E., Davidson, R.N., Griffiths, C.J., and Wilkinson, R.J. (2007). Neutrophil-mediated innate immune resistance to mycobacteria. J Clin Invest *117*, 1988-1994.

Maruyama, I.N., Rakow, T.L., and Maruyama, H.I. (1995). cRACE: a simple method for identification of the 5' end of mRNAs. Nucleic Acids Research *23*, 3796-3797.

Masaki, T., Qu, J., Cholewa-Waclaw, J., Burr, K., Raaum, R., and Rambukkana, A. (2013). Reprogramming adult Schwann cells to stem cell-like cells by leprosy bacilli promotes dissemination of infection. Cell *152*, 51-67.

Mayer-Barber, K.D., Andrade, B.B., Oland, S.D., Amaral, E.P., Barber, D.L., Gonzales, J., Derrick, S.C., Shi, R., Kumar, N.P., Wei, W.*, et al.* (2014). Host-directed therapy of tuberculosis based on interleukin-1 and type I interferon crosstalk. Nature *511*, 99-103.

Mayer-Barber, K.D., Barber, D.L., Shenderov, K., White, S.D., Wilson, M.S., Cheever, A., Kugler, D., Hieny, S., Caspar, P., Nunez, G.*, et al.* (2010). Cutting Edge: Caspase-1 Independent IL-1 Production Is Critical for Host Resistance to Mycobacterium tuberculosis and Does Not Require TLR Signaling In Vivo. The Journal of Immunology *184*, 3326-3330.

McShane, H., Pathan, A.A., Sander, C.R., Goonetilleke, N.P., Fletcher, H.A., and Hill, A.V. (2005). Boosting BCG with MVA85A: the first candidate subunit vaccine for tuberculosis in clinical trials. Tuberculosis (Edinb) *85*, 47-52.

Medzhitov, R. (2007). Recognition of microorganisms and activation of the immune response. Nature *449*, 819-826.

Mishra, B.B., Moura-Alves, P., Sonawane, A., Hacohen, N., Griffiths, G., Moita, L.F., and Anes, E. (2010). Mycobacterium tuberculosis protein ESAT-6 is a potent activator of the NLRP3/ASC inflammasome. Cell Microbiol *12*, 1046-1063.

Mogues, T., Goodrich, M.E., Ryan, L., LaCourse, R., and North, R.J. (2001). The relative importance of T cell subsets in immunity and immunopathology of airborne Mycobacterium tuberculosis infection in mice. The Journal of experimental medicine *193*, 271-280.

Monack, D.M. (2013). Helicobacter and salmonella persistent infection strategies. Cold Spring Harb Perspect Med *3*, a010348.

Moran, A.P. (2007). Lipopolysaccharide in bacterial chronic infection: insights from Helicobacter pylori lipopolysaccharide and lipid A. Int J Med Microbiol *297*, 307-319.

Mosser, D.M., and Edwards, J.P. (2008). Exploring the full spectrum of macrophage activation. Nat Rev Immunol *8*, 958-969.

Movahedi, M., Aghamohammadi, A., Farhoudi, A., Moin, M., Pourpak, Z., Gharagozlou, M., Mansouri, D., Babaei Jandaghi, A., Shahnavaz, N., Rezaei, N.*, et al.* (2003). Respiratory manifestations of chronic granulomatous disease; a clinical survey of patients from Iranian primary immunodeficiency registry. Iran J Allergy Asthma Immunol *2*, 45-51.

Murayama, E., Kissa, K., Zapata, A., Mordelet, E., Briolat, V., Lin, H.F., Handin, R.I., and Herbomel, P. (2006). Tracing hematopoietic precursor migration to successive hematopoietic organs during zebrafish development. Immunity *25*, 963-975.

Murry, J.P., Pandey, A.K., Sassetti, C.M., and Rubin, E.J. (2009). Phthiocerol dimycocerosate transport is required for resisting interferon-gamma-independent immunity. The Journal of Infectious Diseases *200*, 774-782.

Nandi, B., and Behar, S.M. (2011). Regulation of neutrophils by interferon-γ limits lung inflammation during tuberculosis infection. J Exp Med *208*, 2251-2262.

Niethammer, P., Grabher, C., Look, A.T., and Mitchison, T.J. (2009). A tissue-scale gradient of hydrogen peroxide mediates rapid wound detection in zebrafish. Nature *459*, 996-999.

Nolz, J.C., and Harty, J.T. (2014). IL-15 regulates memory CD8+ T cell O-glycan synthesis and affects trafficking. J Clin Invest *124*, 1013-1026.

Onwueme, K.C., Vos, C.J., Zurita, J., Ferreras, J.A., and Quadri, L.E.N. (2005). The dimycocerosate ester polyketide virulence factors of mycobacteria. Progress in Lipid Research *44*, 259-302.

Ordway, D., Henao-Tamayo, M., Harton, M., Palanisamy, G., Troudt, J., Shanley, C., Basaraba, R.J., and Orme, I.M. (2007). The hypervirulent Mycobacterium tuberculosis strain HN878 induces a potent TH1 response followed by rapid down-regulation. Journal of immunology (Baltimore, Md : 1950) *179*, 522-531.

Pagán, A.J., and Ramakrishnan, L. (2014). Immunity and Immunopathology in the Tuberculous Granuloma. Cold Spring Harb Perspect Med.

Parsons, L.M., Jankowski, C.S., and Derbyshire, K.M. (1998). Conjugal transfer of chromosomal DNA in Mycobacterium smegmatis. Mol Microbiol *28*, 571-582.

Pedrosa, J., Saunders, B.M., Appelberg, R., Orme, I.M., Silva, M.T., and Cooper, A.M. (2000). Neutrophils play a protective nonphagocytic role in systemic Mycobacterium tuberculosis infection of mice. Infect Immun *68*, 577-583.

Persson, Y.A., Blomgran-Julinder, R., Rahman, S., Zheng, L., and Stendahl, O. (2008). Mycobacterium tuberculosis-induced apoptotic neutrophils trigger a pro-inflammatory response in macrophages through release of heat shock protein 72, acting in synergy with the bacteria. Microbes Infect *10*, 233-240.

Philips, J.A., and Ernst, J.D. (2012). Tuberculosis Pathogenesis and Immunity. Annual Review of Pathology: Mechanisms of Disease *7*, 353-384.

Price, N.M., Farrar, J., Tran, T.T., Nguyen, T.H., Tran, T.H., and Friedland, J.S. (2001). Identification of a matrix-degrading phenotype in human tuberculosis in vitro and in vivo. J Immunol *166*, 4223-4230.

Ramakrishnan, L. (2012). Revisiting the role of the granuloma in tuberculosis. Nature Reviews Immunology, 1-15.

Ramakrishnan, L. (2013). The Zebrafish Guide to Tuberculosis Immunity and Treatment. Cold Spring Harb Symp Quant Biol *78*, 179-192.

Ramakrishnan, L., Federspiel, N.A., and Falkow, S. (2000). Granuloma-specific expression of Mycobacterium virulence proteins from the glycine-rich PE-PGRS family. Science *288*, 1436-1439.

Ransohoff, R.M., and Perry, V.H. (2009). Microglial physiology: unique stimuli, specialized responses. Annu Rev Immunol *27*, 119-145.

Reed, M.B., Domenech, P., Manca, C., Su, H., Barczak, A.K., Kreiswirth, B.N., Kaplan, G., and Barry, C.E. (2004). A glycolipid of hypervirulent tuberculosis strains that inhibits the innate immune response. Nature *431*, 84-87.

Reichenbach, J., Rosenzweig, S., Döffinger, R., Dupuis, S., Holland, S.M., and Casanova, J.L. (2001). Mycobacterial diseases in primary immunodeficiencies. Curr Opin Allergy Clin Immunol *1*, 503-511.

Reichler, M.R., Reves, R., Bur, S., Thompson, V., Mangura, B.T., Ford, J., Valway, S.E., and Onorato, I.M. (2002). Evaluation of Investigations Conducted to Detect and Prevent Transmission of Tuberculosis. JAMA *287*, 991-995.

Rengarajan, J., Bloom, B.R., and Rubin, E.J. (2005). Genome-wide requirements for Mycobacterium tuberculosis adaptation and survival in macrophages. Proc Natl Acad Sci U S A *102*, 8327-8332.

Renshaw, S.A., Loynes, C.A., Trushell, D.M., Elworthy, S., Ingham, P.W., and Whyte, M.K. (2006). A transgenic zebrafish model of neutrophilic inflammation. Blood *108*, 3976-3978.

Reyes-Ruvalcaba, D., González-Cortés, C., and Rivero-Lezcano, O.M. (2008). Human phagocytes lack the ability to kill Mycobacterium gordonae, a non-pathogenic mycobacteria. Immunol Lett *116*, 72-78.

Rittershaus, E.S., Baek, S.H., and Sassetti, C.M. (2013). The normalcy of dormancy: common themes in microbial quiescence. Cell Host Microbe *13*, 643-651.

Roach, D.R., Bean, A.G.D., Demangel, C., France, M.P., Briscoe, H., and Britton, W.J. (2002). TNF regulates chemokine induction essential for cell recruitment, granuloma formation, and clearance of mycobacterial infection. Journal of immunology (Baltimore, Md : 1950) *168*, 4620-4627.

Robertson, H.E. (1933). The Persistence of Tuberculous Infections. Am J Pathol *9*, 711-718.711.

Roca, F.J., and Ramakrishnan, L. (2013). TNF Dually Mediates Resistance and Susceptibility to Mycobacteria via Mitochondrial Reactive Oxygen Species. Cell *153*, 521-534.

Rohde, K., Yates, R.M., Purdy, G.E., and Russell, D.G. (2007). Mycobacterium tuberculosis and the environment within the phagosome. Immunol Rev *219*, 37-54.

Rosenthal, S., and Tager, I.B. (1975). Prevalence of gram-negative rods in the normal pharyngeal flora. Annals of internal medicine *83*, 355-357.

Rutledge, B.J., Rayburn, H., Rosenberg, R., North, R.J., Gladue, R.P., Corless, C.L., and Rollins, B.J. (1995). High level monocyte chemoattractant protein-1 expression in transgenic mice increases their susceptibility to intracellular pathogens. J Immunol *155*, 4838-4843.

Rydell-Törmänen, K., Uller, L., and Erjefält, J.S. (2006). Neutrophil cannibalism--a back up when the macrophage clearance system is insufficient. Respir Res *7*, 143.

Saunders, B.M., Briscoe, H., and Britton, W.J. (2004). T cell-derived tumour necrosis factor is essential, but not sufficient, for protection against Mycobacterium tuberculosisinfection. Clinical and experimental immunology *137*, 279-287.

Saunders, B.M., and Cooper, A.M. (2000). Restraining mycobacteria: role of granulomas in mycobacterial infections. Immunol Cell Biol *78*, 334-341.

Schiffmann, E., Corcoran, B.A., and Wahl, S.M. (1975). N-formylmethionyl peptides as chemoattractants for leucocytes. Proc Natl Acad Sci U S A *72*, 1059-1062.

Schnappinger, D., Ehrt, S., Voskuil, M.I., Liu, Y., Mangan, J.A., Monahan, I.M., Dolganov, G., Efron, B., Butcher, P.D., Nathan, C.*, et al.* (2003). Transcriptional Adaptation of Mycobacterium tuberculosis within Macrophages: Insights into the Phagosomal Environment. J Exp Med *198*, 693-704.

Scott, H.M., and Flynn, J.L. (2002). Mycobacterium tuberculosis in chemokine receptor 2-deficient mice: influence of dose on disease progression. Infection and Immunity *70*, 5946-5954.

Sepkowitz, K.A. (1996). How contagious is tuberculosis? Clin Infect Dis *23*, 954-962.

Serbina, N.V., Jia, T., Hohl, T.M., and Pamer, E.G. (2008). Monocyte-Mediated Defense Against Microbial Pathogens. Annual Review of Immunology *26*, 421-452.

Serhan, C.N. (2007). Resolution phase of inflammation: novel endogenous anti-inflammatory and proresolving lipid mediators and pathways. Annu Rev Immunol *25*, 101-137.

Shafer, R.W., Bloch, A.B., Larkin, C., Vasudavan, V., Seligman, S., Dehovitz, J.D., DiFerdinando, G., Stoneburner, R., and Cauthen, G. (1996). Predictors of survival in HIV-infected tuberculosis patients. AIDS *10*, 269-272.

Shafiani, S., Dinh, C., Ertelt, J.M., Moguche, A.O., Siddiqui, I., Smigiel, K.S., Sharma, P., Campbell, D.J., Way, S.S., and Urdahl, K.B. (2013). Pathogen-specific Treg cells expand early during mycobacterium tuberculosis infection but are later eliminated in response to Interleukin-12. Immunity *38*, 1261-1270.

Shafiani, S., Tucker-Heard, G., Kariyone, A., Takatsu, K., and Urdahl, K.B. (2010). Pathogen-specific regulatory T cells delay the arrival of effector T cells in the lung during early tuberculosis. J Exp Med *207*, 1409-1420.

Sharma, S.K., Mohan, A., Sharma, A., and Mitra, D.K. (2005). Miliary tuberculosis: new insights into an old disease. The Lancet Infectious Diseases *5*, 415-430.

SHEPARD, C.C. (1957). Growth characteristics of tubercle bacilli and certain other mycobacteria in HeLa cells. J Exp Med *105*, 39-48.

Siegrist, M.S., and Bertozzi, C.R. (2014). Mycobacterial lipid logic. Cell Host Microbe *15*, 1-2.

Silva, M.T., Silva, M.N., and Appelberg, R. (1989). Neutrophil-macrophage cooperation in the host defence against mycobacterial infections. Microb Pathog *6*, 369-380.

Sinsimer, D., Huet, G., Manca, C., Tsenova, L., Koo, M.S., Kurepina, N., Kana, B., Mathema, B., Marras, S.A.E., Kreiswirth, B.N.*, et al.* (2008). The Phenolic Glycolipid of Mycobacterium tuberculosis Differentially Modulates the Early Host Cytokine Response but Does Not in Itself Confer Hypervirulence. Infection and Immunity *76*, 3027-3036.

Solomon, J.M., Leung, G.S., and Isberg, R.R. (2003). Intracellular replication of Mycobacterium marinum within Dictyostelium discoideum: efficient replication in the absence of host coronin. Infect Immun *71*, 3578-3586.

Speert, D.P., Bond, M., Woodman, R.C., and Curnutte, J.T. (1994). Infection with Pseudomonas cepacia in chronic granulomatous disease: role of nonoxidative killing by neutrophils in host defense. J Infect Dis *170*, 1524-1531.

Srivastava, S., Ernst, J.D., and Desvignes, L. (2014). Beyond macrophages: the diversity of mononuclear cells in tuberculosis. Immunol Rev *262*, 179-192.

Steinmüller, C., Franke-Ullmann, G., Lohmann-Matthes, M.L., and Emmendörffer, A. (2000). Local activation of nonspecific defense against a respiratory model infection by application of interferon-gamma: comparison between rat alveolar and interstitial lung macrophages. Am J Respir Cell Mol Biol *22*, 481-490.

Stillie, R., Farooq, S.M., Gordon, J.R., and Stadnyk, A.W. (2009). The functional significance behind expressing two IL-8 receptor types on PMN. J Leukoc Biol *86*, 529-543.

Stinear, T.P., Seemann, T., Harrison, P.F., Jenkin, G.A., Davies, J.K., Johnson, P.D., Abdellah, Z., Arrowsmith, C., Chillingworth, T., Churcher, C.*, et al.* (2008). Insights from the complete genome sequence of Mycobacterium marinum on the evolution of Mycobacterium tuberculosis. Genome Res *18*, 729-741.

Sugawara, I., Udagawa, T., and Yamada, H. (2004). Rat neutrophils prevent the development of tuberculosis. Infect Immun *72*, 1804-1806.

Swaim, L.E., Connolly, L.E., Volkman, H.E., Humbert, O., Born, D.E., and Ramakrishnan, L. (2006). Mycobacterium marinum Infection of Adult Zebrafish Causes Caseating Granulomatous Tuberculosis and Is Moderated by Adaptive Immunity. Infection and Immunity *74*, 6108-6117.

Szumowski, J.D., Adams, K.N., Edelstein, P.H., and Ramakrishnan, L. (2013). Antimicrobial efflux pumps and Mycobacterium tuberculosis drug tolerance: evolutionary considerations. Curr Top Microbiol Immunol *374*, 81-108.

Sørensen, A.L., Nagai, S., Houen, G., Andersen, P., and Andersen, A.B. (1995). Purification and characterization of a low-molecular-mass T-cell antigen secreted by Mycobacterium tuberculosis. Infect Immun *63*, 1710-1717.

Takaki, K., Cosma, C.L., Troll, M.A., and Ramakrishnan, L. (2012). An in vivo platform for rapid high-throughput antitubercular drug discovery. Cell reports *2*, 175-184.

Takaki, K., Davis, J.M., Winglee, K., and Ramakrishnan, L. (2013). Evaluation of the pathogenesis and treatment of Mycobacterium marinum infection in zebrafish. Nature Protocols *8*, 1114-1124.

Tameris, M.D., Hatherill, M., Landry, B.S., Scriba, T.J., Snowden, M.A., Lockhart, S., Shea, J.E., McClain, J.B., Hussey, G.D., Hanekom, W.A.*, et al.* (2013). Safety and efficacy of MVA85A, a new tuberculosis vaccine, in infants previously vaccinated with BCG: a randomised, placebo-controlled phase 2b trial. Lancet *381*, 1021-1028.

Tan, B.H., Meinken, C., Bastian, M., Bruns, H., Legaspi, A., Ochoa, M.T., Krutzik, S.R., Bloom, B.R., Ganz, T., Modlin, R.L.*, et al.* (2006). Macrophages acquire neutrophil granules for antimicrobial activity against intracellular pathogens. J Immunol *177*, 1864-1871.

Taylor, J.L., Hattle, J.M., Dreitz, S.A., Troudt, J.M., Izzo, L.S., Basaraba, R.J., Orme, I.M., Matrisian, L.M., and Izzo, A.A. (2006). Role for matrix metalloproteinase 9 in granuloma formation during pulmonary Mycobacterium tuberculosis infection. Infect Immun *74*, 6135-6144.

Thwaites, G.E., Chau, T.T., Stepniewska, K., Phu, N.H., Chuong, L.V., Sinh, D.X., White, N.J., Parry, C.M., and Farrar, J.J. (2002). Diagnosis of adult tuberculous meningitis by use of clinical and laboratory features. Lancet *360*, 1287-1292.

Tobin, D.M., and Ramakrishnan, L. (2008). Comparative pathogenesis of Mycobacterium marinum and Mycobacterium tuberculosis. Cell Microbiol *10*, 1027-1039.

Tobin, D.M., Roca, F.J., Oh, S.F., McFarland, R., Vickery, T.W., Ray, J.P., Ko, D.C., Zou, Y., Bang, N.D., Chau, T.T.*, et al.* (2012). Host genotype-specific therapies can optimize the inflammatory response to mycobacterial infections. Cell *148*, 434-446.

Tobin, D.M., Vary, J.J.C., Ray, J.P., Walsh, G.S., Dunstan, S.J., Bang, N.D., Hagge, D.A., Khadge, S., King, M.-C., Hawn, T.R.*, et al.* (2010). The lta4h Locus Modulates Susceptibility to Mycobacterial Infection in Zebrafish and Humans. Cell *140*, 717-730.

Truman, R.W., Singh, P., Sharma, R., Busso, P., Rougemont, J., Paniz-Mondolfi, A., Kapopoulou, A., Brisse, S., Scollard, D.M., Gillis, T.P.*, et al.* (2011). Probable zoonotic leprosy in the southern United States. N Engl J Med *364*, 1626-1633.

Tsai, M.C., Chakravarty, S., Zhu, G., Xu, J., Tanaka, K., Koch, C., Tufariello, J., Flynn, J., and Chan, J. (2006). Characterization of the tuberculous granuloma in murine and human lungs: cellular composition and relative tissue oxygen tension. Cell Microbiol *8*, 218-232.

Tunkel, A.R., and Scheld, W.M. (1993). Pathogenesis and pathophysiology of bacterial meningitis. Clin Microbiol Rev *6*, 118-136.

van der Vaart, M., van Soest, J.J., Spaink, H.P., and Meijer, A.H. (2013). Functional analysis of a zebrafish myd88 mutant identifies key transcriptional components of the innate immune system. Disease Models & Mechanisms *6*, 841-854.

van der Wel, N., Hava, D., Houben, D., Fluitsma, D., van Zon, M., Pierson, J., Brenner, M., and Peters, P.J. (2007). M. tuberculosis and M. leprae translocate from the phagolysosome to the cytosol in myeloid cells. Cell *129*, 1287-1298.

Vermaelen, K., and Pauwels, R. (2004). Accurate and simple discrimination of mouse pulmonary dendritic cell and macrophage populations by flow cytometry: methodology and new insights. Cytometry A *61*, 170-177.

Volkman, H.E., Clay, H., Beery, D., Chang, J.C.W., Sherman, D.R., and Ramakrishnan, L. (2004). Tuberculous Granuloma Formation Is Enhanced by a Mycobacterium Virulence Determinant. PLoS Biology *2*, e367.

Volkman, H.E., Pozos, T.C., Zheng, J., Davis, J.M., Rawls, J.F., and Ramakrishnan, L. (2010). Tuberculous Granuloma Induction via Interaction of a Bacterial Secreted Protein with Host Epithelium. Science *327*, 466-469.

von Bernuth, H., Picard, C., Puel, A., and Casanova, J.-L. (2012). Experimental and natural infections in MyD88- and IRAK-4-deficient mice and humans. European Journal of Immunology *42*, 3126-3135.

Walburger, A., Koul, A., Ferrari, G., Nguyen, L., Prescianotto-Baschong, C., Huygen, K., Klebl, B., Thompson, C., Bacher, G., and Pieters, J. (2004). Protein kinase G from pathogenic mycobacteria promotes survival within macrophages. Science *304*, 1800-1804.

Walters, K.B., Dodd, M.E., Mathias, J.R., Gallagher, A.J., Bennin, D.A., Rhodes, J., Kanki, J.P., Look, A.T., Grinblat, Y., and Huttenlocher, A. (2009). Muscle degeneration and leukocyte infiltration caused by mutation of zebrafish Fad24. Dev Dyn *238*, 86-99.

Walters, K.B., Green, J.M., Surfus, J.C., Yoo, S.K., and Huttenlocher, A. (2010). Live imaging of neutrophil motility in a zebrafish model of WHIM syndrome. Blood *116*, 2803-2811.

Wang, J., and Behr, M.A. (2014). Building a better bacillus: the emergence of Mycobacterium tuberculosis. Front Microbiol *5*, 139.

Wang, N., Tytell, J.D., and Ingber, D.E. (2009). Mechanotransduction at a distance: mechanically coupling the extracellular matrix with the nucleus. Nat Rev Mol Cell Biol *10*, 75-82.

Watson, R.O., Manzanillo, P.S., and Cox, J.S. (2012). Extracellular M. tuberculosis DNA targets bacteria for autophagy by activating the host DNA-sensing pathway. Cell *150*, 803-815.

Weiser, J.N. (2009). The pneumococcus: why a commensal misbehaves. Journal of Molecular Medicine *88*, 97-102.

Wells, W.F., Ratcliffe, H.L., and Grumb, C. (1948). On the mechanics of droplet nuclei infection; quantitative experimental air-borne tuberculosis in rabbits. American journal of hygiene *47*, 11-28.

Wertheim, H.F.L., Melles, D.C., Vos, M.C., van Leeuwen, W., van Belkum, A., Verbrugh, H.A., and Nouwen, J.L. (2005). The role of nasal carriage in Staphylococcus aureus infections. The Lancet Infectious Diseases *5*, 751-762.

Williams, L.T., Snyderman, R., Pike, M.C., and Lefkowitz, R.J. (1977). Specific receptor sites for chemotactic peptides on human polymorphonuclear leukocytes. Proc Natl Acad Sci U S A *74*, 1204-1208.

Wolf, A.J., Linas, B., Trevejo-Nuñez, G.J., Kincaid, E., Tamura, T., Takatsu, K., and Ernst, J.D. (2007). Mycobacterium tuberculosis infects dendritic cells with high frequency and impairs their function in vivo. Journal of immunology (Baltimore, Md : 1950) *179*, 2509-2519.

Yang, C.-T., Cambier, C.J., Davis, J.M., Hall, C.J., Crosier, P.S., and Ramakrishnan, L. (2012). Neutrophils Exert Protection in the Early Tuberculous Granuloma by Oxidative Killing of Mycobacteria Phagocytosed from Infected Macrophages. Cell Host & Microbe *12*, 301-312.

Yu, J., Tran, V., Li, M., Huang, X., Niu, C., Wang, D., Zhu, J., Wang, J., Gao, Q., and Liu, J. (2012). Both Phthiocerol Dimycocerosates and Phenolic Glycolipids Are Required for Virulence of Mycobacterium marinum. Infection and Immunity *80*, 1381-1389.

Zhang, Y.J., Reddy, M.C., Ioerger, T.R., Rothchild, A.C., Dartois, V., Schuster, B.M., Trauner, A., Wallis, D., Galaviz, S., Huttenhower, C.*, et al.* (2013). Tryptophan biosynthesis protects mycobacteria from CD4 T-cell-mediated killing. Cell *155*, 1296-1308.

Zumla, A., Raviglione, M., Hafner, R., and von Reyn, C.F. (2013). Tuberculosis. N Engl J Med *368*, 745-755.